Materials Advances

ROYAL SOCIETY OF CHEMISTRY

REVIEW

View Article Online
View Journal

Check for updates

Cite this: DOI: 10.1039/d6ma00219f

Emerging processes, machine learning and applications in composite additive manufacturing

Md Zillur Rahman, * H K Mahedi Azad and Morad Hossain Diganto

Composite additive manufacturing (CAM) enables the development of architected, multifunctional composites, yet industrial uptake, particularly in safety-critical settings, remains limited by process–structure–property uncertainty driven by coupled interface and defect mechanisms, including nonuniform reinforcement dispersion and orientation drift, weak interfacial/interlayer bonding, voids, lack-of-fusion defects, residual stress, and defect-sensitive property scatter. This review synthesizes four interdependent pillars, composite feedstock design, CAM process physics, multiscale modeling, and machine-learning (ML) methods, into an interface-centered process–structure–property–control framework linking manufacturing conditions to microstructural evolution, anisotropy, and performance across polymer, ceramic, and metal matrix systems. This review summarizes emerging composite materials, compares major CAM routes together with new modalities and hybrid approaches, including hybrid and multi-material systems, and examines modeling and simulation strategies from defect-informed RVEs and solidification-aware DED process maps to multiscale physics models, alongside ML architectures and workflows relevant to CAM. Quantitative benchmarking metrics are emphasized across mechanical response, porosity/defect tolerance, geometric and surface quality, anisotropy, productivity, and energy input. Application drivers are highlighted in aerospace and unmanned aerial vehicle structures, biomedical implants and scaffolds, automotive components, and soft robotic systems, where orientation control, interlayer integrity, fatigue/defect tolerance, and traceable quality assurance are decisive. The analysis further evaluates how ML addresses core CAM bottlenecks, including porosity and melt-pool behavior prediction, fiber orientation control, *in situ* defect detection, and real-time process tuning, using task-specific model selection, design-of-experiments, active learning, transfer/domain adaptation, simulation pretraining, physics-informed learning, calibrated uncertainty, explainability, and out-of-distribution validation, and outlines future directions toward passive-to-active, physics-informed, uncertainty-aware digital twins, standardized benchmarking, and qualification-ready digital threads supported by auditable regulatory evidence packages for scalable and certifiable CAM.

Received 16th February 2026,
Accepted 5th June 2026

DOI: 10.1039/d6ma00219f

rsc.li/materials-advances

Open Access Article. Published on 19 June 2026. Downloaded on 6/19/2026 11:23:52 PM.
This article is licensed under a Creative Commons Attribution 3.0 Unported Licence.

1. Introduction

Additive manufacturing (AM) is undergoing a fundamental transition from a geometry-driven prototyping technology to a manufacturing platform capable of producing architected, multifunctional, and application-specific components. Within this transition, composites play an increasingly decisive role because reinforcement architecture enables the simultaneous tailoring of stiffness, strength, damping, thermal and electrical response, lightweight performance, and biofunctionality while preserving the geometric freedom intrinsic to AM. As a result, composite additive manufacturing (CAM) is emerging as a critical enabling technology for high-value sectors, including aerospace, automotive systems, biomedical devices, and soft robotics.[1–8] Despite this momentum, the broader maturation of CAM remains constrained by an incomplete understanding of how feedstock design, process physics, microstructural evolution, and digital decision systems jointly govern process–structure–property relationships. Unlike monolithic AM, in which process parameters are often evaluated primarily against density, dimensional accuracy, surface condition, or scalar mechanical properties, CAM requires simultaneous control of reinforcement dispersion, fiber or particle orientation, matrix wetting, interphase formation, bead-to-bead bonding, porosity, lack-of-fusion defects, and residual-stress development.[9–12] These phenomena are strongly coupled: rheology and reinforcement transport influence deposition stability; thermal history affects residual stress, crystallinity, and interfacial bonding; and defect nucleation governs anisotropy, property scatter, and ultimately qualification confidence. Consequently, CAM cannot be fully understood by considering materials, machines, or

Department of Mechanical Engineering, Ahsanullah University of Science and Technology, Dhaka 1208, Bangladesh. E-mail: md.zillur.rahman.phd@gmail.com

© 2026 The Author(s). Published by the Royal Society of Chemistry

Open Access Article. Published on 19 June 2026. Downloaded on 6/19/2026 11:23:52 PM. This article is licensed under a Creative Commons Attribution 3.0 Unported Licence.

algorithms in isolation. Instead, it requires an integrated framework that connects composite interface behavior with process physics, predictive modeling, monitoring, and qualification.

The current literature provides valuable but fragmented foundations for this integration. Prior reviews have examined composite feedstock systems and printable material innovations,[9,12,13] AM process mechanisms and parameter–property relationships,[14–19] and machine-learning (ML) methods for AM data analytics, monitoring, topology optimization, and property prediction.[10,11,20–22] Digital-twin reviews have clarified physical–virtual synchronization, *in situ* monitoring architectures, simulation modules, and real-time decision support for AM systems.[23–26] Composite-oriented AM reviews have focused mainly on polymer-fiber printable materials, process categories, and reinforcement strategies.[9] Qualification-focused reviews and standards have described certification concepts, production-site quality requirements, traceability, controls, and documentation for AM.[27,28] These contributions are essential; however, they generally treat ML and digital twins, composite feedstock architecture, AM process physics, and qualification evidence as separate domains rather than as interdependent components of a CAM-specific manufacturing ecosystem.

The main novelty of this review is therefore not the isolated discussion of ML, digital twins, benchmarking, or qualification, but the use of the composite interface as the organizing variable within a CAM-specific process–structure–property–control framework. From this perspective, reinforcement dispersion, orientation drift, interfacial bonding, void morphology, lack of fusion, residual stress, and anisotropic property scatter are not independent failure modes; rather, they are coupled targets for materials design, process optimization, sensing, modeling, benchmarking, and qualification. This interface-centered framing is particularly important because weak or inconsistent interfacial load transfer remains one of the main reasons why CAM parts often fail to reach their theoretical performance potential, even when reinforcement content and geometric reliability appear favorable.

Accordingly, this review advances four linked contributions. First, it provides a cross-process synthesis connecting polymer-, ceramic-, and metal-matrix composite feedstocks with the process physics that govern their printability and microstructural evolution. Second, it establishes quantitative benchmarking criteria for mechanical performance, geometric accuracy, defect tolerance, anisotropy, and productivity across CAM platforms. Third, it offers problem-specific guidance for matching ML model classes, including artificial neural networks, convolutional neural networks, recurrent neural networks, and ensemble methods, to CAM tasks such as porosity prediction,

Md Zillur Rahman

Dr Md Zillur Rahman is an Associate Professor of Mechanical Engineering at the Ahsanullah University of Science and Technology, Dhaka, Bangladesh. He earned his PhD and MEng from the University of Auckland, New Zealand, and his BSc (Eng) from BUET. His research focuses on fiber-reinforced composites, nanocomposites, hybrid and biocomposites, structural vibration, damping, durability, bio-inspired design, and computational simulation, with emphasis on sustainable natural fiber composites. He has authored over 160 publications, has an h-index of 40 with more than 4400 citations, is currently editing 32 books with Elsevier, Springer, and ACS, and was included in the 2025 Stanford-Elsevier Top 2% Scientists list.

H K Mahedi Azad

H K Mahedi Azad is a PhD student in Mechanical Engineering at Virginia Tech, USA. He holds a Master's degree in Engineering Technology from Bowling Green State University, USA, with a Bachelor of Science in Mechanical Engineering from the Ahsanullah University of Science and Technology, Dhaka, Bangladesh. His research focuses on materials design and discovery using physics-informed machine learning, multiscale simulation, and experimental characterization. His work integrates mechanical and microstructural analysis with data-driven modeling to enhance material performance and reliability across engineering applications.

Morad Hossain Diganto

Morad Hossain Diganto holds a Bachelor of Science in Mechanical Engineering from the Ahsanullah University of Science and Technology, Dhaka, Bangladesh. His research spans renewable energy systems, composite materials, and additive manufacturing. He is interested in advancing industry-integrated research on advanced materials and 3D printing using machine learning and digital twin frameworks for real-time control, optimization, and system diagnostics.

© 2026 The Author(s). Published by the Royal Society of Chemistry

Open Access Article. Published on 19 June 2026. Downloaded on 6/19/2026 11:23:52 PM. This article is licensed under a Creative Commons Attribution 3.0 Unported Licence.

melt-pool instability detection, reinforcement-orientation control, and geometric-deviation compensation.[29–31] Fourth, it develops a qualification-oriented roadmap that links designed datasets, uncertainty-aware prediction, closed-loop control, digital twins, and auditable digital-thread evidence.

Several persistent barriers motivate this integrated treatment. Nonuniform reinforcement dispersion, orientation drift, weak interfacial bonding, stochastic porosity, lack-of-fusion defects, and limited closed-loop process control continue to restrict repeatability, scalability, and certification readiness in CAM. ML-enhanced AM has shown substantial promise for topology optimization, *in situ* monitoring, parameter selection, and predictive quality assurance.[29–31] However, most current implementations remain narrowly scoped and do not yet provide a systematic pathway for integration across the complete CAM workflow. At the same time, emerging AM modalities, including volumetric stereolithography and advanced directed-energy or jetting-based approaches, are challenging conventional assumptions of layerwise fabrication, yet their implications for composite microstructural evolution, interfacial quality, and qualification remain insufficiently explored.[16,32,33]

These gaps persist even as materials discovery, digital-twin simulation, and closed-loop AM control are becoming increasingly inseparable within ML-driven manufacturing frameworks.[30,34] To address this need, the present review develops an integrated analysis that treats materials, processes, modeling, ML, and qualification as mutually dependent drivers of next-generation CAM. Specifically, this review: (i) maps composite feedstock architecture to process-dependent microstructural evolution across major AM platforms;[4,12,35] (ii) links multiscale modeling with ML-enabled prediction and optimization to support transferable and uncertainty-aware process design;[30] (iii) evaluates the suitability of different ML model classes for CAM-specific prediction, monitoring, optimization, and control task[29–31] and (iv) identifies convergent opportunities for intelligent and autonomous CAM through physics-informed ML and digital-twin environments.[25,30,36,37] Accordingly, this review is driven by the following explicit research questions: RQ1: How can emerging ML frameworks be systematically integrated into CAM workflows to enable predictive design, real-time control, and autonomous quality assurance? RQ2: What unresolved mechanistic links between composite feedstock characteristics, AM process physics, and resulting performance should be clarified to achieve reliable, scalable CAM? RQ3: Which emerging CAM modalities and hybridized manufacturing routes offer the most promising pathways for high-performance, sustainable composite production?

By addressing these questions, this review advances a holistic roadmap for transforming CAM from a predominantly empirical practice into a data-rich, simulation-driven, ML-enabled, and qualification-ready manufacturing paradigm. Emerging composite materials for AM are first summarized with emphasis on reinforcement types, matrix systems, and structure–property relationships across polymer, ceramic, and metal matrix composites (Section 2). Major CAM processes are then reviewed, including their classifications, operating principles, and suitability for different composite classes, followed by a dedicated discussion of composite-specific processing challenges related to reinforcement orientation, dispersion, feedstock stability, interfacial bonding, and defect formation (Sections 3 and 3.1). Recent developments in key CAM routes, including stereolithography, binder jetting, fused deposition modeling, selective laser sintering, and directed energy deposition, are subsequently discussed (Sections 3.2–3.6), followed by emerging hybrid printing and multi-material CAM systems (Section 3.7). Quantitative performance metrics and benchmarking criteria for mechanical, physical, geometric, surface, and productivity-based comparison of CAM processes are then presented in Section 3.8. Section 4 discusses emerging modeling and simulation techniques for CAM, while Section 5 synthesizes ML methods relevant to CAM, including common model architectures, ML-integrated workflows, data-efficient learning strategies, and problem-specific model selection for trustworthy and uncertainty-aware prediction. Section 6 reviews applications in aerospace, automotive, biomedical, and soft robotics fields, while Sections 7, 8, and 9 outline key prospects and challenges, a roadmap for ML-enabled CAM, and concluding perspectives, respectively.

2. Emerging composite materials

2.1 Polymer matrix composites

Polymers are the most widely used feedstocks in AM methods.[12,38] However, selecting polymers for AM is critical due to their characteristics. Typically, thermoplastics, thermosets (UV-curable), and hydrogels are the three most commonly used polymer types in AM. Critical physical properties, molecular structures, printing methods, and subcategories of the various polymers widely used in AM are illustrated in Fig. 1.[12]

Additively manufactured polymer materials often lack functionality and the required mechanical properties. As a result, reinforcements are combined with polymer matrices to achieve the requisite mechanical, electrical, thermal, and other functional properties that are unattainable by any individual constituent alone.[12,39] From the nanoscale (*e.g.*, carbon nanotubes, graphene, and nanoparticles) to the macroscale (*e.g.*, short and long fibers), various materials can serve as reinforcement materials.[12] Additively manufactured polymer composites can be categorized into three types based on the reinforcement materials (Table 1). Regardless of the category, AM technology enables the manufacture of polymer composites with complex geometries with high accuracy and minimal waste.[38,39]

2.2 Ceramic matrix composites

Ceramic matrix composites (CMCs) are low-density materials with an outstanding ability to resist high temperatures. Therefore, it has significant potential in aerospace, aircraft, automotive, energy, environmental, biomedical, military, and other sectors.[40–42] Nowadays, the most used reinforcement materials for CMCs are whiskers, particles, continuous fibers, and staple

Open Access Article. Published on 19 June 2026. Downloaded on 6/19/2026 11:23:52 PM.
This article is licensed under a Creative Commons Attribution 3.0 Unported Licence.

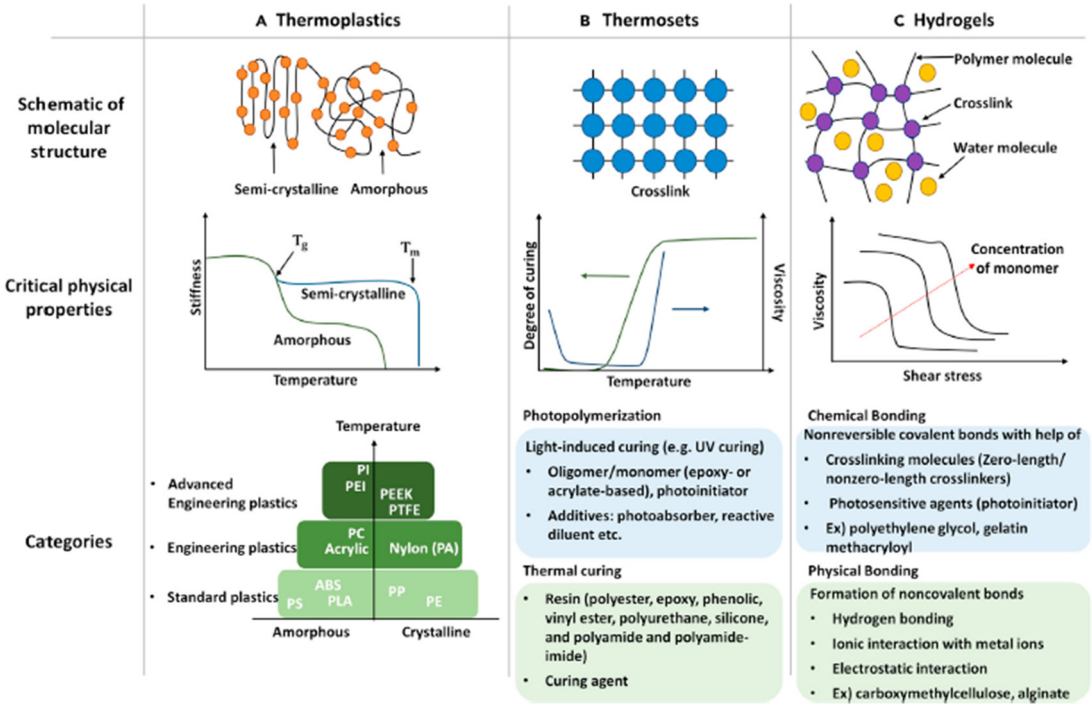

Fig. 1 Frequently used polymer types in AM: (A) thermoplastics, (B) thermosets, and (C) hydrogels, adapted from ref. 12 (open access).

Table 1 Classification, properties, and examples of polymer composites. Adapted from ref. 13 (reused with permission, license number 6212370793093)

Classification	Properties	Examples
Particle-reinforced	Superior tensile and compressive moduli and thermal conductivity Reduced thermal coefficient and enlargement at break	Al-ZrB_2-ABS, Al-Al_2O_3-Nylon 6, $CaTiO_3$-polypropylene, glass bead-polyamide, and diamond-acrylic
Fiber-reinforced	Massive increase in mechanical properties Lightweight	Short glass fiber, ABS short carbon fiber, silicon carbide yarn, nylon
Nanoparticle-reinforced	Enhanced tensile and compressive moduli Reduced elongation and thermal coefficient Increase thermal stability and electrical conductivity	CNF-nylon, graphite-polystyrene, CNF-ABS, and metal nano-powder polymers

fibers.[41,42] Conventional techniques for manufacturing CMCs include sintering, reaction bonding, hot pressing, infiltration, *in situ* chemical reaction, sol-gel, and pyrolysis.[43] However, AM technology is more suitable than conventional techniques for manufacturing CMCs due to its shorter development cycle, lower costs, improved yield, and ability to avoid secondary processing of the produced CMC parts.[41,42] However, utilizing AM technologies to manufacture CMC parts requires a multistep manufacturing process due to the high sintering temperature. ZrO_2–Al_2O_3, SiC_f–SiC, SiC–C, and $TiAl_3$–Al_2O_3 are some examples of CMCs that can be manufactured through AM.[42]

2.3 Metal matrix composites

In metal matrix composites (MMCs), reinforcing materials are continuously dispersed within a monolithic metallic matrix to enhance overall properties.[44,45] Depending on the application, different metal matrices (*e.g.*, magnesium, aluminum, and titanium) are used in MMC for structural and high-temperature applications.[45] The main functionality of such matrices is to provide stability, support the dispersed reinforcements, and help to carry loads to the composite structure.[46] Although silver, beryllium, aluminum, cobalt, iron, copper, nickel, magnesium, and titanium are the most common matrices that are used for commercial applications, it has been reported that 25% of the market uses only copper as the matrix for MMCs.[45] Furthermore, C, Gr, BeO, Mo, NbC, TiB, $TiBl_2$, TiC, SiC, TaC, and Al_2O_3 are commercially used reinforcement materials in MMCs. Moreover, some CAM applications also use MMCs consisting of continuous reinforcement (*i.e.*, SiC, graphite, and Al_2O_3 fiber) and discontinuous reinforcements (*i.e.*, whiskers, short fibers, and particles).[45,46] Recent advancements in MMC materials for AM have opened a range of possibilities in the automotive, aerospace, sports, and structural

© 2026 The Author(s). Published by the Royal Society of Chemistry

Open Access Article. Published on 19 June 2026. Downloaded on 6/19/2026 11:23:52 PM. This article is licensed under a Creative Commons Attribution 3.0 Unported Licence.

industries.[45] Al–GrO, Al–Gr, A332–Al_2O_3–SiC, and Al–SiC are examples of MMCs that can be fabricated using AM.[46]

3. Emerging CAM processes

According to the American Society for Testing and Materials (ASTM), AM processes are classified by the methodologies used to create layers of materials that stack and gradually form the complete object.[7,16,47–53] Various CAM techniques, their classifications, base material types, and typical resolutions are presented in Table 2.

3.1 Composite-specific challenges of AM methods

Beyond geometric capability, composite AM performance is governed by (i) reinforcement orientation/architecture, (ii) dispersion and feedstock stability, and (iii) interfacial bonding (matrix–matrix and matrix-reinforcement). Table 3 compares AM methods and their composite-specific processing challenges (fiber orientation, dispersion, and bonding).

• Vat photopolymerization (SLA/DLP): particle-filled resins are common, but short/continuous fibers are difficult to orient and keep uniformly suspended; increased viscosity and optical scattering reduce cure depth and can create partially cured interlayers. Agglomeration and sedimentation drive spatially varying stiffness, residual stress, and microcracking; surface functionalization and rheology control (thixotropy) are typically required for stable printing.[16]

• Material extrusion (FFF/DIW): shear during extrusion and raster/toolpath design can deliberately align short fibers and place continuous fibers, but dispersion depends strongly on compounding quality (fiber breakage, nozzle filtering, and clogging). The dominant bonding limitation is interlayer welding/diffusion across bead interfaces; fiber-rich boundaries reduce intimate contact and increase voids, leading to anisotropic *Z*-strength unless thermal management (preheating/closed chamber) and consolidation are used.[61,62]

• Powder bed fusion (PBF): for particle-reinforced systems (polymers or MMCs), 'dispersion' is largely set by powder preparation; density/size mismatches cause segregation and reinforcement clustering, which can be exacerbated by melt-pool flow. Bonding is governed by wetting, interfacial reactions, and thermal gradients; lack-of-fusion porosity and hot cracking are key risks, especially when reinforcement alters absorptivity or melt viscosity.[63]

• Binder jetting (BJT): orientation control is minimal (powder-based), so reinforcement architecture is driven by powder morphology and post-processing. Dispersion is sensitive to segregation during recoating and to binder saturation/migration; bonding quality is determined primarily during sintering/infiltration, where differential shrinkage and incomplete densification often dominate final porosity and strength.[64,65]

• Material jetting (MJT): composite 'inks' require long-term dispersion stability (no sedimentation), tight viscosity

Table 2 CAM processes, their classification, and comparison

Processing techniques	Classification	Methods	Base material types	Typical resolution	Re.
Vat photopolymerization	Stereolithography Digital light processing Continuous digital light processing/continuous liquid light processing	Laser treatment Cured with a projector Rehabilitate with LEDs and oxygen	Photopolymer resin (ceramic, metallic, and composite filler)	1–100 μm	13, 16, 54 and 55
Material jetting	Material jetting Nanoparticle jetting Drop on demand	UV treatment Heat treatment Milled to form	Metals, ceramics, polymers, hybrids, and biomaterials	10–25 μm	13 and 54–56
Binder jetting	Binder jetting	Joined by a bonding agent	Ceramics, metals, biomaterials, polymers, composites, and alloys	~100 μm	13, 54, 55 and 57
Material extrusion	Fusion deposition modeling	Filament feeding through the nozzle and extruder is continuous	Polymers and composites	100 μm–1 cm	13 and 52–55
Sheet lamination	Laminated object manufacturing Ultrasonic AM	Adhesives used for bonding Lower temperatures than the melting temperature of raw materials and the normal force used for bonding	Polymers, metals, ceramics, and hybrids	200–300 μm	13, 54, 55, 58 and 59
Powder bed fusion	Direct laser metal sintering Selective laser sintering Direct metal laser sintering/selective laser melting Electron beam method	Fused with agent and energy Laser fusing Laser fusing Fused with an electron beam	Polymers, metals, ceramics, and composites	50–100 μm	13, 51 and 54–56
Direct energy deposition	Laser engineering net shape Electron beam AM	Fused with a laser Fused with an electron beam	Metal and metal hybrids	100 μm–1 cm	13, 54–56 and 60

Open Access Article. Published on 19 June 2026. Downloaded on 6/19/2026 11:23:52 PM.
This article is licensed under a Creative Commons Attribution 3.0 Unported Licence.

Table 3 A comparison of AM methods and their composite-specific processing challenges (fiber orientation, dispersion, and bonding)

ISO/ASTM category	Representative methods	Fiber orientation and reinforcement control	Dispersion/feedstock challenges	Bonding/interface challenges	Typical defects and key refs	Ref.
Vat photopolymerization (VP)	SLA, DLP, CLIP	Mainly particulate fillers, fiber alignment is difficult (limited to short fibers/field-assisted alignment)	Filler sedimentation, viscosity rise, light scattering/absorption can inhibit cure, and agglomeration	Reduced degree of conversion near fillers, cure shrinkage stress, weakened interlayer adhesion if cure is incomplete	Agglomerates, cure-inhibited zones, voids/microcracks	16, 39 and 71–75
Material extrusion (ME)	FFF/FDM, DIW	High: shear + toolpath/raster control aligns short fibers, continuous-fiber placement possible	Compounding quality, nozzle clogging, fiber breakage, filler filtration, rheology/temperature window	Interlayer diffusion/welding limits strength, fiber-rich interfaces reduce intimate contact, void formation	Porosity + weak *Z*-bonds, warpage	61, 62, 69 and 76–82
Powder bed fusion (PBF)	PBF-LB/EB (metals), SLS (polymers)	Low for fibers, particles distribute *via* powder prep, but melt-pool flow can cause clustering/segregation	Powder segregation (density/size), reinforcement clustering, spatter/denudation	Wetting + interfacial reactions (MMC), lack-of-fusion, residual stress cracking	LOF porosity, unmelted clusters, cracks	63, 71 and 83–86
Binder jetting (BJT)	Binder jet + sinter/infiltrate	No intrinsic orientation control (powder-based)	Powder segregation, binder saturation non-uniformity, binder migration	Limited green strength, sintering shrinkage, infiltration/impregnation quality governs bonding	High porosity, distortion, and weak interfaces	64 and 65
Material jetting (MJT)	PolyJet, NPJ/MJM	Typically, none; multi-material voxel placement possible (reinforcement mostly particulate)	Ink/dispersion stability, particle sedimentation, nozzle clogging, droplet consistency	Droplet coalescence + curing, interlayer adhesion for photopolymers, debinding/sintering for metals/ceramics	Voids, delamination, composition gradients	66–68
Directed energy deposition (DED)	Laser DED, WAAM	Limited for reinforcements (usually particles/wires), tracking strategies affect bead geometry	Feed delivery stability, particle entrainment/clustering, dilution control	Metallurgical bonding + remelting, intermetallics/segregation, cracking from thermal gradients	Porosity, dilution/geometry errors, hot cracking	60, 69 and 87–89
Sheet lamination (SHL)/UAM	LOM, UAM/UC	High for sheet/prepreg architectures, UAM enables embedding fibers/foils with controlled layup	Sheet/prepreg uniformity, contamination/oxide layers at interfaces	Adhesive/thermal bonding (LOM) or ultrasonic seam welding (UAM), incomplete welds/voids	Delamination, unbonded interfaces	70 and 90–93

© 2026 The Author(s). Published by the Royal Society of Chemistry

Open Access Article. Published on 19 June 2026. Downloaded on 6/19/2026 11:23:52 PM. This article is licensed under a Creative Commons Attribution 3.0 Unported Licence.

Table 4 Advancement of SLA techniques throughout different generations[71] (open access)

Generation	SLA approaches	Methods	System resolution	Printable size	Printing speed	Light source
1st Gen (1984)	Scanning	Scanned with a focused laser beam to cure resin	~100 nm	10–100 mm	100–1000 mm s^{-1}	UV lights
2nd Gen (1988)	Projection	Projected UV radiation through masks and a piece of flat transparent material simultaneously on the resin	>5 microns	10 mm	10 mm $hour^{-1}$	UV/visible light
3rd Gen (2015)	Continuous	Continuous manufacturing, where cured resin gets mechanically moved and replaced by uncured resin	>5 microns	10 mm	100 mm $hour^{-1}$	UV/visible light
4th Gen (2016)	Volumetric	Directed image subcomponents beam orthogonally at the resin volume	80–300 microns	10 mm	$>10^5$ mm^3 $hour^{-1}$	UV light

windows, and clog-resistant nozzles. Bonding depends on droplet coalescence and curing/solidification (or debinding/sintering for nanoparticle jetting), making interlayer adhesion and trapped-void control central to part integrity.[66–68]

• Directed energy deposition (DED/WAAM): reinforcement control is typically limited to particle or wire feeding; dispersion depends on stable delivery and mixing in the melt pool. Bonding is metallurgical *via* remelting but can be compromised by dilution, segregation, and intermetallic formation at the reinforcement–matrix interface; steep thermal gradients drive residual stress and increase the risk of cracking.[69]

• Sheet lamination/ultrasonic AM (LOM/UAM): when sheets/prepregs define reinforcement architecture, orientation control can be excellent, but bonding is interface-limited: adhesive/thermal bonding (LOM) and oxide/contaminant disruption plus plastic flow (UAM) determine interlayer integrity. Unbonded regions and delamination remain the principal quality threats and require optimization of process parameters and surface preparation.[70]

3.2 Stereolithography

The devices used for AM are generally unable to receive information from 3D CAD files, which contain the objects' design and geometry. Therefore, the CAD files are converted to stereolithography (STL) files, which approximate the 3D model using the simplest triangles and polygons. Secondly, a computer program defines and slices the 3D model into cross-sections. Then, finally, these cross-sections are fabricated and combined to form the 3D model.[4,94,95] Over the years, the SLA technique has made great progress, as evidenced by its approaches, as presented in Table 4.

Volumetric SLA is a recent development in this process, which was introduced by Shusteff *et al.*[32,96] based on holographic lithography. In a volumetric SLA system, the overlapping of patterned optical fields from three orthogonal beams is projected onto a photosensitive resin. By measuring the counterbalance between each beam, 3D geometries can be generated from a single exposure of the intersected profile. Fig. 2(a) illustrates silicon spatial light modulators (SLM), beam blocks to eliminate un-diffracted light (BB), Fourier transform lenses (FLT), hologram planes (HP), ''4-f'' configured telescope lens pairs for beam expansion, pinhole spatial filters (4fn), and 45° prism mirrors for directing image subcomponent beams orthogonally into the resin volume.[32,71]

Further research was conducted on the dual-wavelength process (Fig. 2(b)) to understand volumetric SLA.[97] Furthermore, Kelly *et al.*[72] and Loterie *et al.*[73] proposed a promising volumetric SLA technique based on tomographic reconstruction (Fig. 2(c)). The researchers showed that in tomographic volumetric SLA, simultaneous irradiation is used to expose the entire volume of photosensitive resin. As shown in Fig. 2(c and d), computed light patterns are projected from the side into the rotating cylindrical resin container. The process of light pattern computation using the Radon transform is comparable to topography, and it is presented in synchronization with the resin container's circular movement. In order to create the desired objects, a volume of resin must locally exceed its gelation threshold due to the 3D distribution of the collected light dose (Fig. 2(e and f)).[71]

Volumetric SLA enables the fabrication of complex composite geometries in a single unit operation, making the process faster than other approaches (*e.g.*, scanning, projection, and continuous) that use a layer-by-layer approach. In layer-by-layer approaches, the planarization time and resin surface settling time are slower, which allows the fluid–air interface to create oxygen-concentrated gradients in the object, whereas volumetric SLA can help overcome these bottlenecks.[96] In contrast, studies have shown that multiple SLA approaches can be combined to produce high-performance objects. For instance, researchers have used both scanning and projection approaches in SLA and successfully fabricated 3D structures with higher resolution.[71,98]

3.3 Binder jetting

Patented by Emanuel Sachs in 1993, binder jetting (BJT) was initially developed at the Massachusetts Institute of Technology by using gypsum-type powder and bubble inkjet print heads that deposited binders (*i.e.*, glycerin or water). The method has not been fundamentally changed to date.[33,57] Therefore, the method can be used to manufacture ceramic matrix composites.[99–101] According to ASTM F2792, powder materials are joined selectively using liquid bonding agents in the BJT

Open Access Article. Published on 19 June 2026. Downloaded on 6/19/2026 11:23:52 PM.
This article is licensed under a Creative Commons Attribution 3.0 Unported Licence.

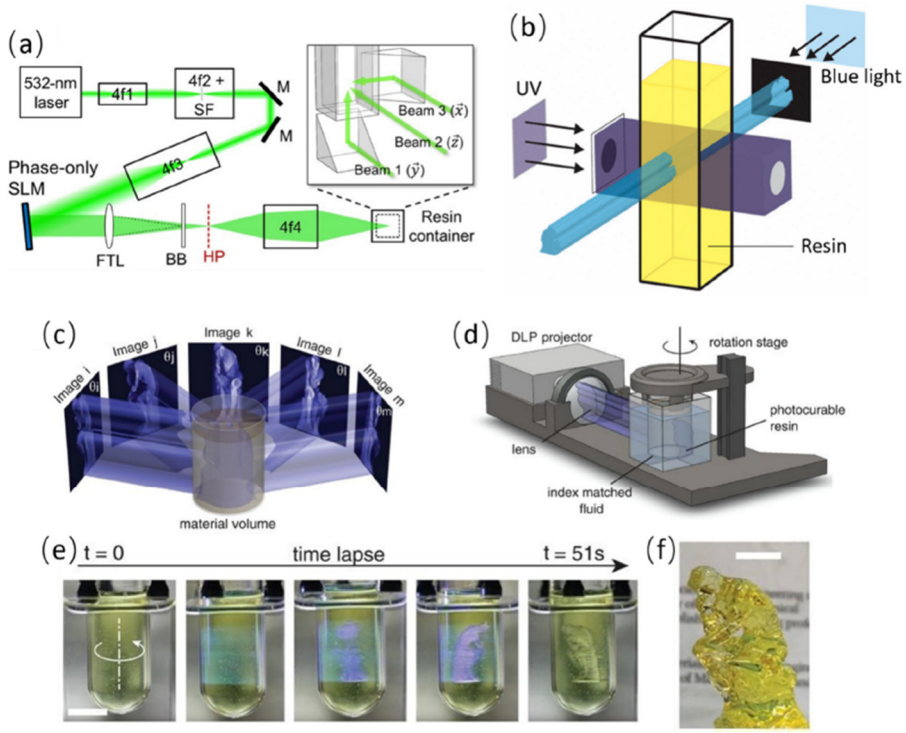

Fig. 2 Schematic diagram of (a) first volumetric SLA, (b) dual-wavelength volumetric polymerization, and volumetric tomographic SLA (c) conceptual diagram, (d) device, and (e) sequential view of the fabrication by volumetric SLA, and (f) fabricated geometry. Adapted from ref. 71 (open access).

process. Afterward, the layers are joined to form a solidified structure in which powders are arranged in the desired 3D geometry.[57] In this process, a small amount of base material is delivered by the print head, while the majority remains in the powder bed. Typically, the binder droplets (~80 μm in diameter) form spherical agglomerates of binder liquid and powder particles while providing bonding strength to the previously printed layer.[56] The schematic diagram of the BJT is shown in Fig. 3.

After printing 3D geometry with BJT, a series of postprocessing operations (Fig. 4) is required. Firstly, the manufactured structure may need to be heated to cure the binder, followed by a de-powdering process to remove excess parts from the powder bed. At this stage, the removed part of the powder bed is called "green" and is not suitable for end use. Following this, infiltration or sintering is performed to achieve desirable mechanical properties, making the greens suitable for end use.[33,57] The post-curing process strengthens its greens and dries the binder.[57] Curing processes (*e.g.*, thermal curing, drying, salt-based binder reduction, and preceramic polymer conversion) should be selected depending on the binder chemistry to produce high-quality products.[33] Generally, the powder bed is detached from the printer during curing. The binder is then heated to dryness, allowing the green geometries to be removed from the powder bed.[33,57] In this process, the "build box" containing the printed parts and the powder bed is heated in an oven to 180–200 °C for hours, depending on the binder characteristics and the build volume. Then the loose powder is removed from the build box by manual brushing and vacuuming. As a result, green geometry becomes loosely bound and is immediately taken to the densification stage, known as sintering or infiltration.[57]

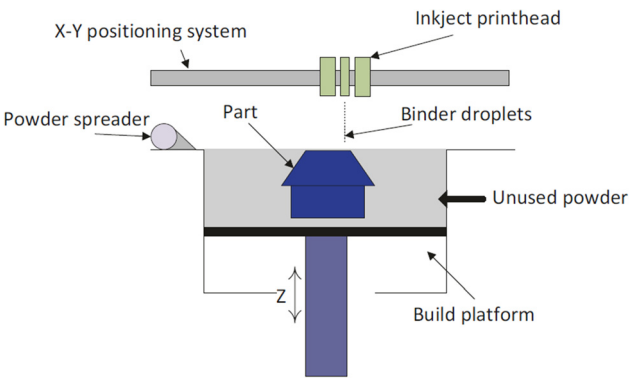

Fig. 3 Schematic diagram of the BJT process. Adapted from ref. 102 (reused with permission, license number 5826971245184).

Green geometries typically obtain 50–60% density after curing and de-powdering. Microscopically, the powder particles at this stage are bound to the polymer at the particle contact points. At this point, desired mechanical properties and density can be achieved through various densification methods, including sintering and infiltration. Before any densification method, a burn-out step at ~600–700 °C is performed to fully pyrolyze the binder. Although sintering characteristics may vary from material to material, practically, they can be controlled by using mixed powders of various sizes and a sintering aid with coated

© 2026 The Author(s). Published by the Royal Society of Chemistry

Open Access Article. Published on 19 June 2026. Downloaded on 6/19/2026 11:23:52 PM.
This article is licensed under a Creative Commons Attribution 3.0 Unported Licence.

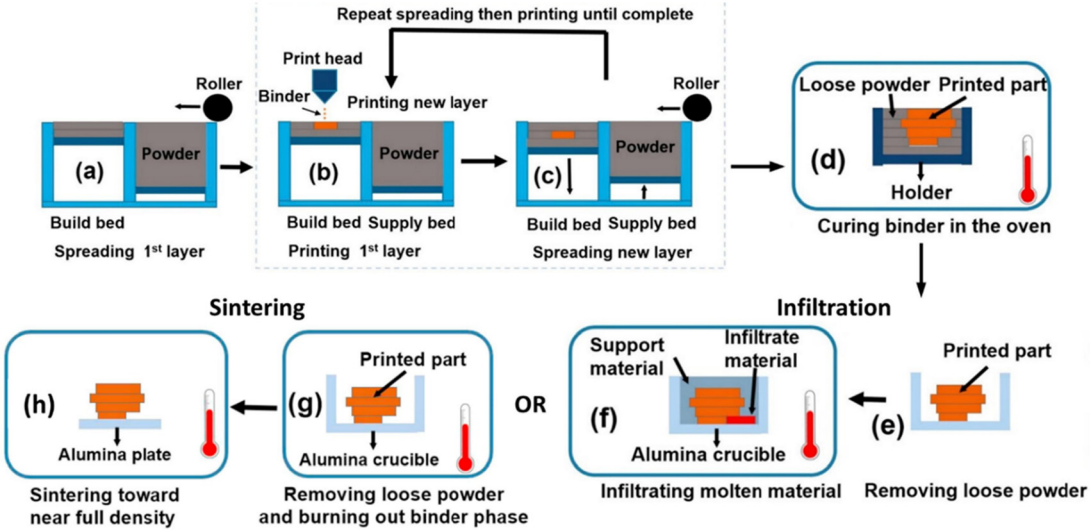

Fig. 4 Schematic diagram of BJT AM and post-processing processes (a) first layer and the foundation preparation, (b) and (c) printing process, (d) binder curing process in the oven, (e) de-powdering followed by the infiltration process, (f) infiltration process, (g) de-powdering followed by sintering, and (h) sintering process in the supervised atmosphere. Adapted from ref. 57 (open access).

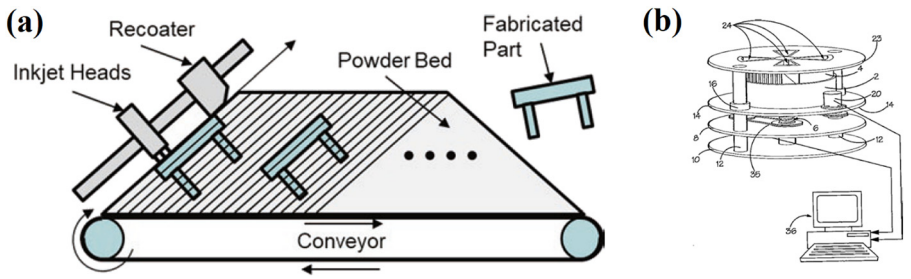

Fig. 5 Schematic diagram of (a) continuous BJT and (b) spiral growth BJT machine, adapted from ref. 102 (reused with permission, license number 5826971245184).

particles. Therefore, densification strategies become different for metals, ceramics, and polymer composites. In addition, design considerations (*i.e.*, section size and part orientation) are crucial for effectively removing bindings and avoiding slumping during sintering.[33,57] According to Mostafaei *et al.*,[57] the average roughness of the fabricated part is about 6 μm after preprocessing. After preprocessing, surface finishing is a common practice. Common surface-finishing techniques include tumble polishing, bead blasting, machining, plating, extrude-horning, and hand polishing.[57]

Although the working principle of most of the commercially available BJT printers remains fundamentally unchanged since their invention, two different types of BJT approaches have been developed in recent years (Fig. 5). In 2013, a German-based machine-industry company, Voxeljet, introduced a strategy based on linear translation of the fabricated part (Fig. 4 (a)). Another approach, known as spiral growth BJT manufacturing, was developed by researchers at the University of Liverpool, United Kingdom, in the early 2000s (Fig. 4(b)). In the Voxeljet, the build surface of the powder bed is 30° inclined, which is less than the critical angle of the powder's repose. BJT and recoating of the powder are carried out on this build surface. In contrast, the spiral BJT printer has four build stations, and printing is performed by rotating the machine plates.[56,102]

3.4 Fused deposition modeling

Fused deposition modeling (FDM) is the most widely used material-extrusion-based AM method,[53] invented in 1989 by Scott Crump, co-founder of Stratasys, a USA-based manufacturer of 3D printers, software, and materials for polymer AM. In FDM, thermoplastic polymers such as acrylonitrile butadiene styrene (ABS), polycarbonate (PC), and polylactic acid (PLA) are used as base materials. As shown in Fig. 6, the extrusion head of the FDM machine is directly connected to the roller where filaments are stored. The extrusion head has motions in the *X*, *Y*, and *Z* directions, where only the build platform moves. Generally, two types of filament materials (*i.e.*, built material and supporting material) are used for FDM, with a typical diameter of 1.75–3 mm.[103,104] Pre-processing, production, and post-processing are the three stages of the FDM manufacturing technique.[104]

Open Access Article. Published on 19 June 2026. Downloaded on 6/19/2026 11:23:52 PM.
This article is licensed under a Creative Commons Attribution 3.0 Unported Licence.

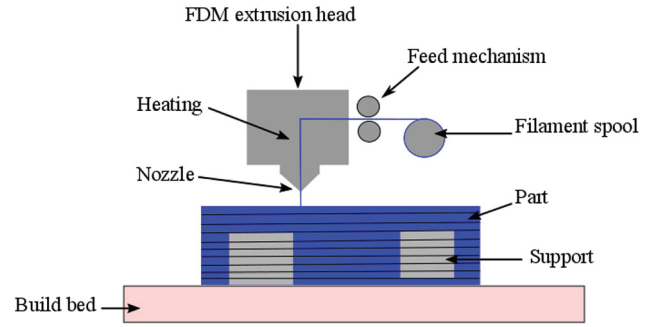

Fig. 6 Schematic diagram of FDM. Adapted from ref. 103 (open access).

The feedstock material attached to the extrusion head is heated to a semi-liquid state before printing begins. Then, 2D layers are stacked on the build platform until the required 3D geometry is fabricated. The filament temperature during printing remains between 150 and 300 °C, and the dimensional printing accuracy is 100 μm.[104] Despite higher accuracy and lower cost, simple post-processing is required to prepare FDM-printed parts for end use.[53,104] According to Kumbhar and Mulay,[105] the main objective of post-processing in FDM is surface finishing using chemical (*i.e.*, heating, coating, and vapor deposition) and mechanical (*i.e.*, sanding, machining, abrasive, barrel, and vibratory finishing) processes. Based on the feed mechanism and the extrusion head, FDM can be classified into three types: single-head, dual-head, and in-nozzle impregnation (Fig. 7a).[54,106] The single-head FDM method is a traditional CAM approach that uses only one filament.[104] However, single-head FDM can print just one material system at a time, and the processing temperature is relatively high. In contrast, dual-head FDM can print two material systems simultaneously, making it suitable for polymer composite manufacturing. The in-nozzle FDM process is the most recent development of FDM technology, in which the nozzle head is reinforced with the heated material to improve mixing and fiber incorporation into the polymer matrix.[54] Regardless of the specific method, FDM can manufacture composite structures efficiently and at relatively low cost; however, as-built surfaces commonly require chemical or mechanical post-processing, and interlayer bonding is often limited by diffusion/welding across bead interfaces, especially when fiber-rich regions reduce intimate contact and promote void formation.[53,61,62,107–109] An iron-ABS composite material manufactured using the FDM technique is shown in Fig. 7b and c.

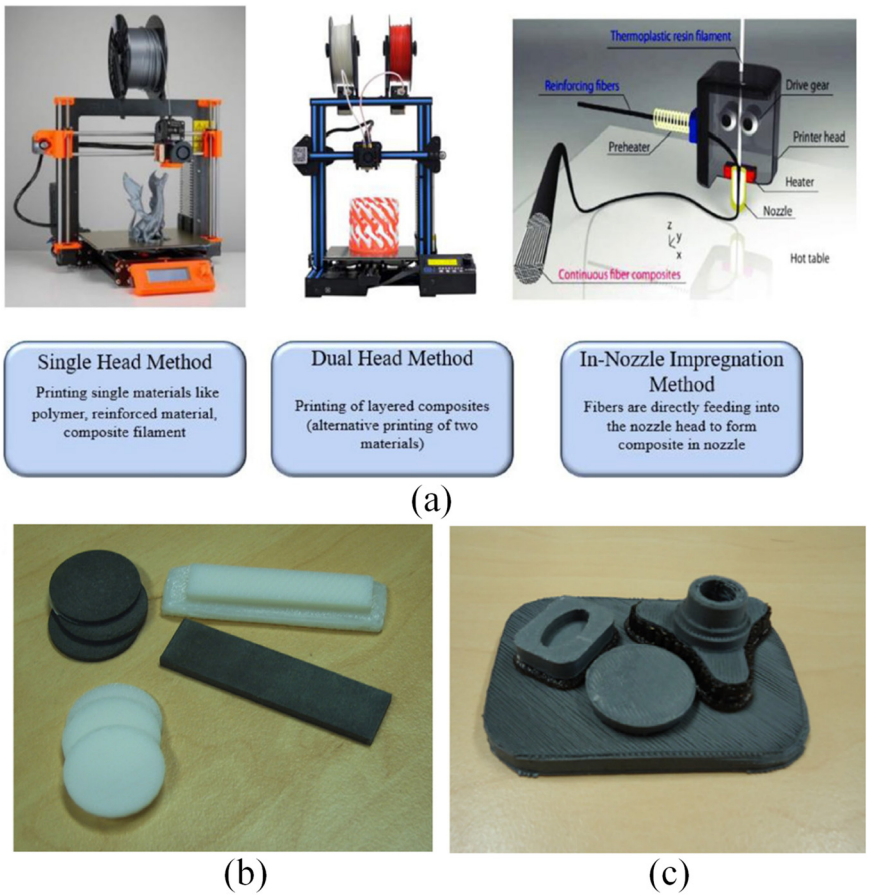

Fig. 7 (a) Different types of FDM methods, adapted from ref. 104 (reused with permission, license number 5826980222657). (b) ABS (white colored) and iron-ABS (black colored) test sample, and (c) Iron–ABS composite structure manufactured using the FDM technique, adapted from ref. 107 (reused with permission, license number 5827071030726).

© 2026 The Author(s). Published by the Royal Society of Chemistry

Open Access Article. Published on 19 June 2026. Downloaded on 6/19/2026 11:23:52 PM.
This article is licensed under a Creative Commons Attribution 3.0 Unported Licence.

3.5 Selective laser sintering

Developed by Carl Deckard in 1989,[110] selective laser sintering (SLS) is a process that uses a selective laser beam to irradiate and solidify the powder material in layers to manufacture complex geometries. In this process, powder materials are preheated to a high temperature before irradiation through a laser beam. The preheating temperature is controlled below the softening temperature of the polymer materials to avoid powder amalgamation. Then the laser is used to heat and selectively solidify the powder material to the sintering temperature. Later, the powder temperature is allowed to decrease gradually after the completion of the sintering process.[111–113] The three steps of the SLS process are illustrated in Fig. 8. The fundamental principle of SLS is quite simple, and it is a cost-effective and feasible technique. In various AM techniques (*e.g.*, FDM, material jetting, and SLA), a support structure is essential, whereas in SLS it is not required, which is considered a critical advantage. This advantage arises because the unsintered powder surrounding the part acts as a self-supporting medium due to powder packing and thermal stability, so separate support structures are typically unnecessary.[112] There are other advantages of SLS, such as durability, an economical and fast process, the ability to manufacture complex and large parts, the production of watertight and sterilizable parts, material versatility, and high printing accuracy.[110] Some SLS-manufactured composite materials are illustrated in Fig. 9.

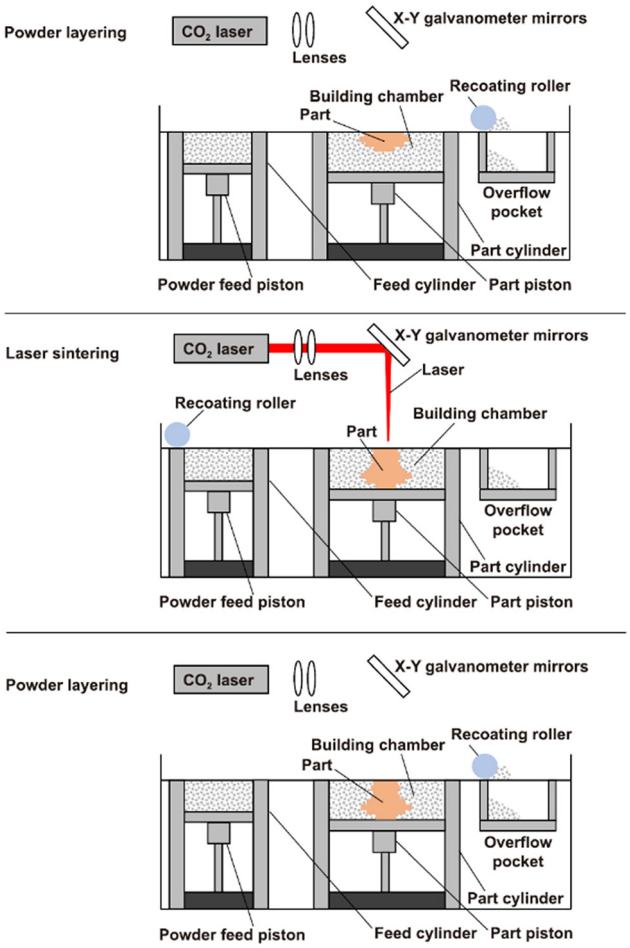

Fig. 8 Schematic diagram of SLS. Adapted from ref. 112 (open access).

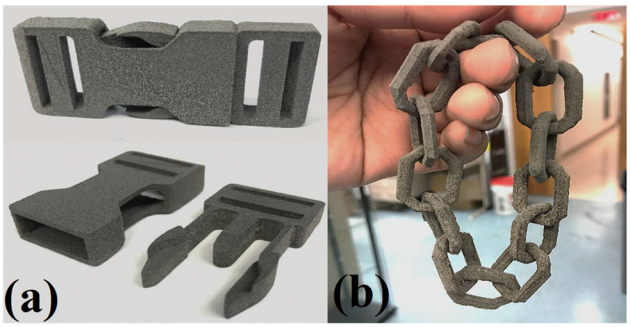

Fig. 9 Composite parts manufactured by SLS; (a) two-part buckle and (b) circular chain, adapted from ref. 112 (open access).

3.6 Direct energy deposition

The direct energy deposition (DED) process uses a focused thermal energy source to melt materials and deposit them to form structures. The basic principle of DED is the formation of material through the combined operation of cladding and welding, using either powder or wire feeding techniques (Fig. 10). Firstly, the adjacent layer of filament material is targeted by the specific thermal energy (*i.e.*, laser, electron beam, or welding heat flux). The targeted zone of thermal energy is then simultaneously supplied with a feedstock containing various types of wires and powders, in the presence of an inert gas. The feedstock and the adjacent layer are both melted in and around the region of concentrated thermal energy, forming a molten pool.[114,115] Moreover, the process can be categorized into wire and powder feeding types based on the feedstock. In wire-feeding processes, a wire is used as feedstock for a plasma arc, and the electron beam, electric

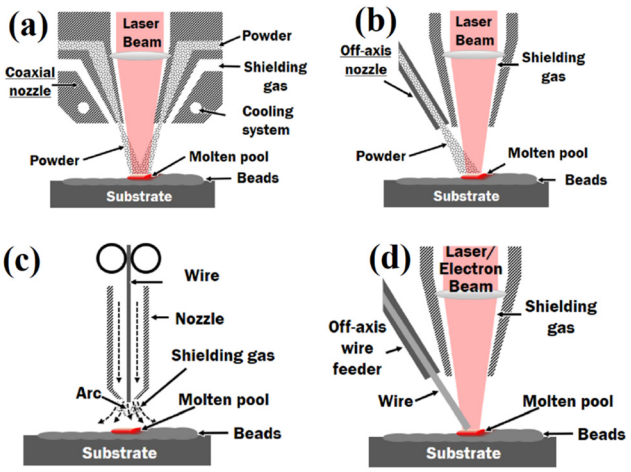

Fig. 10 Schematic diagram of different DED processes showing powder feeding in (a) co-axial direction, (b) off-axis direction, and wire feeding in (c) co-axial direction, (d) off-axis direction. Adapted from ref. 114 (open access).

Open Access Article. Published on 19 June 2026. Downloaded on 6/19/2026 11:23:52 PM. This article is licensed under a Creative Commons Attribution 3.0 Unported Licence.

arc, and laser are used as sources of thermal energy. However, only a laser is used as the thermal energy source for powder-feeding processes.[60,114] This process is highly adaptable for the deposition of high-performance materials, including alloy steels, titanium-based alloys, stainless steels, tool steels, cobalt-based alloys, nickel-based alloys, intermetallics, shape memory alloys, aluminum alloys, high-entropy alloys, ceramics, functionally graded materials, and composites.[60,115,116] Nevertheless, the properties and quality of parts manufactured by DED depend on the category of DED process, interactions between beams and materials, environment of the printing process (*i.e.*, inert gas, vacuum, or ambient), parameters of deposition (*i.e.*, hatch spacing, powder feed rate, laser powder, laser scan speed, and laser scan strategy), and attributes of the feedstock.[116]

DED can also be described in terms of solidification parameters, because bead geometry alone does not determine the microstructure of a deposited composite or metal-matrix build. At the solid–liquid interface, the thermal gradient, G, and local solidification rate, R, determine growth-front stability. A high G/R ratio favors planar or cellular front stability, whereas a lower G/R ratio increases constitutional undercooling and promotes cellular-dendritic or equiaxed dendritic growth, depending on alloy chemistry, nucleant availability, flow, and thermal history.[116–118] The product $G \times R$ is the local cooling rate and is commonly related to cell or dendrite-arm spacing, with higher cooling rates producing finer microstructural length scales.[116,117] In DED of MMCs, these quantities are especially important because reinforcement particles or *in situ* reaction products alter melt viscosity, absorptivity, convection, nucleation, and solute redistribution. As a result, changes in laser power, scan speed, layer reheating, powder or wire feed rate, and shielding conditions can shift the G/R ratio and thereby affect columnar-to-equiaxed transition behavior, dendritic growth, segregation of alloying elements or ceramic reinforcements, and interfacial reaction layers.[116–119] Consequently, DED process maps for CAM should not report only nominal heat input and bead dimensions; they should also include, where possible, measured or simulated G, R, G/R, and $G \times R$ values linked to microsegregation, dendrite spacing, reinforcement distribution, residual stress, and cracking susceptibility. In addition to manufacturing new components, DED is widely used for repair and remanufacturing applications, which can extend component service life and reduce environmental impact.[60,115] Owing to these advantages, DED has gained increasing attention in defense, aerospace, biomedical, and automotive industries.[115]

3.7 Hybrid printing and multi-material systems in CAM

Beyond single-material architectures, contemporary CAM is increasingly driven by hybrid printing and multi-material additive manufacturing (MMAM), which enables spatial control over composition, architecture, and interfaces that is difficult to achieve with monolithic builds. In the strict sense, MMAM refers to the deposition of two or more distinct materials within a single layer or build platform, whereas hybrid manufacturing integrates additive, subtractive, and sometimes forming or joining steps into a single process chain. Recent reviews[120–125] show that multi-material capability is available across almost all major AM modalities, including material extrusion, material jetting, vat photopolymerization, powder-bed fusion, and directed energy deposition. This significantly expands the design possibilities for architected composites compared to single-material processes. Multi-material metal AM, as per the ASTM F2792-12a standard, is shown in Fig. 11.

In polymers, multi-nozzle and single-mixing-nozzle material-extrusion platforms enable sharp or graded transitions between stiff and compliant filaments (*e.g.*, PLA/TPU, PLA/ABS, and PEEK-based systems), as well as between filled and unfilled filaments.[124,126] For example, Baca and Ahmad[127] compared multi-material FDM using a single mixing nozzle *versus* multiple nozzles and reported that interface design and nozzle strategies can change ultimate tensile strength by ~15–30% and strongly affect failure points at material boundaries. Sequential multimaterial printing of functionally graded biopolymer composites has been used to mimic bio-inspired architectures with continuous variations in stiffness, demonstrating that mechanical gradients (*e.g.*, modulus variations of a factor ~3–5 across the structure) can be encoded directly *via* toolpath and feedstock scheduling rather than post-processing.[122,128] In the context of CAM, such platforms are particularly attractive for tailoring local fiber volume fraction, embedding continuous or discontinuous fibers only where load paths demand them, and introducing sacrificial or soluble phases to generate vascular or porous networks.

Vat-photopolymerization and inkjet-based systems have also been extended to multi-material composites. Multi-vat vat-photopolymerization has enabled graded ceramic suspensions, permitting spatial control of ceramic loading and thus local stiffness and sintered density within a single part.[129] Similarly, direct ink writing (DIW) has been used to co-print multi-material reactive composites, where a structural matrix is locally co-deposited with energetic or functional phases; these studies highlight that tuning interface geometry and the sequence of material deposition can change measured compressive strength and energy-release characteristics by more than an order of magnitude.[130] At the structural scale, multi-material AM of Ti-, Mg-, and Fe-based alloys has been explored for graded biomedical implants, where compositionally graded interfaces reduce local stress concentrations and improve fatigue performance relative to sharp bi-metal transitions fabricated by conventional joining.[123,131]

Hybrid additive–subtractive manufacturing adds another layer of flexibility for CAM. In hybrid systems, material deposition (*e.g.*, directed energy deposition or laser powder-bed fusion) is interleaved with high-precision milling or turning, enabling near-net-shape deposition of difficult-to-machine composites followed by local machining to achieve tight tolerances and improved surface integrity. Hybrid metal AM can achieve relative densities ≥99.5%, fatigue strengths comparable to wrought alloys, and machined surface roughness (R_a) below ≈1–2 μm, while reducing total process time by 20–40%

© 2026 The Author(s). Published by the Royal Society of Chemistry

Open Access Article. Published on 19 June 2026. Downloaded on 6/19/2026 11:23:52 PM.
This article is licensed under a Creative Commons Attribution 3.0 Unported Licence.

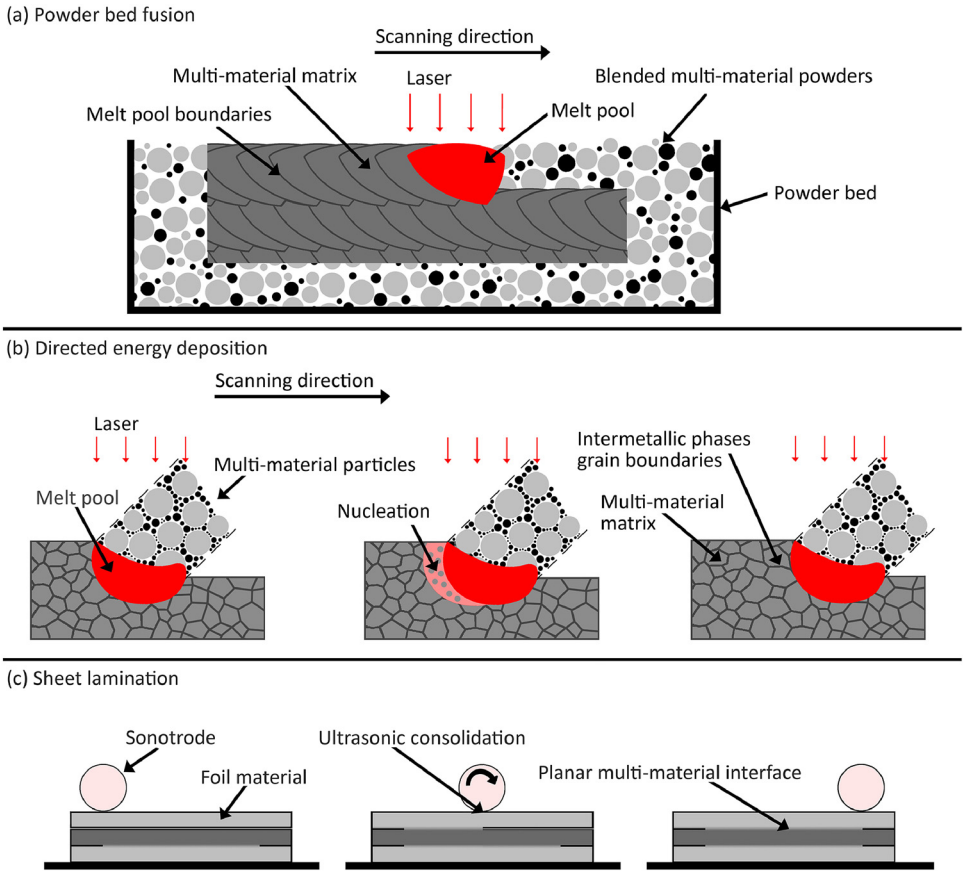

Fig. 11 Laser and ultrasonic multi-material AM for metals according to the process classifications of ASTM F2792-12a: (a) powder bed fusion, (b) directed energy deposition, and (c) sheet lamination, adapted from ref. 122 (open access).

compared with sequential AM followed by stand-alone machining.[132–136] For fiber-reinforced systems, hybrid routes are particularly relevant when continuous fibers are locally interrupted for inserts or load-transfer features, since *in situ* machining can re-establish the designed surface quality and geometry at these interruptions. Hybrid AM also synergizes with the machine-learning-driven process-planning strategies, because data from both additive and subtractive stages (*e.g.*, in-process metrology, cutting forces, and tool wear) can be fused to close the loop on part-quality prediction across the entire composite process chain.

Despite these advances, challenges remain in hybrid and multi-material CAM relevant to structural reliability. First, thermal and elastic mismatches at material or phase boundaries can lead to interfacial residual stresses, delamination, and microcracking; interfacial strength reduction of 10–40% can occur when high-modulus and low-modulus polymers are sharply juxtaposed without designed transition zones.[121,122] Second, process planning and path scheduling for MMAM and hybrid machines are far from mature: multi-objective optimization should simultaneously consider collision-free toolpaths, support-free deposition of overhangs, thermal management across dissimilar materials, and accessibility for *in situ* machining, all under manufacturing time and cost constraints.[135] Addressing these multi-physics, multi-material interactions and quantifying their influence on long-term fatigue, creep, and environmental durability remains a critical frontier for achieving reliable CAM components in safety-critical applications.

3.8 Quantitative performance metrics and benchmarking for CAM processes

Quantitative performance metrics allow a more objective comparison between processes. For CAM, such metrics should span (i) mechanical performance (tensile, flexural, interlaminar, and fatigue properties), (ii) physical metrics (density and porosity), (iii) geometric and surface metrics (dimensional accuracy and roughness), and (iv) process and productivity metrics (build rate, energy input, and throughput). Reporting only qualitative advantages (*e.g.*, "high design freedom") is insufficient; instead, process–structure–property relationships should be framed using consistent, experimentally measured ranges.[137]

For material-extrusion-based polymer composites, mechanical properties are now well-quantified. A study[138] reported tensile strengths of 36.5–70 MPa and elastic moduli of ~1.1–4 GPa for FDM-printed PLA, depending on print orientation and process parameters, with compressive strengths of 31–80 MPa. A process-parameter study[139] in polymers showed that,

Open Access Article. Published on 19 June 2026. Downloaded on 6/19/2026 11:23:52 PM. This article is licensed under a Creative Commons Attribution 3.0 Unported Licence.

for PLA, increasing the infill to 100% and optimizing the layer thickness ($\approx$0.2–0.4 mm) yield tensile strengths of 45–50 MPa, whereas lower infill fractions and coarser layers can reduce strength by 30–40%. Comparative experiments across PLA, ABS, PETG, and PEEK indicated that, under comparable FDM conditions, PLA and PETG typically show higher tensile and compressive strengths than ABS, whereas PEEK exhibits superior stiffness but is more sensitive to processing temperature and crystallinity; analysis of variance consistently identifies infill percentage and layer thickness as the dominant factors governing tensile and flexural response.[140] In addition, Kargar and Ghalebahman[141] reported that sub-optimal raster orientations can reduce fatigue life by more than an order of magnitude at a fixed stress amplitude, even when static tensile strengths differ by less than 20%. These data highlight the need to report mechanical anisotropy ratios (*e.g.*, strength parallel *vs.* perpendicular to build layers) and S–N behavior, not only single-point strengths.

For powder-bed fusion of polymers, quantitative benchmarks are emerging as well. SLS- and MJF-processed PA12 routinely achieve tensile strengths around 45–50 MPa and moduli of $\sim$1.5–1.8 GPa, with differences in tensile and flexural strengths between SLS and MJF of only a few percent when process windows are optimized.[142] Another study[143] on PA12 powder composition and reuse showed that entirely virgin powder can deliver tensile strengths of $\approx$46 MPa and an as-built R_a of $\approx$10–11 μm. In contrast, increased recycled content leads to reduced strength and higher roughness, demonstrating a clear trade-off between sustainability and part performance. Importantly, these works couple mechanical metrics with geometric and productivity indicators: for example, in manufacturing PA12 forearm orthoses, SLS and MJF yield statistically similar tensile and flexural strengths, while MJF offers higher weekly production capacity at fixed mechanical targets and comparable dimensional accuracy.[142] For CAM applications, such coupled metrics (mechanical performance *vs.* throughput and surface quality) are essential to justify process selection beyond simple strength comparisons.

In metallic systems, laser powder-bed fusion (LPBF/SLM) of 316L stainless steel serves as a well-studied reference for high-performance AM. A systematic parameter-optimization study[144] demonstrated that relative densities of 99.6–99.97% are routinely achievable, with yield strengths of 400–420 MPa and an elongation at failure of $\sim$40–42% for optimized parameter sets. Another study[145] reported even higher tensile properties: ultimate tensile strengths of $\sim$650–770 MPa, yield strengths of $\sim$410–580 MPa, and elongations of $\sim$40–46%, depending on energy density and scan strategy, exceeding the performance of many wrought 316L products. At the same time, SLM surface roughness on as-built 316L surfaces is typically an order of magnitude higher than that of machined surfaces (R_a on the order of several micrometres for up-skin surfaces and higher for down-skin) and is strongly affected by laser power, scan speed, hatch spacing, and scan strategy.[146] Multi-objective optimization and machine-learning-based models have therefore moved toward treating relative density, surface roughness, and mechanical properties as simultaneous design objectives, rather than independent quantities.[147]

From a fatigue and defect-tolerance perspective, quantitative metrics are again critical for CAM. AM metals showed that pores, lack-of-fusion defects, and surface notches can reduce high-cycle fatigue strength by 30–60% relative to fully dense, polished specimens, even when static tensile properties are similar.[148] Fatigue-critical design thus requires metrics such as defect size distributions (*e.g.*, maximum pore size and area parameters), near-surface defect densities, and surface topography parameters (S_a, S_z, not just R_a), in addition to conventional S–N curves. For continuous-fiber and short-fiber CAM, these metrics should be enhanced by interfacial measures, such as interlaminar shear strength, mode I/II fracture toughness, and fiber pull-out energy, since the primary failure modes often shift from matrix-dominated to interface-dominated.

Overall, the literature clearly supports (i) the important role of hybrid and multi-material processing routes in expanding the design possibilities for CAM, and (ii) the need to report quantitative performance metrics such as mechanical, geometric, and process-level when comparing processes and designing composite architectures. Integrating these metrics into data-driven process-selection and optimization frameworks is a necessary step toward reliable, certifiable deployment of composite AM in high-value engineering applications.

4. Emerging modeling and simulation techniques of CAM

The properties of additive-manufactured composite materials depend on various processing parameters, such as base materials, layer thicknesses, layer proportions, and reinforcement orientation.[149,150] Therefore, the microstructure of additive-manufactured composites differs from the microstructure of conventionally manufactured composites. Moreover, because the microstructure of composite materials influences the properties of manufactured objects, AM techniques enable the manufacture of composites with higher performance.[151] However, it is essential to determine the optimal processing parameters for manufacturing such composites. In recent years, various modeling and simulation techniques (*e.g.*, representative volume element, moving laser source method, and multi-scale physical modeling) have emerged as convenient methods for optimizing the process parameters of unique and multi-physical CAM processes. Furthermore, such techniques can help determine the effects of reinforcement percentage, reinforcement orientation, fatigue properties, porosity, and laser energy density on composite materials manufactured by the AM.[152]

4.1 Representative volume element method

The representative volume element (RVE) method provides a micromechanical route for linking the heterogeneous microstructure of CAM materials to homogenized properties used in layer- or part-scale simulations. An RVE should be sufficiently

© 2026 The Author(s). Published by the Royal Society of Chemistry

Open Access Article. Published on 19 June 2026. Downloaded on 6/19/2026 11:23:52 PM.
This article is licensed under a Creative Commons Attribution 3.0 Unported Licence.

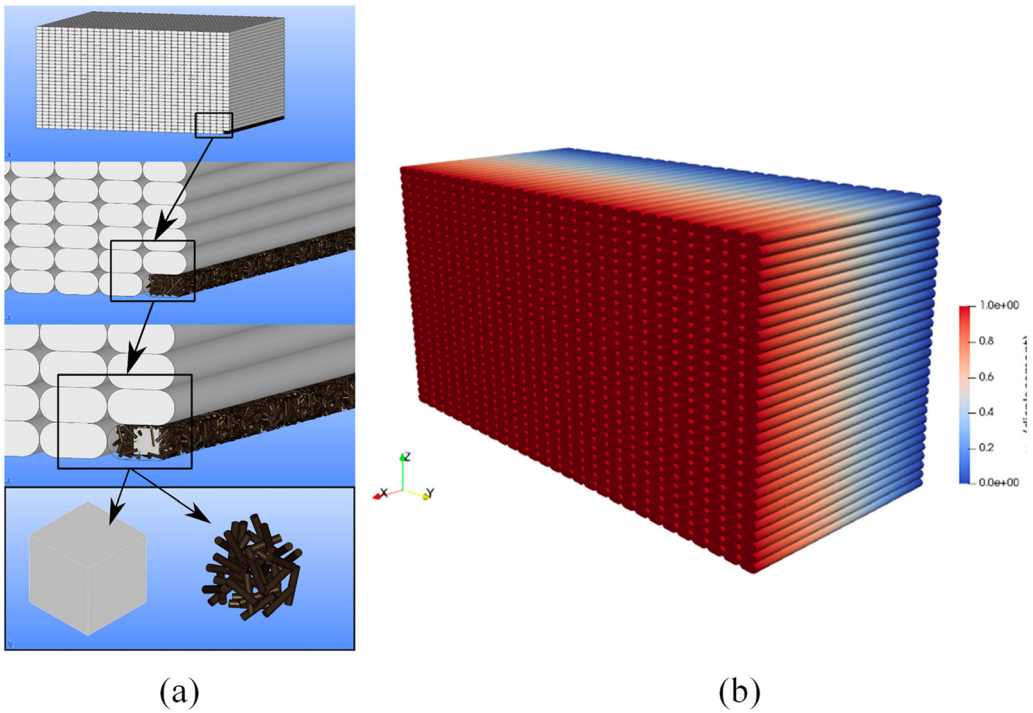

Fig. 12 (a) Step-by-step procedure for developing an RVE model from the layered inner structure of an FDM-manufactured component, and (b) FEM simulation of composite materials is demonstrated at the mesoscale, with one fixed end and the other end shifted by displacement. Adapted from ref. 159 (open access).

large to contain statistically representative microstructural information, yet sufficiently small relative to the macroscopic body to justify continuum homogenization.[152,153] In material-extrusion CAM, this requirement is difficult to satisfy because the printed microstructure is not a simple random or periodic fiber-matrix system. Fiber alignment induced by extrusion, fiber length and volume fraction, bead-to-bead bonding, raster architecture, voids, and interlayer interfaces all contribute to anisotropic and defect-sensitive mechanical behavior.[154,155]

For this reason, idealized RVEs with perfect fiber-matrix bonding, an isotropic matrix, unchanged fiber geometry, and no voids should be interpreted as upper-bound baselines rather than realistic representations of printed composites. Such models are useful for isolating the effects of fiber content, fiber length, and nominal orientation, but they omit process-induced mechanisms that often control stiffness, strength, and failure in CAM parts. Experiments and micromechanical studies show that printed fiber-reinforced thermoplastics can contain inter-filament and intra-filament voids, imperfect impregnation, weak interlaminar bonding, fiber-rich and matrix-rich regions, fiber-orientation heterogeneity, and interfacial damage.[156–160] These features reduce effective stiffness, introduce nonlinear response, and promote debonding, pull-out, interlayer delamination, and anisotropic damage accumulation.[157,161,162]

A more defensible RVE workflow is therefore hierarchical and experimentally informed. First, a void-free, perfectly bonded RVE can be used to establish a reference homogenized response. The model should then be refined using measured microstructural descriptors obtained from microscopy or X-ray microCT, including fiber spatial distribution, fiber volume fraction, orientation statistics, raster-level porosity, and bead-interface geometry.[160,161] Fig. 12 illustrates a hierarchical RVE modelling workflow for FDM/CAM composites, progressing from the layered printed structure to a representative microstructural volume and mesoscale FEM simulation under displacement-controlled loading. Interfacial failure should not be represented solely by displacement and traction continuity at the fiber–matrix boundary. Cohesive elements, cohesive contact formulations, or imperfect-interface conditions can be calibrated from fiber pull-out, microbond, short-beam shear, interlaminar fracture, or inverse-identification tests.[161,163,164] When sizing chemistry, thermal history, or reaction products that produce an interphase with a finite thickness, an explicit interphase layer may be assigned independent stiffness, strength, thermal expansion, and damage parameters; alternatively, finite normal and tangential compliances can be prescribed at the interface.[163,164]

Although these refinements increase computational cost and introduce additional calibration uncertainty, they improve the physical credibility of CAM RVE predictions. The most reliable multiscale strategy is to progress from ideal homogenization to defect-informed RVEs, then transfer the resulting effective properties and damage variables to mesoscale bead, layer, or part simulations. Future work may focus on uncertainty-aware RVE generation, standardized calibration of cohesive and interphase parameters, and validation against

Open Access Article. Published on 19 June 2026. Downloaded on 6/19/2026 11:23:52 PM.
This article is licensed under a Creative Commons Attribution 3.0 Unported Licence.

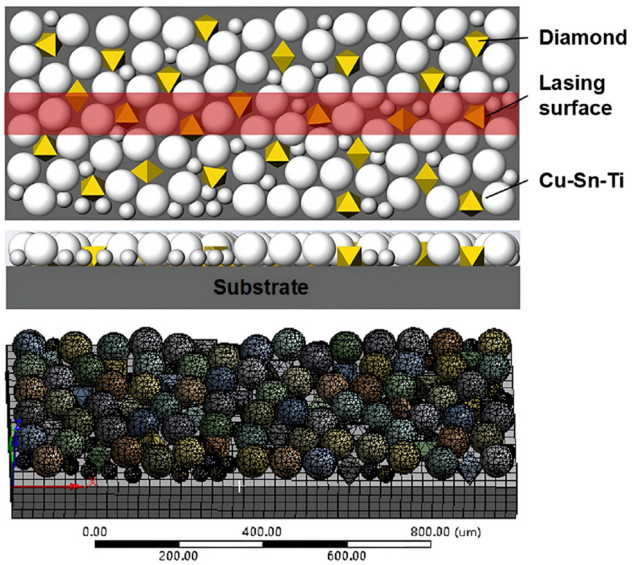

Fig. 13 Model geometry developed in SolidWorks for powder bed AM using a moving laser source. Adapted from ref. 165 (reused with permission, license number 5827071444018).

full-field strain measurements and failure observations across multiple print paths, materials, and loading modes.

4.2 Moving laser source method

Powder bed AM methods, such as SLS and SLM, require simulation to model the spreading of a composite powder layer, which is usually performed in MATLAB or SolidWorks (Fig. 13).[165,166] The position of each spherical particle of composite powders is determined using a random function that complies with the non-overlap criterion. Furthermore, the layer of powders is scanned by a moving laser source, and the laser source simulation is performed using ABAQUS,[167] ANSYS,[165,168] or LAMPS.[168] Then various physical processes involving energy transfer take place, such as the absorption and dispersion of laser light, melting, heat transfer, fluid flow within molten pools, chemical reactions, and evaporation. The particles in the powder bed absorb the laser energy, initiating melting as the temperature reaches the material's melting point.[152]

4.3 Multiscale physical modeling

AM methods, for instance, SLA, are critical processes that require multiscale physical modeling due to the complexity of the entire procedure.[169,170] SLA starts with the addition of fibers to the polymer resin, which increases the intricacy of the required physical processes. Moreover, heat transfer, material solidification, and chemical reactions in the matrix material are usually the foundations of the microscale mathematical model used to simulate SLA printing. When exposed to a light source, the liquid polymers begin to solidify, and the solidification rate is determined by both monomer concentration and light intensity. The polymerization process is an exothermic reaction that generates heat. Therefore, liquid polymers experience thermal stress throughout this solidification process. Thus, appropriate boundary conditions are imposed at the mesoscale, thereby emphasizing the identification of the effects of lighting conditions and layer thickness on polymerization process parameters to perform multiscale physical modeling.[152] A graphical illustration of the multi-scale structure utilized in SLA printing is depicted in Fig. 14.

4.4 Impact of simulation results in CAM

Simulation results can be used to analyze, modify, and optimize the cellular structures, fatigue properties, energy density effects, and so on of materials manufactured using the CAM technique. The voids produced during the fabrication process are commonly referred to as porosity, a prevalent issue in AM, as they can reduce the mechanical properties of the final products. The porosity percentage increases during CAM when reinforcement particles are printed into the polymer matrix,

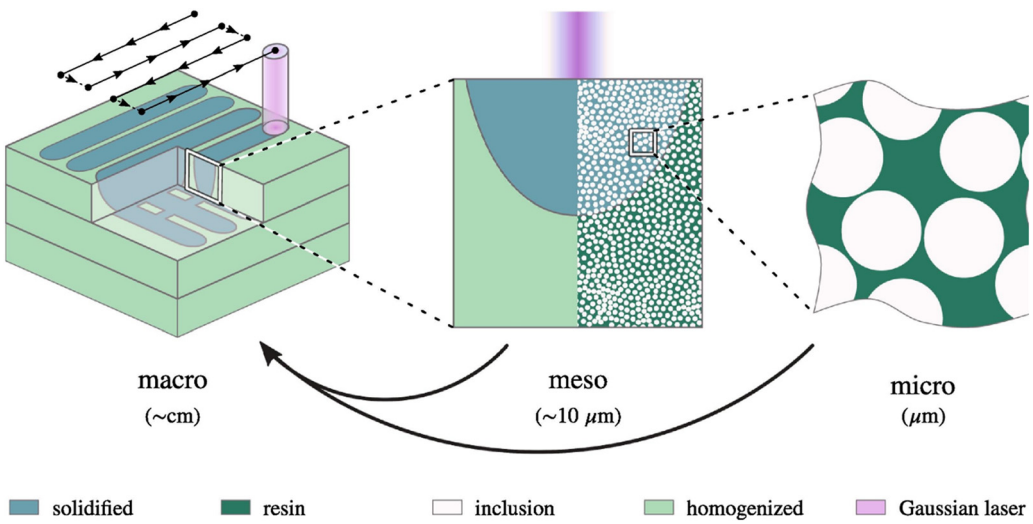

Fig. 14 A graphical representation of the multi-scale framework. Adapted from ref. 170 (open access).

© 2026 The Author(s). Published by the Royal Society of Chemistry

Open Access Article. Published on 19 June 2026. Downloaded on 6/19/2026 11:23:52 PM.
This article is licensed under a Creative Commons Attribution 3.0 Unported Licence.

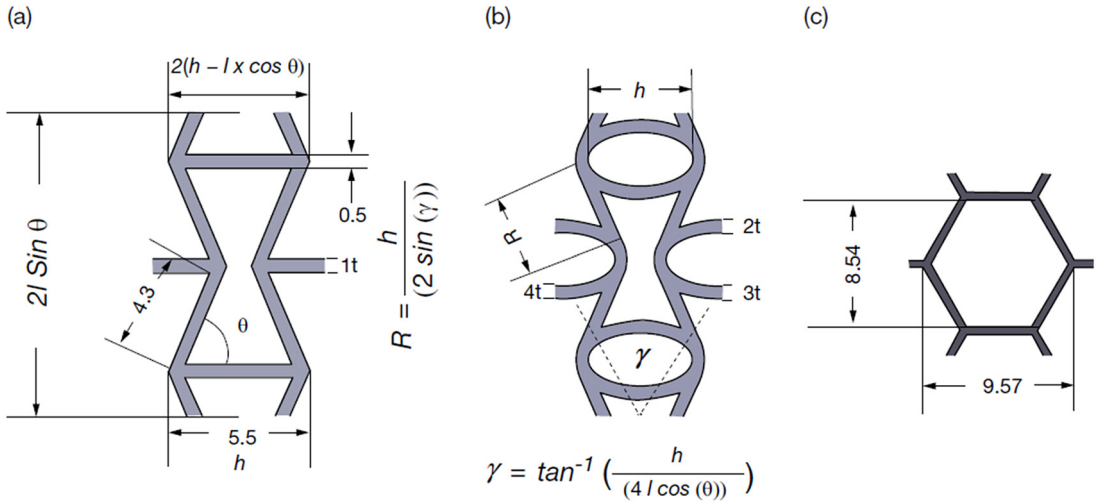

Fig. 15 Cellular structure of carbon fiber-reinforced PETG with (a) re-entrant design, (b) circle design, and (c) hexagonal design. Adapted from ref. 171 (open access).

due to the size, shape, and spatial distribution of the printing part. Researchers in recent years have used simulation techniques to study the impact of porosity on the mechanical properties of composites and to reduce its occurrence, since an increase in porosity decreases the composite's tensile modulus.[158,159] Moreover, cellular structures of the objects made with CAM can be customized and modified using simulation techniques.[169] Porous architectures featuring repeating unit cells and lightweight structures capable of absorbing energy can be manufactured using AM techniques. Alarifi[171] replicated the mechanical properties of carbon fiber-reinforced polyethylene terephthalate glycol (PETG) into their specimens with three different types of unit cells (*i.e.*, re-entrant, hexagonal, and circular) using FDM (Fig. 15). It was observed that the changes in the cellular structure of materials imply changes in their mechanical properties. Specimens with re-entrant unit cells exhibited the highest flexural stress at the breakpoint, while those with circular unit cells showed maximum compressive and tensile strengths due to the homogeneous stress distribution and load transfer. Moreover, circular unit cells reduced stress concentrations and prevented isolated failures in the composite specimens. Re-entrant unit cells created multiple load paths, dispersing load and lowering stress concentrations under bending conditions.[152]

In contrast, the study of the fatigue properties of composites has not received much attention yet.[172,173] However, the mechanical properties of the Kevlar-reinforced polymer matrix were numerically studied by Pertuz-Comas *et al.*[174] to determine the fatigue life of composite materials. The study compared numerical simulation data with experimental data, with a difference of only 2.5%. Nonetheless, the greater portion of the simulated cycles showed that the simulation result has a propensity to overestimate failure cycles,[152] as shown in Fig. 16a. Laser energy is another commonly used technique in AM methods, such as SLS and SLM, to sinter or melt powder, with reinforcing particles affecting the sintering process. Higher energy density creates a greater temperature gradient, increasing fluid flow, reducing fluid density, and ultimately influencing particle dispersion.[168] Moreover, the increase in laser power is responsible for the increase in the molten pool temperature, though the temperature distribution varies across the matrix and reinforcement materials.[175] Gan *et al.*[165] simulated the SLM of the Cu–SnTi/diamond composite, showing that Cu–Sn–Ti alloy particles reach 1500 °C with increasing power or energy density, as shown in Fig. 16b. Conversely, the temperature of diamond particles initially rises and then drops below 1000 °C. The lower thermal conductivity of Cu–Sn–Ti alloys compared to diamond causes significant heat accumulation in the powder bed, leading to ineffective heat transport within the material structure.

5. Machine learning techniques

Machine learning (ML) techniques are increasingly being used in AM systems for various purposes such as material design,[176,177] topology optimization,[30,178] parameter optimization,[179,180] process optimization,[176] field monitoring,[181] defect monitoring,[176] and anomaly detection[30] due to the advancements in data science and storage technologies.[53] During AM processes, the machine's embedded sensor collects data of various dimensions (*i.e.*, 1D, 2D, and 3D), while cameras can capture close-up images.[182] The collected data during such manufacturing processes can later be used for dataset training using various algorithms[176] (*i.e.*, supervised, unsupervised, and reinforcement learning) and further analysis using artificial intelligence (AI) methods[53] such as machine learning (*e.g.*, artificial neural network, convolutional neural network, recurrent neural network, and so on) and deep learning techniques.[183] Studies have shown that ML techniques can be used to characterize, assess quality, and optimize the overall CAM process for additive-manufactured composites.[53,115,180,184] Some emerging ML techniques are briefly

Open Access Article. Published on 19 June 2026. Downloaded on 6/19/2026 11:23:52 PM.
This article is licensed under a Creative Commons Attribution 3.0 Unported Licence.

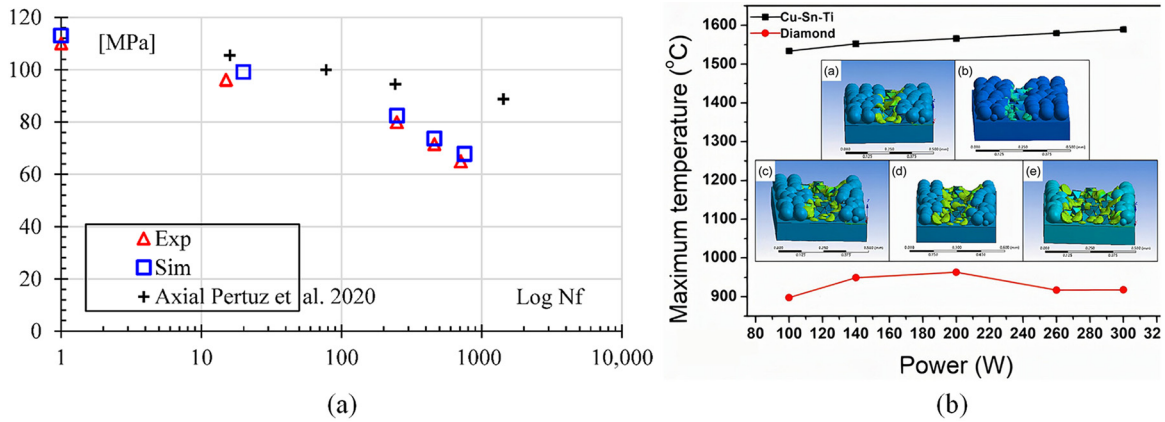

Fig. 16 (a) Stress-life curve for experimental and simulation data. Adapted from ref. 174 (open access). (b) Graphical representation of powder bed's temperature *vs.* power. Adapted from ref. 165 (reused with permission, license number 5827071444018).

described in this section, and the potential applications of ML in composite AM are shown in Fig. 17.

To make ML actionable (not merely predictive) in CAM, it should be embedded in an end-to-end workflow that connects (i) data acquisition (design/material/process descriptors plus *in situ* and *ex situ* measurements), (ii) model development (surrogate or deep models for process–structure–property and defect prediction with uncertainty quantification), and (iii) optimization and decision-making (process-parameter tuning, toolpath planning, and closed-loop control actions). A ML-integrated CAM workflow is illustrated in Fig. 18. The recent AM literature increasingly frames this as a digital-thread/digital-twin paradigm: physics- or data-informed surrogates are continuously updated from monitoring data, while Bayesian optimization and related strategies propose parameter trajectories that improve target properties under manufacturing constraints. This iterative workflow, progressing from data to modeling, optimization, and verification, is particularly important in CAM because fiber orientation, porosity, and interlayer bonding are strongly coupled and can shift with minor changes in thermal history, rheology, and path scheduling.[10,185,186]

However, a primary barrier to ML deployment in CAM is the limited availability of high-quality labeled datasets linking process signatures to composite-specific outcomes (*e.g.*, porosity distributions, interlayer bonding metrics, fiber orientation fields, and anisotropic mechanical properties). Many "labels" require destructive testing or high-cost metrology

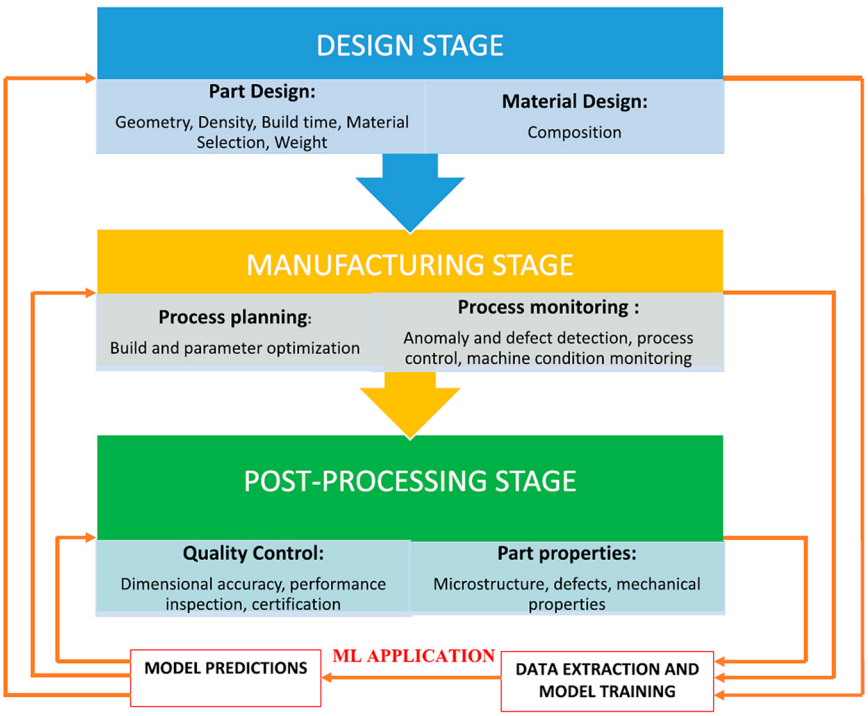

Fig. 17 ML at different stages of CAM. Adapted from ref. 11 (open access).

© 2026 The Author(s). Published by the Royal Society of Chemistry

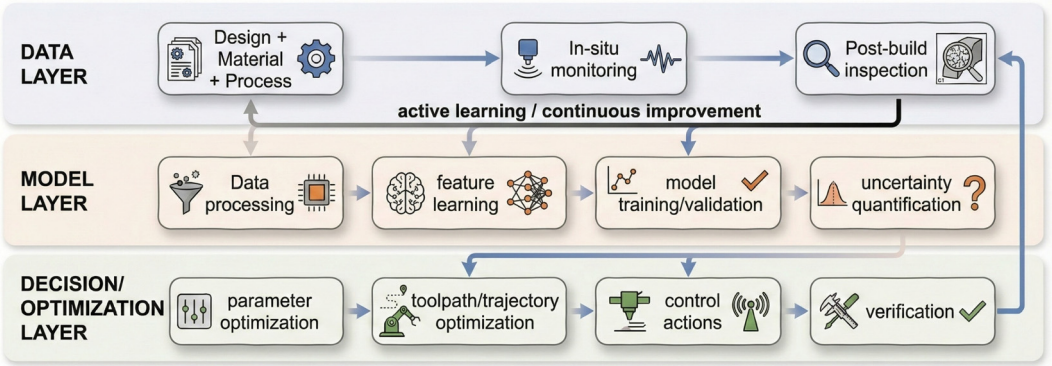

Fig. 18 ML-integrated CAM workflow progressing from data to modeling, optimization, and closed-loop control for CAM.

Open Access Article. Published on 19 June 2026. Downloaded on 6/19/2026 11:23:52 PM. This article is licensed under a Creative Commons Attribution 3.0 Unported Licence.

(*e.g.*, micro-CT, microscopy, ultrasonic C-scan, or standardized mechanical test specimens), which restricts dataset size and diversity and can reduce model generalization across machines, materials, and geometries. Consequently, the recent AM literature increasingly emphasizes data-efficient learning strategies such as semi-supervised learning, weak/active labeling, and anomaly detection, enabling models to exploit abundant in-process unlabeled images/signals while minimizing manual annotation. For example, semi-supervised deep learning has been shown to reduce labeling requirements while maintaining high defect-detection performance on powder-bed datasets, illustrating a practical pathway for AM quality inspection when labels are scarce.[187] Integrated sensing should be co-registered with machine states (position, speed, extrusion/laser power, layer number, and toolpath ID) and synchronized across sensors (thermal/visible/coaxial vision, pyrometry, acoustic emission, vibration/force/torque, and electrical signals), because many defects are only detectable when signals are interpreted in the context of where and when they occur along the toolpath. Reviews[188,189] of *in situ* monitoring noted that building reliable monitoring systems requires careful calibration, timing alignment, and robust feature extraction/data fusion, and highlighted standardization and interoperability as recurring gaps, especially when transitioning from lab demonstrations to industrial platforms. Real-time ML should meet latency constraints from sensing through inference, decision-making, and actuation, and define a decision policy (*e.g.*, early warning, parameter adjustment, local repair, or stop-build). The laser AM monitoring/control literature[189,190] frames this as moving from ''detect-only'' to adaptive quality enhancement, where multi-sensor monitoring and ML models support in-process remediation strategies rather than post-build rejection. Recent work[191] also demonstrated that data-driven approaches for closed-loop tuning (*e.g.*, Bayesian optimization for *in situ* controller autotuning in LPBF) can be used to execute monitoring, modeling, optimization, and control during the build rather than offline.

Because CAM datasets are costly to label and highly sensitive to feedstock batch, toolpath, machine state, and thermal history, dataset generation should be planned using design-of-experiments (DoE) principles rather than assembled solely from convenience trials. Full factorial designs are useful when the number of factors is limited and key interactions, such as layer thickness × raster angle, nozzle temperature × print speed, or laser power × scan speed, must be estimated directly. When many variables must be screened, fractional factorial or Taguchi-style orthogonal-array designs can reduce the required build count; however, the aliasing or confounding structure should be reported so that unresolved effects are not incorrectly interpreted as material trends.[192] Randomization, replication, and blocking by machine, feedstock batch, build plate position, or production day should also be considered to separate true process–material relationships from experimental noise.

After influential variables have been identified, response-surface designs are appropriate for local process-window modeling. Central composite designs support second-order models and include axial points for curvature estimation, whereas Box–Behnken designs use three-level factor combinations that avoid simultaneous extreme settings, which can be useful when extreme parameter combinations lead to failed builds or unsafe thermal conditions.[193,194] For ML-enabled CAM, DoE can be combined with adaptive sampling: an initial factorial or fractional-factorial stage screens dominant process and material variables, a central composite or Box–Behnken stage refines nonlinear process–response relationships, and a final active-learning or Bayesian-optimization stage selects new experiments in regions of high prediction uncertainty or high expected improvement.[192–196] This hybrid DoE–ML strategy improves data efficiency, preserves interpretability of main effects and interactions, and supports more defensible training, validation, and test partitions, particularly when holdout sets are structured by machine, feedstock batch, geometry, or toolpath. AM composite studies combining response-surface or Taguchi-style experimental plans with ANN and other ML models demonstrate the practical value of structured experimental design for property prediction and parameter optimization, although broader validation across machines, feedstock batches, geometries, and loading conditions remains necessary.[195,196]

5.1 Artificial neural network

An artificial neural network (ANN) is one of the most frequently used ML techniques[55] that can identify intricate relationships among nonlinear variables (*i.e.*, process parameters of AM)

Open Access Article. Published on 19 June 2026. Downloaded on 6/19/2026 11:23:52 PM.
This article is licensed under a Creative Commons Attribution 3.0 Unported Licence.

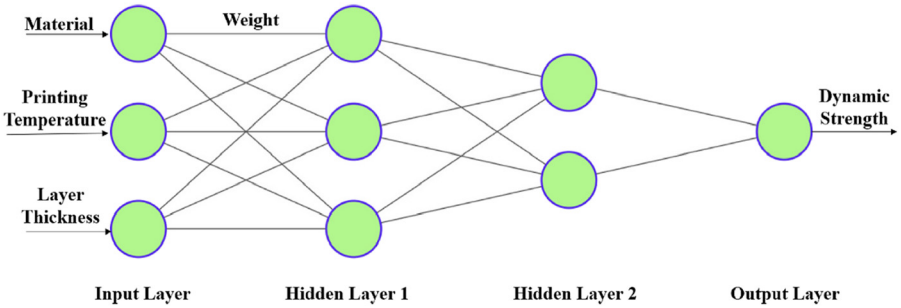

Fig. 19 Architecture of the ANN model used to determine additive-manufactured composites' dynamic strength, adapted from ref. 183 (open access).

without relying on a physical model or domain-specific expertise. This characteristic constitutes ANN a significant advantage over conventional methodologies (*i.e.*, experimental methods). A recent study[183] showed that ANNs can predict the dynamic strength of additive-manufactured composites (*e.g.*, polypropylene-based composites) with high accuracy by comparing their predictions with experimental data. The dynamic strength was predicted (see Fig. 19) using an input data set of three process parameters (*i.e.*, material type, printing temperature, and each layer thickness) measured at the initial point of CAM. The study showed that any required properties of additive-manufactured composites can be achieved by changing the aforementioned parameters, which can change the way CAM is performed to date. Beyond property prediction, ANNs are increasingly used as surrogate models to optimize print parameters when experiments are sparse or expensive. Deka and Hall[197] proposed a five-step framework that uses an ANN to enhance limited/non-systematic experimental datasets, builds response-surface models, and then performs optimization (including genetic-algorithm-based searches) to identify process settings that simultaneously maximize multiple mechanical properties in FDM. This workflow is especially relevant to CAM because the "best" parameter set is typically multi-objective, balancing stiffness/strength against porosity suppression, interlayer welding quality, and reinforcement-induced rheology constraints. Practically, ANN-driven optimization can be formulated to target composite-critical outputs (*e.g.*, void fraction, inter-bead bonding strength, and fiber alignment proxies) as constraints or penalty terms, enabling process windows that are robust to feedstock variability and reinforcement dispersion challenges.

Marko *et al.*[184] predicted the quality and defects of the manufactured object using the process-monitoring signal from the AM machine *via* an ANN model. Mahmood *et al.*[55] summarized that an ANN can be used for various applications in CAM, such as design and process planning, feature recommendation, microstructure optimization, geometric orientation, and stress prediction. In recent years, researchers have compared the precision and efficiency of ANN models with other predictive models (Fig. 20), such as k-nearest neighbors (KNN), extreme gradient boosting (XGB), random forest (RF), support vector regression (SVR), and decision tree (DT), and found that the prediction error for ANN was below 4%. Furthermore, the ANN was the most efficient among the six models.[183] Recent work has also demonstrated that self-learning ANN models, particularly when integrated with simulation-based datasets, can autonomously refine predictions over time. These models evaluate composite performance using feedback from virtual

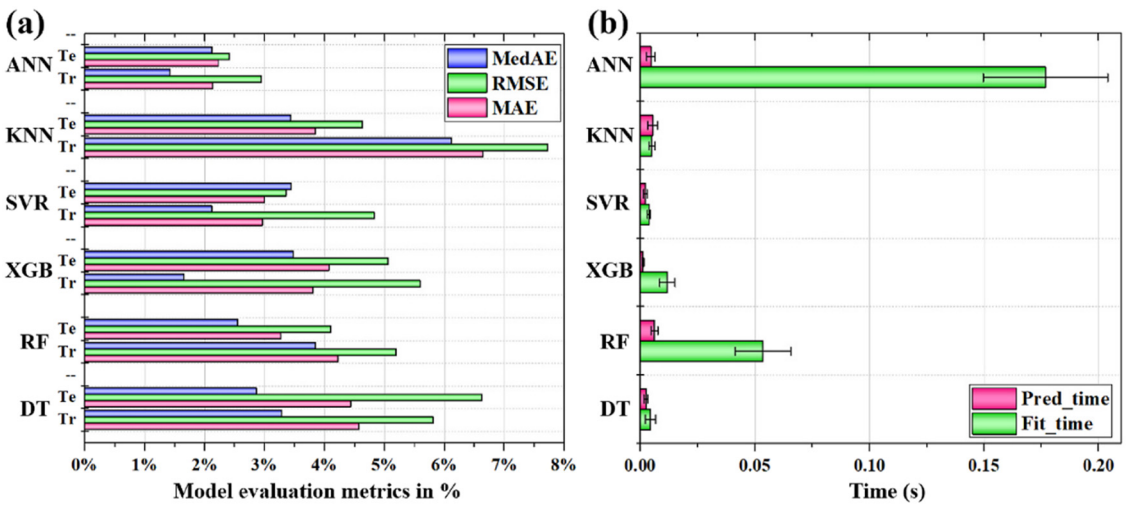

Fig. 20 Comparison of (a) accuracy and (b) efficiency of various ML models, adapted from ref. 183 (open access).

© 2026 The Author(s). Published by the Royal Society of Chemistry

Open Access Article. Published on 19 June 2026. Downloaded on 6/19/2026 11:23:52 PM.
This article is licensed under a Creative Commons Attribution 3.0 Unported Licence.

tests (*e.g.*, finite element simulations) and adjust internal weights to eliminate suboptimal design paths. This continuous learning loop significantly enhances prediction accuracy in dynamic manufacturing environments.[34]

5.2 Convolutional neural network

A convolutional neural network (CNN) is a widely used ML technique that operates *via* convolutional layers composed of functional numerical filters. Each filter in such a network is updated using input from the previous layer, generates values, and feeds them to the next layer. These connected convolutions make the model highly efficient in terms of computational power compared to other ML models.[198] CNNs can be used to design composites,[34] optimize their structures,[198] and predict their properties.[199] Although CNNs are primarily used for prediction in image processing,[200,201] a paradigm shift has occurred in recent years, as models can now predict acoustically with high efficiency[202] by suppressing environmental noise.[203] Furthermore, CNNs can make real-time predictions with 92.7% accuracy,[204] with great potential for the CAM industry.[29] CNNs have matured into practical porosity-detection engines for powder-bed fusion, where defect formation is strongly tied to local thermal history and melt-pool stability. In laser powder bed fusion (LPBF), Klein *et al.*[205] trained a CNN on in-process melt-pool monitoring data and labeled the ground truth using X-ray microCT, enabling automated discrimination between porous and non-porous regions; interpretability was enhanced using Grad-CAM to localize image evidence associated with porosity. Complementarily, Ansari *et al.*[206] demonstrated CNN-based classification of seeded pores in powder-bed fusion imagery, showing that careful labeling (CAD- *vs.* X-ray microCT-assisted) and dataset balancing can substantially improve precision/recall and enable detection of small pores (down to ~0.2 mm), thereby supporting a data-driven closed-loop framework for monitoring, porosity inference, and intervention in AM quality assurance. For CAM, the same CNN can be extended to composite-relevant defect signatures (*e.g.*, lack-of-fusion voids, reinforcement-rich clustering, or inter-bead void networks in short-fiber systems) by pairing *in situ* imagery/thermography/acoustics with post-build CT or microscopy labels, thereby converting porosity from a post-mortem metric into a controllable process variable. Beyond image-based monitoring, CNNs have also been applied to acoustic sensing in CAM. Shevchik *et al.*[203] monitored the additive-manufactured composites' quality and performed further analysis through CNNs. The sound emitted during CAM was captured by a sensor and fed as the received data to a CNN model that predicted the quality of printed composite layers (Fig. 21). CNNs have also been employed in self-optimizing frameworks, where the network iteratively selects and retains high-performing composite geometries from a pool of candidates. By using performance feedback from simulation or experimental data, CNNs can evolve better microstructural designs through successive generations. This approach is particularly useful in designing bioinspired, hierarchical composites with tailored mechanical responses.[34]

5.3 Reinforcement learning

Reinforcement learning (RL) provides a natural framework for toolpath/scan-strategy planning because deposition and

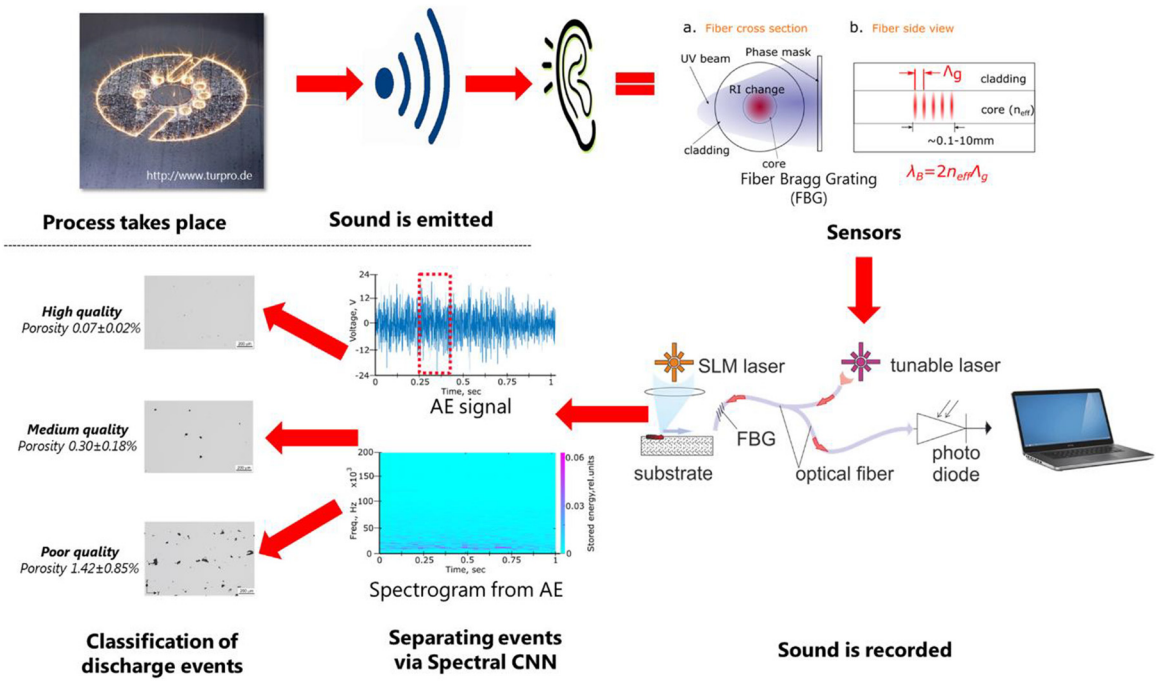

Fig. 21 Illustration of CAM quality monitoring and analysis using CNNs. Adapted from ref. 203 (reused with permission, license number 5827080424221).

Open Access Article. Published on 19 June 2026. Downloaded on 6/19/2026 11:23:52 PM.
This article is licensed under a Creative Commons Attribution 3.0 Unported Licence.

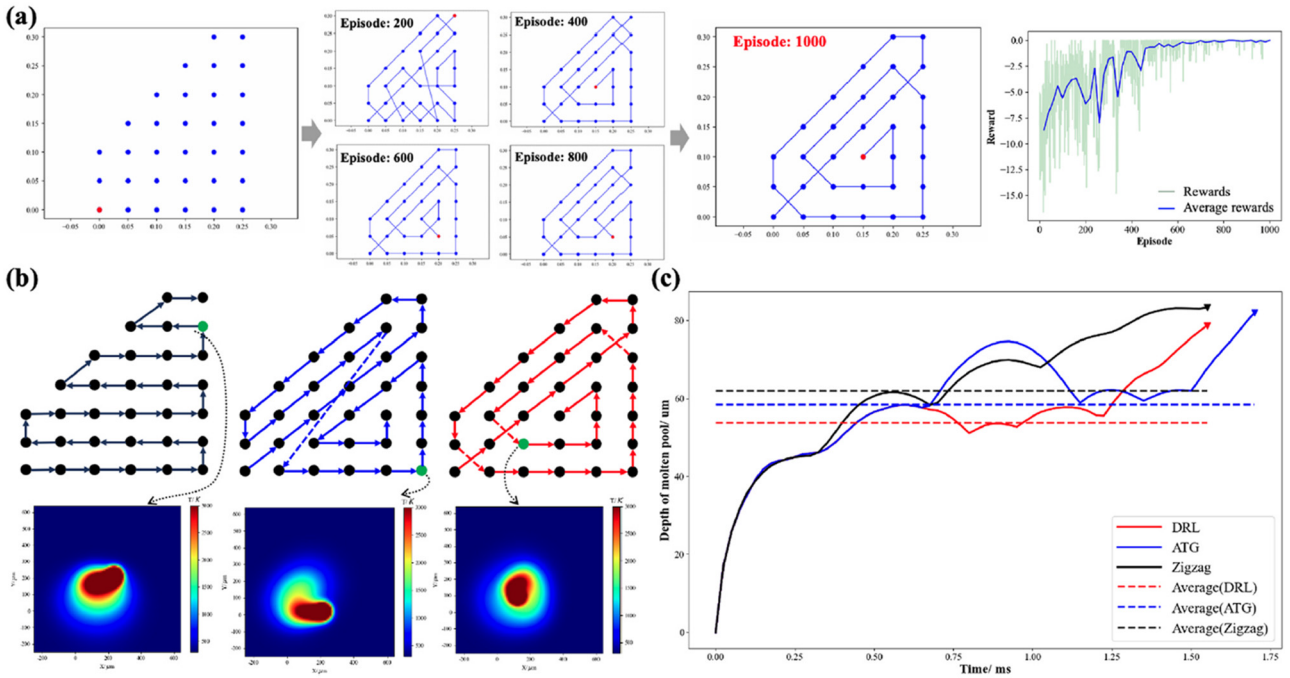

Fig. 22 Numerical modeling of three representative scan-strategy approaches applied to a polygonal build region. (a) Workflow of scan-path optimization using a DRL framework, including the evolution of the training reward over learning episodes, (b) side-by-side comparison of conventional zigzag scanning, ATG, and the DRL-optimized strategy, illustrating the resulting scan trajectories and corresponding simulated thermal distributions, and (c) temporal evolution of melt-pool penetration depth during the simulated build, where dashed lines denote mean values and inverted triangle markers indicate maximum excursions, adapted from ref. 207, (reused with permission, license number 6212380932298).

scanning are sequential decision processes with delayed consequences (thermal accumulation, distortion, bonding quality, and defect risk). Fig. 22 illustrates a deep reinforcement learning (DRL)-based scan-path optimization framework for polygonal regions, showing improved thermal uniformity and melt-pool stability compared with conventional zigzag and alternating traversal generation (ATG) strategies. Recent work by Qin *et al.*[207] developed a deep-RL-based toolpath generation strategy for LPBF to promote thermal uniformity and avoid extreme heat accumulation by designing reward functions that penalize unstable thermal states while enforcing feasible movement constraints; the approach is positioned as a route to reduce residual-stress-driven distortion compared with conventional scan patterns. Earlier RL toolpath concepts have also been explored for AM path design (*e.g.*, deep RL for deposition-path decisions) and as a foundation for "intelligent toolpaths" that adapt based on process feedback.[208,209] In CAM, RL is especially promising for continuous-fiber and short-fiber extrusion toolpaths, where action choices (raster direction, steering curvature, dwell time, and local compaction/heating moves) can be optimized against rewards defined by predicted fiber orientation quality, bead-to-bead bonding, porosity risk, and geometric deviation, enabling genuinely autonomous process planning rather than static, heuristic toolpath rules.

5.4 Recurrent neural network

A recurrent neural network (RNN) is a predictive model primarily employed for time-series sequential data[26,30,176,210] when researchers must rely on historical data.[211] The model predicts future outputs by evaluating past information[210] through its feedback connection system.[212] An RNN processes the input data at each neuron using its memory state to predict the required output.[213] Different types of path-dependent mechanical behavior of materials (*e.g.*, cracking,[214] plastic flow,[215] and so on) have been predicted in recent years by using RNNs.[210] The model can efficiently predict the complex behavior of materials that change with time[211] and other conditions. Moreover, RNNs can process datasets of any length, as the model's size does not expand during computation, which enables the predictive model to learn quickly despite data variation[216] and dynamics in the study system.[212] In recent years, Yanamandra *et al.*[26] predicted fiber orientation in additive-manufactured composites using an RNN. Sun *et al.*[210] demonstrated the process to manufacture 4D composites using CAM (Fig. 23). Furthermore, they predicted the nonlinear deformation or shape-change under thermal conditions using RNNs (Fig. 24). Beyond time-dependent predictions, RNNs can be trained to recognize patterns in evolving structural datasets and suggest process parameter changes in real time. When used in conjunction with reinforcement learning principles, RNN-based systems can adaptively control CAM parameters (*e.g.*, laser speed and feed rate) to optimize the final composite structure during fabrication.[34] Zha *et al.*[217] applied an RNN-inspired framework using an attention-based CNN to predict stress-aligned toolpaths in continuous fiber composites. By replacing FEA with learned sequential predictions,

© 2026 The Author(s). Published by the Royal Society of Chemistry

Open Access Article. Published on 19 June 2026. Downloaded on 6/19/2026 11:23:52 PM.
This article is licensed under a Creative Commons Attribution 3.0 Unported Licence.

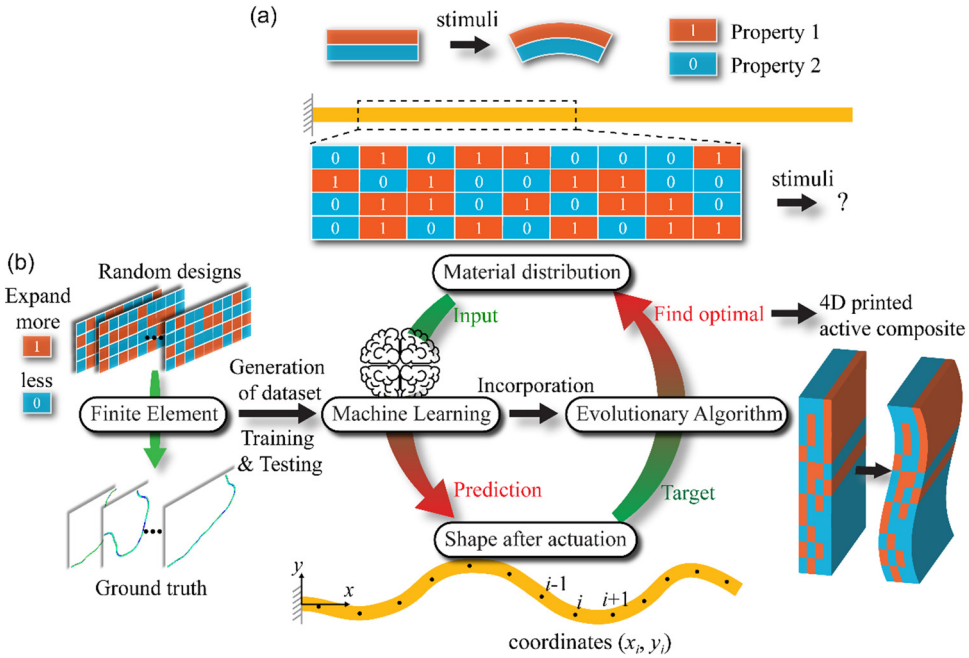

Fig. 23 4D printed composite beam designing proposal using CAM that shows (a) composite design with different inherent properties and (b) from design to composite manufacturing using ML. Adapted from ref. 210 (reused with permission, license number 5827080677155).

the method reduced computation time by 87% while maintaining accuracy within 10°, demonstrating the efficiency of temporal learning in AM process planning.

5.5 Other ML techniques

Some other recently used ML techniques for CAM include XGBoost,[115] decision trees (DTs), *k*-nearest neighbors (KNNs),

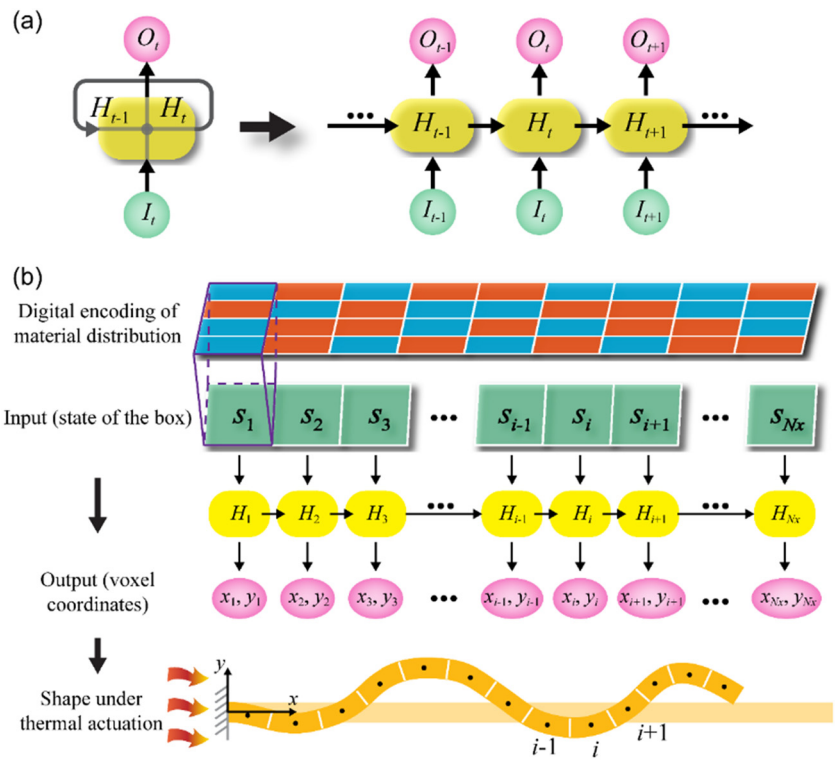

Fig. 24 (a) Architecture of RNNs and (b) used model of RNNs to predict additive manufactured composite beams' nonlinear deformation. Adapted from ref. 210 (reused with permission, license number 5827080677155).

Open Access Article. Published on 19 June 2026. Downloaded on 6/19/2026 11:23:52 PM. This article is licensed under a Creative Commons Attribution 3.0 Unported Licence.

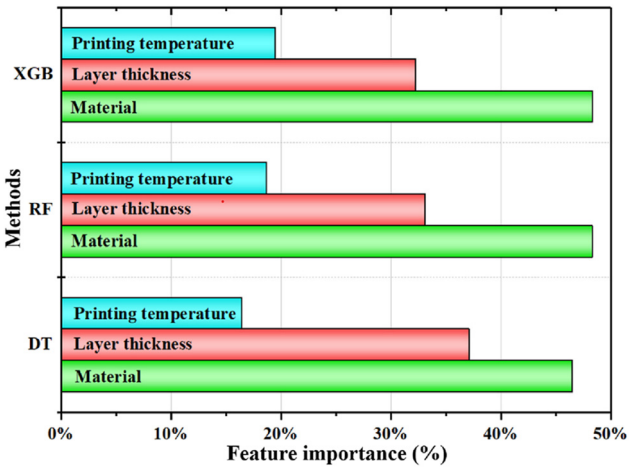

Fig. 25 Process parameters importance predicted by XGB, RF, and DT. Adapted from ref. 183 (open access).

random forests (RFs), support vector regression (SVR), and XGB.[183] The XGBoost predictive model showed that the mechanical properties of manufactured composites are influenced by process parameters during DED.[115] The other models, such as XGB, RF, and DT, can also be used to predict the important features of CAM (Fig. 25) that can improve the quality of composites, process parameters, and CAM performance. Recently, generative adversarial networks (GANs) and variational autoencoders (VAEs) have emerged as promising tools for composite design. These models learn from existing CAM datasets to generate entirely new material configurations with enhanced mechanical performance or customized structural attributes. Such generative models not only reduce reliance on heuristic methods but also accelerate the discovery of previously unexplored design solutions.[34] Moreover, ongoing advances have demonstrated the efficacy of ensemble learning techniques for refining post-processing outcomes in AM. Kiadarbandsari *et al.*[218] employed a stacked ensemble model to accurately predict improvements in surface roughness of SLA-printed dental components subjected to chemo-mechanical finishing.

By combining multiple base learners and optimizing model parameters through Bayesian techniques, the approach achieved a test R^2 of 0.96, surpassing the performance of standalone models. Although computational demand increased, the enhanced accuracy in predicting post-process quality metrics supports the growing adoption of ensemble strategies in AM surface engineering. Mahapatra *et al.*[219] applied ML to predict tensile properties of 3D-printed lattice composites using features such as cell geometry, material type, and relative density. The model achieved accurate forecasts with minimal experimental input, emphasizing the value of data-driven methods in optimizing lightweight AM designs. Tian *et al.*[220] developed an ML approach using extended support vector regression (X-SVR) to assess the influence of geometric inaccuracies on the structural stability of 3D-printed lattice-core sandwich composites. By modeling imperfections such as node displacement and surface waviness, the method achieved accurate predictions with significantly reduced computational effort compared to conventional Monte Carlo simulations. Chang *et al.*[221] used XGBoost with an evolutionary algorithm to predict magnetic properties in SLM-fabricated soft magnetic composites. By mapping key inputs (*e.g.*, oxygen concentration, laser power, and scan speed) to outputs (*e.g.*, permeability and iron loss), the model enabled rapid, accurate parameter selection, outperforming traditional trial-and-error approaches.

5.6 Problem-specific model selection and trustworthy ML in CAM

The selection of an ML model for CAM should be governed by the manufacturing objective, data modality, data volume, physical constraints, and required decision output, rather than by a generic preference for a particular algorithm. For tabular descriptors, including feedstock composition, fiber volume fraction, raster angle, layer thickness, nozzle or laser settings, and post-processing conditions, ANN, RF, XGBoost, SVR, and GPR models are widely used for process–structure–property prediction and process optimization.[11,31,179,183] Image-based data from melt-pool monitoring, layerwise inspection, thermal imaging, microscopy, and X-ray microCT are commonly addressed using CNNs, vision transformers, or encoder–decoder segmentation models for porosity detection, lack-of-fusion identification, reinforcement clustering, and surface-anomaly analysis.[187,205,206] Sequential and path-dependent signals, including toolpath history, acoustic emission, thermal histories, and layer-by-layer process signatures, are better modeled using temporal CNNs, recurrent models, transformers, state-space models, or hybrid architectures because defect formation, fiber orientation, residual stress, and interlayer bonding evolve cumulatively during the build.[26,203,206,210] For scan-path or toolpath planning, reinforcement learning and model-predictive control approaches may be appropriate, as each manufacturing action modifies the subsequent thermal, geometric, and reinforcement states.[207,217] Table 5 summarizes problem-specific ML approaches for CAM by linking manufacturing objectives, data modalities, decision requirements, and suitable model families.

Beyond selecting models according to data modality and decision task, ML-enabled CAM also requires careful validation, uncertainty quantification, physics consistency, and transparent reporting to ensure that predictions are trustworthy across machines, materials, and build conditions. The main limitation for ML-enabled CAM is the scarcity of high-quality labeled datasets. Labels for porosity, fiber orientation, interfacial bonding, residual stress, and anisotropic mechanical properties often require destructive testing or high-cost characterization, including X-ray microCT, microscopy, ultrasonic inspection, and standardized tensile, flexural, fatigue, or interlaminar tests.[187–189] CAM datasets are also highly heterogeneous, combining scalar process parameters, 2D images, 3D defect fields, toolpath histories, thermal signals, acoustic signatures, and post-build mechanical measurements.

© 2026 The Author(s). Published by the Royal Society of Chemistry

Open Access Article. Published on 19 June 2026. Downloaded on 6/19/2026 11:23:52 PM. This article is licensed under a Creative Commons Attribution 3.0 Unported Licence.

Table 5 Problem-specific ML approaches for composite additive manufacturing, including data-scarce, physics-informed, uncertainty-aware, and certification-oriented applications

CAM problem/decision task	Recommended ML approaches	Rationale	Ref.
Process–structure–property prediction	ANN, RF, XGBoost, SVR, GPR, Bayesian models, physics-guided surrogate models	Suitable for mapping feedstock composition, fiber volume fraction, raster angle, layer thickness, toolpath, thermal history, nozzle or laser settings, and post-processing conditions to porosity, microstructure, stiffness, strength, and dynamic response. GPR and Bayesian models are especially useful when datasets are small and predictive uncertainty is required	11, 31, 179, 183, 219, 222 and 223
Porosity, lack of fusion, voids, and reinforcement clustering	CNN, U-Net/encoder–decoder segmentation, vision transformers, semi-supervised learning, anomaly detection, spatial GPR	Defects and reinforcement heterogeneity are spatially localized and are commonly detected from layer images, thermal maps, melt-pool images, X-ray microCT, microscopy, or optical inspection. Semi-supervised and anomaly-detection methods reduce labeling burden, while spatial GPR can support uncertainty-aware defect-field interpolation in small datasets	179, 187, 205, 206 and 222
In situ monitoring and defect precursor detection	CNN, temporal CNN, RNN/LSTM/GRU, transformers, state-space models, multimodal fusion, online anomaly detection	Thermal, acoustic, optical, vibration, and process-signal streams are time-dependent and should be integrated with toolpath position, layer number, and local thermal history. Temporal and multimodal models are therefore more appropriate than static classifiers alone	181, 182, 188, 189 and 203
Process optimization and closed-loop control	GPR surrogate models, Bayesian optimization, active learning, constrained or multi-objective optimization, model-predictive control, reinforcement learning	GPR and Bayesian optimization reduce experimental cost in small-data regimes. Active learning identifies the most informative experiments, while reinforcement learning or model-predictive learning is useful for sequential scan-path, toolpath, or control decisions that influence later thermal, geometric, and defect states	180, 185, 191, 207 and 224
Fiber orientation prediction and continuous-fiber path planning	RNN/LSTM, temporal CNN, CNN-based field prediction, graph neural networks, geometric/path-planning models, reinforcement learning	Fiber orientation depends on toolpath, shear history, deposition sequence, curvature, compaction, and local stress fields. Sequential, field-based, and graph-based models can connect path planning to reinforcement alignment and load-bearing trajectories	26, 210 and 217
Interfacial bonding and interlayer adhesion	RF, XGBoost, SVR, ANN, GPR, physics-guided ML, physics-informed surrogate models	Bond quality depends on temperature, pressure, residence time, diffusion or wetting, surface state, fiber-rich interfaces, and local thermal history. Physics-guided descriptors can reduce nonphysical extrapolation outside the tested processing window	180 and 223
Residual stress, distortion, and thermal history	Physics-informed surrogate models, PINNs, thermomechanical field surrogates, RNN/LSTM, graph-based field models	Thermal conduction, heat accumulation, scan order, cooling rate, material anisotropy, and thermoelastic constraints govern distortion and residual stress. PINNs (physics-informed neural networks) are most appropriate when reliable governing equations, boundary conditions, and thermal constraints are available	207, 223 and 225
Mechanical performance, fatigue, and lattice or sandwich response	ANN, RF, XGBoost, SVR, GPR, BNN, MC dropout, deep ensembles, graph neural networks, reliability-aware models	Nonlinear interactions among material composition, geometry, layer thickness, raster angle, defects, fiber architecture, and interfacial quality govern mechanical response. Bayesian models, MC dropout, and ensembles provide uncertainty estimates, while graph-based models are useful for lattice, sandwich, or topology-dependent structures	183, 219, 220 and 226–230
Data-scarce and cross-domain CAM learning	Transfer learning, domain adaptation, self-supervised learning, semi-supervised learning, simulation-pretrained models	CAM datasets are often small, expensive, machine-specific, and difficult to label. Transfer learning and domain adaptation can reduce data requirements when source and target domains share relevant physical similarity, while self-supervised and simulation-pretrained models can exploit unlabeled or synthetic data	224 and 231–233
Certification, reliability, and trustworthy ML	Calibrated GPR, BNN, MC dropout, deep ensembles, conformal prediction, OOD detection, XAI	Certification-oriented CAM requires more than point accuracy. Models should provide calibrated uncertainty, detect out-of-distribution process conditions, and offer physically interpretable explanations linking predictions to process, material, sensor, or microstructural descriptors	229, 230 and 234–237

Open Access Article. Published on 19 June 2026. Downloaded on 6/19/2026 11:23:52 PM. This article is licensed under a Creative Commons Attribution 3.0 Unported Licence.

Reproducibility and transferability are further limited when publications omit essential metadata, such as fiber length distribution, sizing chemistry, fiber volume fraction, rheological state, drying history, chamber temperature, humidity, toolpath identifier, sensor calibration, spatial registration, and post-processing conditions. Consequently, ML studies in CAM should report not only the dataset and model architecture but also the domain of validity, including machine type, feedstock batch, geometry class, sensor configuration, train–test split strategy, external validation procedure, and out-of-distribution checks.[10,189,238]

Transfer learning, domain adaptation, and self-supervised learning are promising routes to mitigate data scarcity in CAM. A model trained on a source task, such as defect detection in a related polymer, composite, or metal AM process, can be adapted to a target CAM task using a limited number of target labels. This approach is most defensible when the source and target domains share relevant physical similarity, including comparable thermal histories, bead geometry, reinforcement morphology, interlayer bonding mechanisms, or imaging conditions. However, transfer learning should be treated as a domain-adaptation problem rather than a simple model-reuse strategy, because negative transfer can occur when the source data encodes processes inconsistent with the target machine, material, geometry, or sensor configuration. Practical implementation should therefore include source–target similarity assessment, frozen or partially fine-tuned feature extractors, few-shot target calibration, and independent validation on a separate CAM build.[224]

Synthetic and simulation-derived data can further reduce the experimental burden, but they should complement rather than replace experimental evidence. Depending on the CAM process, finite-element simulations, computational homogenization, voxel-based mesostructure models, cure- or heat-transfer simulations, extrusion-flow models, fiber-orientation predictions, and melt-pool simulations can generate controlled examples of orientation fields, void morphology, thermal gradients, residual stresses, and interfacial damage states that are difficult to sample experimentally. Such data are valuable for pretraining, sensitivity analysis, active-learning acquisition, and rare-defect augmentation, but they should be accompanied by domain randomization, mesh and discretization checks, uncertainty estimates, and validation against independent builds. A defensible workflow is to train surrogate or deep models first on simulation-derived data, update or fine-tune them using a small number of experimentally measured CAM cases, and then reserve at least one feedstock batch, geometry, and machine condition for external validation.[34,222–225]

Physics-informed and physics-guided ML are needed because purely data-driven models can learn correlations that do not remain valid outside the tested process window. In CAM, physical knowledge can be introduced through engineered features, constrained architectures, simulation-informed priors, hybrid surrogate models, or loss-function penalties. Relevant constraints include heat conduction and cooling rate for thermal history, mass conservation and melt-pool continuity for fusion-based processes, rheology and shear-induced alignment for extrusion, cure kinetics for photopolymerization, rule-of-mixtures and micromechanics relations for stiffness prediction, orientation tensors for fiber architecture, wetting and diffusion descriptors for interfacial bonding, and thermoelastic balance for residual stress. These constraints are especially important when labels are sparse, process parameters interact nonlinearly, or models are expected to generalize across feedstock batches, machine platforms, and build geometries.[223,225]

Uncertainty quantification should be treated as a required component of ML-enabled CAM rather than an optional post-processing step. CAM contains aleatoric uncertainty arising from process noise, feedstock variability, sensor noise, and stochastic defect nucleation, as well as epistemic uncertainty arising from limited data, distribution shift, and model-form error.[222] GPR models are appropriate for small tabular datasets and Bayesian optimization because they provide both mean predictions and uncertainty estimates.[179,185,191] Bayesian neural networks can represent uncertainty in model weights and are relevant for nonlinear process–structure–property prediction when safety margins must be quantified.[228] Monte Carlo dropout provides a computationally convenient approximation for uncertainty estimation in deep networks used for image- or sequence-based monitoring,[229] whereas deep ensembles are useful when practical uncertainty estimates are required without fully Bayesian training.[230] These methods should be assessed using calibration metrics, coverage probability, reliability diagrams, and out-of-distribution tests. In CAM, calibrated uncertainty estimates can support conservative parameter selection, active learning, targeted inspection, build interruption, or local repair when uncertainty exceeds an acceptable threshold.[191,222]

For certification-oriented CAM, explainable artificial intelligence is as important as numerical accuracy. A high-area-under-curve defect classifier or low-error property predictor is not sufficient when the model cannot identify which process, sensor, or material descriptors drove the decision. In safety-critical settings, black-box predictions should be accompanied by physically interpretable evidence, such as feature attributions showing sensitivity to energy input, chamber temperature, layer time, raster angle, fiber volume fraction, local curvature, melt-pool dimensions, or acoustic-emission features; saliency or localization maps tied to X-ray microCT-verified pores or lack-of-fusion regions; and counterfactual tests showing how process changes would reduce defect probability or improve anisotropic properties. Interpretability should also be evaluated for stability and physical consistency across machines and feedstock batches. When *post hoc* explanations are used, they should be treated as diagnostic aids, whereas qualification claims should preferentially rely on interpretable models, physics-constrained surrogates, uncertainty-calibrated predictions, and traceable decision rules.[239,240] Because ML-enabled CAM models are often trained on small, heterogeneous, and process-specific datasets, model accuracy alone is insufficient for judging reliability. Table 6 summarizes

© 2026 The Author(s). Published by the Royal Society of Chemistry

Open Access Article. Published on 19 June 2026. Downloaded on 6/19/2026 11:23:52 PM. This article is licensed under a Creative Commons Attribution 3.0 Unported Licence.

Table 6 Validation, uncertainty, and reporting requirements for trustworthy ML-enabled CAM studies[a]

Requirement	What should be reported	Why it matters for CAM
Dataset description	Machine type, feedstock batch, fiber type, fiber length distribution, fiber volume fraction, matrix type, geometry class, build orientation, raster angle, layer thickness, nozzle or laser settings, chamber temperature, humidity, and post-processing conditions	CAM datasets are highly process- and material-specific. Without detailed metadata, results cannot be reproduced or transferred across machines, materials, or geometries
Label definition	Whether labels represent final properties, binary defects, porosity fraction, fiber-orientation tensor, void network, interfacial strength, crystallinity, degree of cure, residual strain, or thermal history	Mechanism-aware labels are more informative than simple pass/fail labels or final tensile strength alone
Train–test strategy	Random split, build-wise split, geometry-wise split, batch-wise split, machine-wise split, or external validation split	Random splitting can overestimate model performance when specimens from the same build or geometry are included in both the training and test sets
External validation	Independent validation using a different build, feedstock batch, geometry, machine, sensor setup, or environmental condition	Demonstrates whether the model generalizes beyond the narrow training dataset
Out-of-distribution testing	Performance under unseen process windows, new geometries, new feedstocks, sensor drift, or changed environmental conditions	CAM models can fail when deployed outside the training domain; OOD (out-of-distribution) checks are essential for safe use
Uncertainty quantification	Prediction intervals, epistemic uncertainty, aleatoric uncertainty, calibration curves, coverage probability, reliability diagrams, or conformal prediction sets	Point predictions are insufficient for process qualification, defect acceptance, and closed-loop control
Physics consistency	Heat-transfer consistency, mass conservation, cure kinetics, fiber-orientation constraints, micromechanics relations, or thermoelastic constraints	Helps prevent physically implausible predictions and improves extrapolation outside the tested process window
Explainability	Feature attribution, saliency maps, counterfactual tests, sensitivity analysis, interpretable surrogate models, or physically meaningful decision rules	Important for certification, troubleshooting, process optimization, and trust in safety-critical CAM applications
Data scarcity strategy	Transfer learning, domain adaptation, self-supervised learning, active learning, simulation pretraining, or rare-defect augmentation	CAM labels are expensive because they often require X-ray microCT, microscopy, destructive testing, or long-term mechanical testing
Reproducibility	Code availability, model hyperparameters, preprocessing steps, sensor calibration, spatial registration, data normalization, and evaluation metrics	Enables fair comparison across studies and reduces irreproducible model claims

[a] For certification-oriented CAM, model accuracy should be reported together with uncertainty calibration, external validation, OOD behavior, and physical interpretability. Accuracy alone is insufficient for qualification-relevant decisions.

the validation, uncertainty, physics-consistency, explainability, and reproducibility requirements.

ML predictions in CAM should be interpreted within the process–structure–property chain rather than as direct correlations between processing parameters and final part performance. Therefore, target variables should extend beyond ultimate tensile strength, modulus, or binary defect labels. More informative labels include fiber-orientation tensors, fiber length distributions, void-network descriptors, reinforcement-rich clusters, interphase thickness, interfacial strength, crystallinity, degree of cure, residual strain, and layer-wise thermal history. These mechanism-aware descriptors are essential because printed composites exhibit direction-dependent, spatially heterogeneous, and path-dependent behavior. Future ML-CAM studies should therefore prioritize physically meaningful, spatially resolved labels over purely empirical performance metrics.

6. Applications of additive-manufactured composites

6.1 Application drivers for fiber-orientation control and anisotropic performance in CAM

In many safety- and stiffness-critical CAM applications, performance is more strongly influenced by orientation-driven anisotropy (fiber trajectory, continuity, and interlayer bonding) than by bulk material properties, making fiber-orientation control and verification a primary design requirement. For example, in aerospace and UAV structures, the principal advantage of CAM is the ability to steer continuous fibers along load paths to maximize specific stiffness/specific strength, while keeping mass low and enabling integrated geometries that are difficult to achieve with conventional laminate layups. A representative demonstration is the meter-scale continuous carbon-fiber-reinforced wing spar produced by material-extrusion-based printing, where the combination of topology optimization and fiber-reinforced deposition targets lightweight, stiffness-critical performance typical of flight structures. Such components are susceptible to orientation-driven anisotropy: small deviations in fiber trajectory or local discontinuities can shift load transfer to weaker matrix-dominated directions, making orientation control and verification essential for certification-relevant properties.[241,242] Rehabilitation devices (*e.g.*, prosthetic sockets and orthoses) require custom geometry yet should sustain long-term, directionally biased loads; therefore, fiber placement strategies that align reinforcement with expected stress paths are critical. A recent continuous-fiber reinforced transfemoral prosthetic socket study[243] explicitly links path planning to mechanical performance by generating fiber trajectories that better match the

Open Access Article. Published on 19 June 2026. Downloaded on 6/19/2026 11:23:52 PM.
This article is licensed under a Creative Commons Attribution 3.0 Unported Licence.

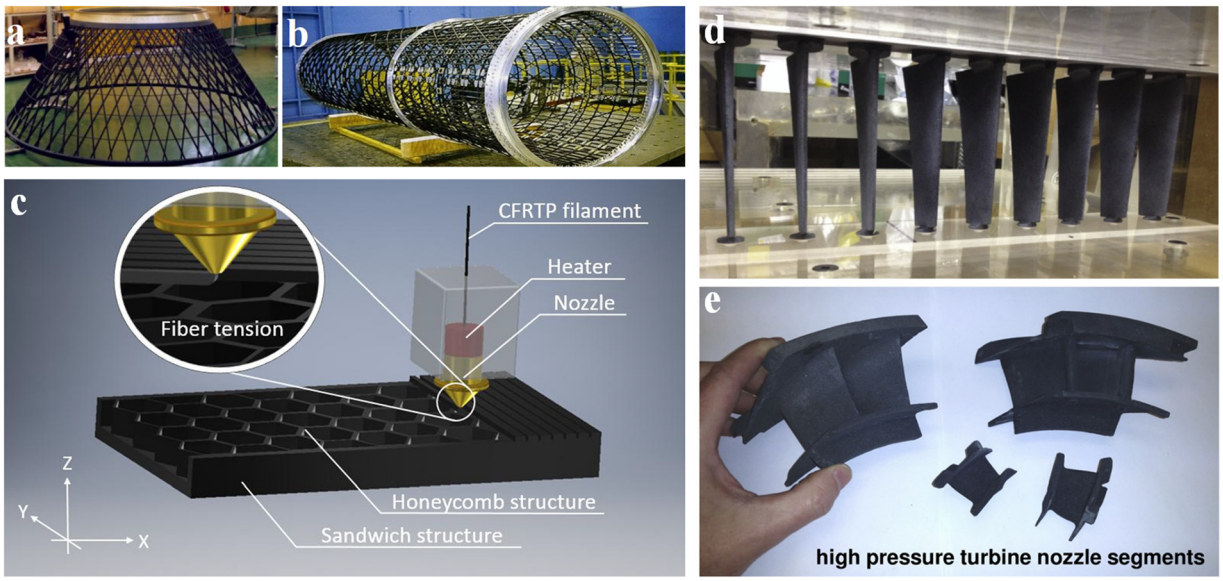

Fig. 26 Additive manufactured composite structures for aerospace showing (a) lattice payload adapter and (b) spacecraft frame, adapted from ref. 251 (open access), (c) AM of composite honeycomb sandwich structure, adapted from ref. 249 (open access), (d) inlet guide vanes of compressor made of polyetherimide composite using FDM, and (e) nozzle segments of turbine made of ceramic composite using AM, adapted from ref. 252 (reused with permission, license number 5827080925988).

service load environment, precisely the kind of anisotropy-sensitive use case where CAM's toolpath-level control becomes a functional requirement rather than an aesthetic choice. Across stiffness-critical parts (aerospace brackets, robotic arms, protective shells, and lightweight frames), continuous-fiber CAM can be viewed as manufacturing a transversely isotropic material field whose strength/stiffness is maximized when the fiber direction aligns with the principal stress direction. A recent work[217] on ML-assisted path planning operationalizes this idea by learning stress fields (*via* CNN-style models) and mapping fiber paths accordingly, highlighting that the "right" anisotropy is beneficial only if the reinforcement direction is controlled and consistently reproduced.

6.2 Application in aerospace

The techniques for fabricating composite materials *via* AM have revolutionized the aerospace industry by enabling the production of lightweight, multifunctional, complex geometries.[244] Aerospace was one of the earliest industries to adopt AM, and it has been reported that 18.2% of the total AM market is attributed to the aerospace industry.[245] The technology of AM has the potential to reduce material wastage in the aerospace industry and reduce the annual expense of fuel by USD 3000 for every kilogram of saved materials.[246,247] Moreover, automated CAM technology has reduced man-hours by 80% in the aerospace industry.[248] Additively manufactured composite structures for aerospace applications can meet requirements for stiffness, stability, and strength under specific loads and conditions.[247] Aerospace structures, such as lattice payload adapters (Fig. 26a), spacecraft frames (Fig. 26b), and sandwich structures (Fig. 26c) for aircraft, can be manufactured from composite materials using AM techniques. The first use of composite honeycomb sandwich structures in aerospace was initiated by the United States to develop the Convair B-58 bomber aircraft, which could reach Mach 2.4.[245,249] Composite sandwich structures manufactured *via* AM technology can also reduce the complexity of aerospace spare parts production.[245] Furthermore, complex aerospace components such as inlet guide vanes (Fig. 26d) and turbine nozzles (Fig. 26e), as well as aircraft camera fairings,[250] have been fabricated using CAM.

6.3 Application in automotive

The automotive industry is highly competitive, with innovative design and manufacturing trends occurring regularly. Therefore, innovation in manufacturing processes is required to meet the demands of the automobile industry.[253,254] The application of CAM techniques in the automotive industry can increase production flexibility, reduce product design and development time, and provide optimized components and bespoke vehicle products on demand.[254–257] Although AM in the automotive industry started with the production of soft assembly tools using FDM and SLS,[254] it has since expanded to include a wide range of applications. These applications include electrical sensors, engine components, suspension systems, exterior panels, trims, interiors, and seating. In recent years, the side-view mirror shells of racing cars competing in NASCAR events in Chicago were fabricated using CAM, demonstrating the reliability of such techniques even under harsh conditions (Fig. 27a).[244,258] Moreover, the use of CAM is increasing in vehicle restoration, customization, and redesign. For instance, the Oak Ridge National Laboratory (ORNL) fabricated a full-scale replica of the Shelby Cobra for its 50th anniversary. The entire car was manufactured using Big Area Additive Manufacturing (BAAM) technology, excluding

© 2026 The Author(s). Published by the Royal Society of Chemistry

Open Access Article. Published on 19 June 2026. Downloaded on 6/19/2026 11:23:52 PM.
This article is licensed under a Creative Commons Attribution 3.0 Unported Licence.

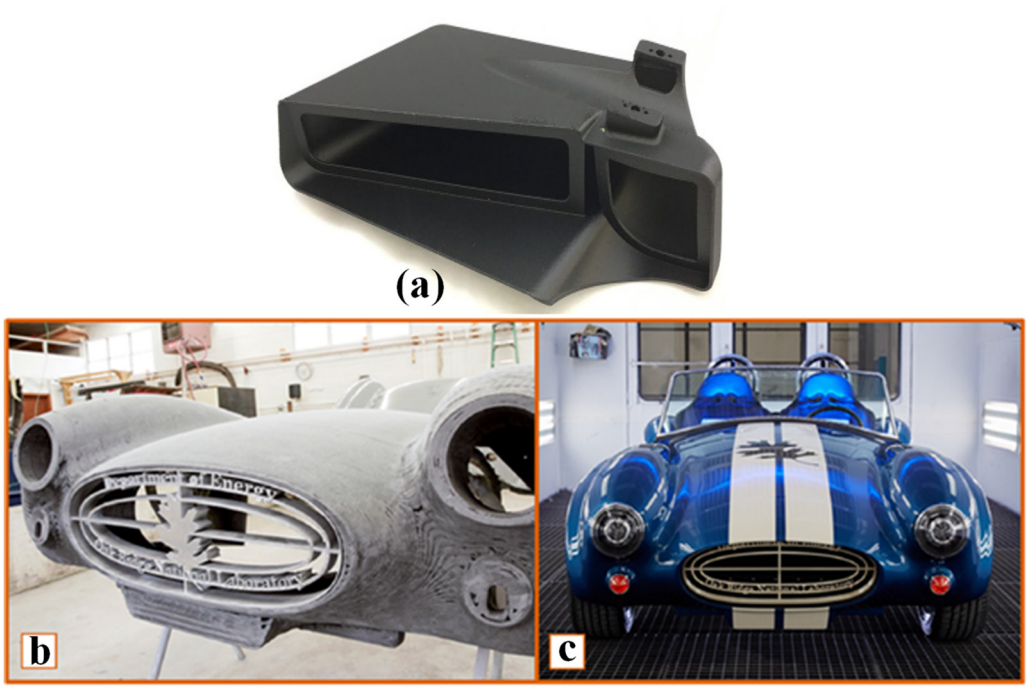

Fig. 27 (a) Side view mirror shell of a racing car participating in NASCAR. Adapted from ref. 244 (reused with permission, license number 5827081166703). Full-scale car reconstruction using CAM showing (b) rough bodywork and (c) finished bodywork. Adapted from ref. 258 (open access).

Fig. 28 Spare part reconstruction using CAM showing (a) inlet duct made of carbon fiber, (b) body components of Maserati MV 3200 GTC, and (c) related tooling, adapted from ref. 258 (open access).

electrical components and the engine. Firstly, a composite consisting of carbon fiber and ABS plastic was used to fabricate the chassis. Secondly, other components were separately fabricated and assembled to form the entire body (Fig. 27(b)). Finally, the entire car was painted (Fig. 27(c)) to replicate the original model.[248,258,259] Moreover, vehicle spare parts (*i.e.*, inlet ducts, body components, and tools) can also be reconstructed using CAM, as shown in Fig. 28.[258]

6.4 Application in soft robotics

At present, multi-material AM techniques can fabricate complex structures with precision, enabling the production of

Open Access Article. Published on 19 June 2026. Downloaded on 6/19/2026 11:23:52 PM.
This article is licensed under a Creative Commons Attribution 3.0 Unported Licence.

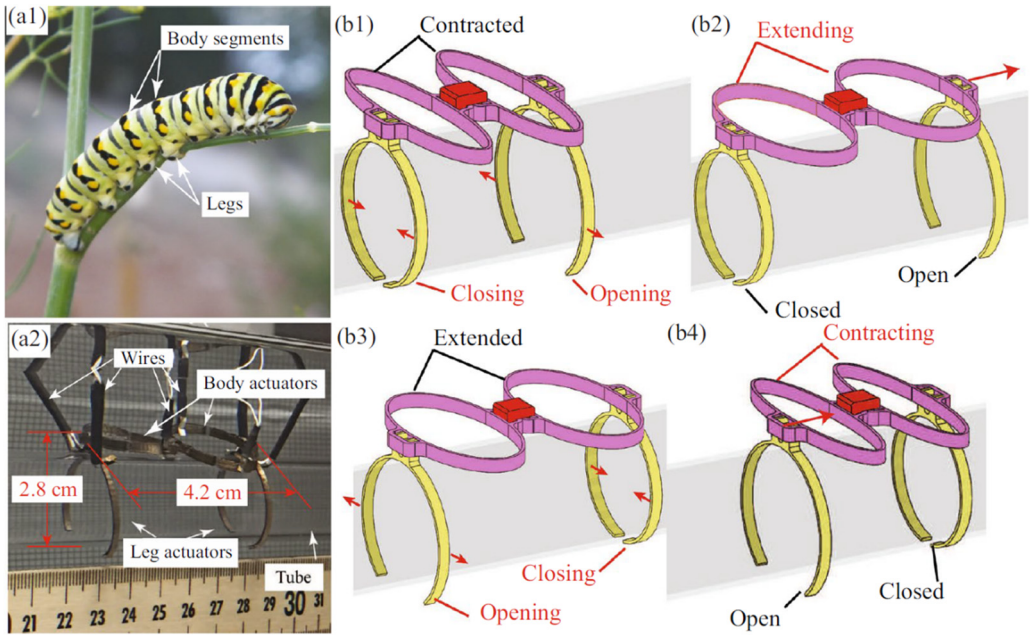

Fig. 29 (a1) Biological caterpillar, (a2) manufactured robot using the CAM technique, and (b1)–(b4) schematic diagram of the robot showing the actuator movement angle, adapted from ref. 266 (open access).

soft actuators with intricate geometries. Compared to conventional manufacturing methods, AM offers a significantly more convenient approach to fabricating soft actuators.[260] Multi-material AM is not only suitable for producing components of soft robots, such as soft actuators, but it also offers significant advantages in fabricating entire soft robots. Research by Bartlett *et al.* and Yap *et al.*[261,262] has demonstrated the potential of additively manufactured soft actuators in robotics. Soft magnetic composites (SMCs) are emerging materials that offer flexibility and magnetic responsiveness, making them ideal for flexible, untethered robotics.[263–265] These materials can be 3D printed into complex forms that integrate structural flexibility with magnetic functionality, enabling novel actuation and sensing. Their mechanical–magnetic synergy is well-suited to applications involving 3D-printed magnetic components under mechanical stress.[263] To minimize eddy current losses, preserving the insulating coating is crucial—binder-jet printing supports this, while DMLS offers high-density structures suitable for durable soft robotics.[264] In recent years, CAM has been extensively used to fabricate soft robots. For instance, Carrico *et al.*[266] additively manufactured a soft crawling robot using ionic polymer–metal composites that could simulate the movement of a biological caterpillar, as shown in Fig. 29. The researchers successfully created custom-shaped designs capable of performing nonlinear movements through CAM. This task would have been considerably challenging with conventional manufacturing techniques.[266] This issue can be addressed by altering the printer to incorporate softer materials into the filament feeding system, selecting a more ductile polymer for the matrix, or adding compounds that enhance the composite's overall ductility.[263] CAM can also produce an on-demand drug delivery soft robot that can deliver drugs inside the human body by crawling and non-linear movement, as demonstrated in Fig. 30.[260] Moreover, recent progress in AM of soft magnetic composites has enabled the fabrication of magnetic structures embedded in elastomers, well-suited for remotely controlled, flexible devices.[267] Concurrently, shape memory alloy actuators with built-in self-sensing functions have shown great potential for developing compact, high-strain morphing components in robotic systems.[265,268]

6.5 Applications in the biomedical industry

In the biomedical industry, the fabrication of composite materials has become feasible due to the integration of AM technology. These additively manufactured composite materials exhibit superior physical strength, mechanical properties, and biological characteristics, including biocompatibility, cell adhesion, cell proliferation, and non-toxicity, making them suitable for biomedical applications compared to conventional materials.[269,270] For instance, carbon fiber-reinforced polyether ether ketone (PEEK) composites exhibit superior cell adhesion, biocompatibility, and regeneration capability compared to pure PEEK.[270,271] In organ and tissue transplantation, the manufacture of artificial tissues and organs has emerged as one of the most promising solutions to address limitations in current approaches, such as donor shortages, immunological rejection, and high costs.[12] Hydroxyapatite/titanium composites are considered suitable materials for implant applications in bone tissue engineering.[270,271] Moreover, the development of functionally graded material implants has been enabled by CAM.[4,270] Fig. 31 shows a scaffold made of the nano-hydroxyapatite/poly-ε-caprolactone composite that was applied to a defective rabbit femur due to its biocompatibility,

© 2026 The Author(s). Published by the Royal Society of Chemistry

Open Access Article. Published on 19 June 2026. Downloaded on 6/19/2026 11:23:52 PM.
This article is licensed under a Creative Commons Attribution 3.0 Unported Licence.

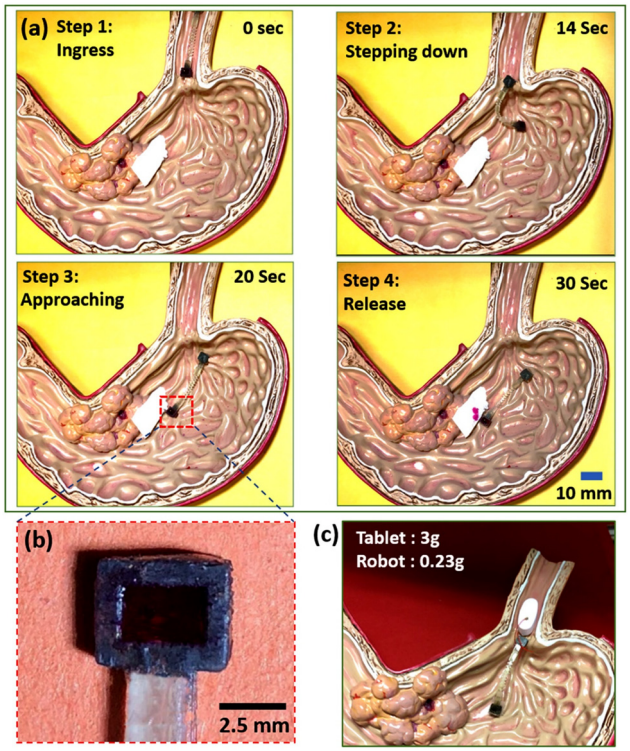

Fig. 30 Additive manufactured composite soft robot for drug delivery in the human body showing (a) traveling process of the soft robot inside the human body, (b) integrated reservoir for drugs, and (c) composite soft robot carrying a capsule, adapted from ref. 260 (reused with permission, license number 5827090073224).

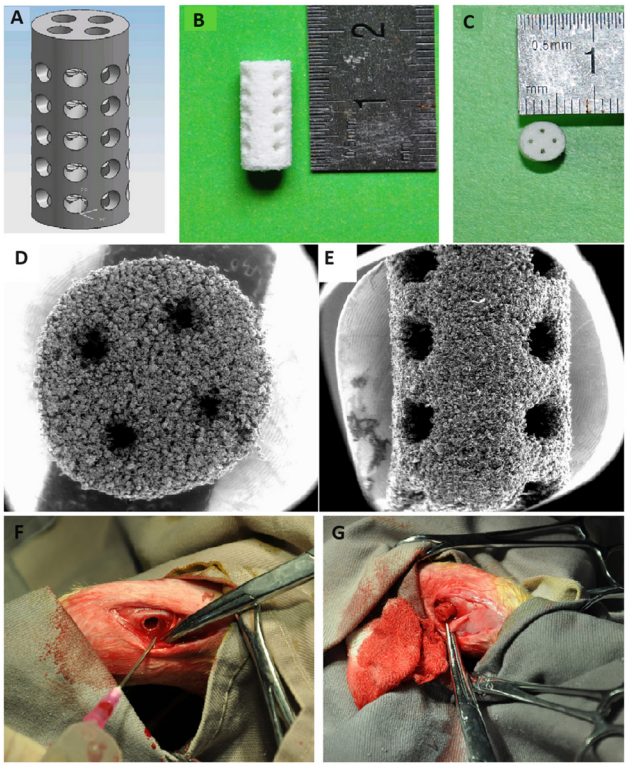

Fig. 31 (A) CAD model of the scaffold, (B) and (C) SLS fabricated scaffold, (D) and (E) scanning electron microscopy of the scaffold, and (F)–(G) application of the scaffold in the defective femur of the rabbit. Adapted from ref. 272 (open access).

degradability, and ability to accomplish expected cellular interactions.[12,272]

7. Prospects and challenges

CAM is approaching a transition point where incremental improvements in hardware and feedstock will not, by themselves, deliver the repeatability required for safety-critical adoption. The central barrier is not geometric capability but manufacturing stability: fiber orientation/architecture, void formation, and interfacial bonding evolve dynamically with thermal history, rheology, and path scheduling, and small disturbances can amplify into property scatter. Consequently, the next step-change in CAM reliability is expected to come from sensor-rich data streams coupled with ML models explicitly designed to support optimization and control, rather than *post hoc* quality classification.[273,274]

7.2 Data scarcity and the label bottleneck

A persistent obstacle for ML-enabled CAM is the shortage of high-quality labeled datasets that link process signals, microstructure, or defects to resulting properties. This bottleneck is well recognized in AM broadly: destructive testing is slow and expensive, while ground-truth defect labels (*e.g.*, CT-derived porosity) require specialized metrology and careful registration to *in situ* signals.[188,190,274] A practical path forward for CAM is to combine three complementary strategies: (i) physics-informed or hybrid substitutes that reduce dependence on dense labels by embedding known process constraints, (ii) active-learning acquisition that prioritizes experiments/inspections where model uncertainty is highest, and (iii) community benchmark datasets and protocols that enable reproducible comparisons across machines and materials. The AM-Bench framework[275] demonstrates how shared measurement datasets can accelerate model validation and trust, an approach that CAM urgently needs for fiber-reinforced systems (including standardized reporting of reinforcement morphology, fiber volume fraction, and anisotropic properties).

7.3 Sensor integration, synchronization, and multimodal monitoring

To move from "ML as analytics" to "ML as a manufacturing tool," CAM requires instrumentation that is (a) synchronized, (b) calibrated, and (c) informative for the dominant failure modes. Reviews[188,274] of *in situ* monitoring across both polymer and metal AM emphasize that single sensors are rarely sufficient; robust inference typically requires multimodal data fusion (*e.g.*, vision or thermography combined with force/torque or drive signals and acoustic or vibration measurements), together with accurate time-stamping and spatial registration to the toolpath. For material extrusion CAM in particular, *in situ* monitoring frameworks highlight the role of

Open Access Article. Published on 19 June 2026. Downloaded on 6/19/2026 11:23:52 PM.
This article is licensed under a Creative Commons Attribution 3.0 Unported Licence.

extrusion dynamics, bead geometry, thermal management, and layerwise imaging for detecting porosity, under-extrusion, and interlayer bonding defects.[274] For laser-based processes, monitoring should capture melt-pool/track stability and thermal gradients that govern defect formation and interfacial quality, variables that directly affect reinforcement distribution, residual stress, and cracking susceptibility in composite or particulate-reinforced systems.[276]

7.4 From monitoring to real-time decision-making and control

A key point repeatedly raised in the AM literature is that detection alone is insufficient: actionable ML should connect monitoring outputs to control levers (*e.g.*, process parameters, toolpath updates, or energy input adjustments).[188,276] A study[276] synthesizing ML-assisted closed-loop strategies frames the problem in terms of observability (the ability to measure defect precursors) and controllability (the availability of actuators capable of correcting deviations within the required time scale). For CAM, the most meaningful near-term control targets are: (i) porosity suppression (*via* thermal management, flow stabilization, and consolidation), (ii) interlayer/interface strengthening (*via* temperature/pressure history control), and (iii) reinforcement architecture fidelity (*via* path scheduling, shear history management, and continuous-fiber placement logic). Implementations should report not only accuracy metrics but also latency, robustness under drift, and uncertainty, because control decisions should be made under sensor noise and changing boundary conditions.[25,276]

7.5 Standardization, qualification, and benchmarking for ML-CAM

For high-impact publication and transferability beyond a single machine, ML-enabled CAM studies should converge on: (i) shared data schemas and metadata, (ii) benchmark artifacts coupled with standardized test plans, and (iii) qualification-aligned reporting. Benchmark initiatives explicitly designed around high-quality measurements (*e.g.*, AM-Bench) provide a proven model for cross-comparison and should be adapted to CAM with composite-specific descriptors (fiber type/length distribution, sizing chemistry, dispersion metrics, and anisotropic mechanical test suites).[275,277] In parallel, qualification-oriented standards for critical AM processes illustrate how workflow structuring, spanning personnel, digital data, equipment, feedstock, qualification, and the manufacturing plan can be formalized; CAM roadmaps should therefore align ML data collection and model validation with these qualification steps, rather than treating ML as an isolated research add-on.[278]

7.6 Digital twins, cloud/edge deployment, and the digital thread

A realistic action plan for ML-enabled CAM can be framed as a digital-twin/digital-thread architecture, in which design and toolpath files, machine states, *in situ* sensor streams, inspection results, and qualification data remain connected across the build lifecycle. Within this loop, models are updated from process data and used to predict quality outcomes under candidate parameter or toolpath changes. As summarized in Fig. 32, AM digital twins combine process sensing and control with training and testing data, mechanistic models, and dynamic feedback so that monitoring, prediction, and optimization can support both low-latency edge decisions and scalable cloud-based data management.[25,276] Validated multiphysics models and data-driven surrogates can therefore support process planning, defect mitigation, and qualification, which is especially important in CAM because process history strongly affects anisotropic microstructure and performance.[25,279]

This architecture can be implemented first as a passive twin and then matured into an active, closed-loop control. A passive

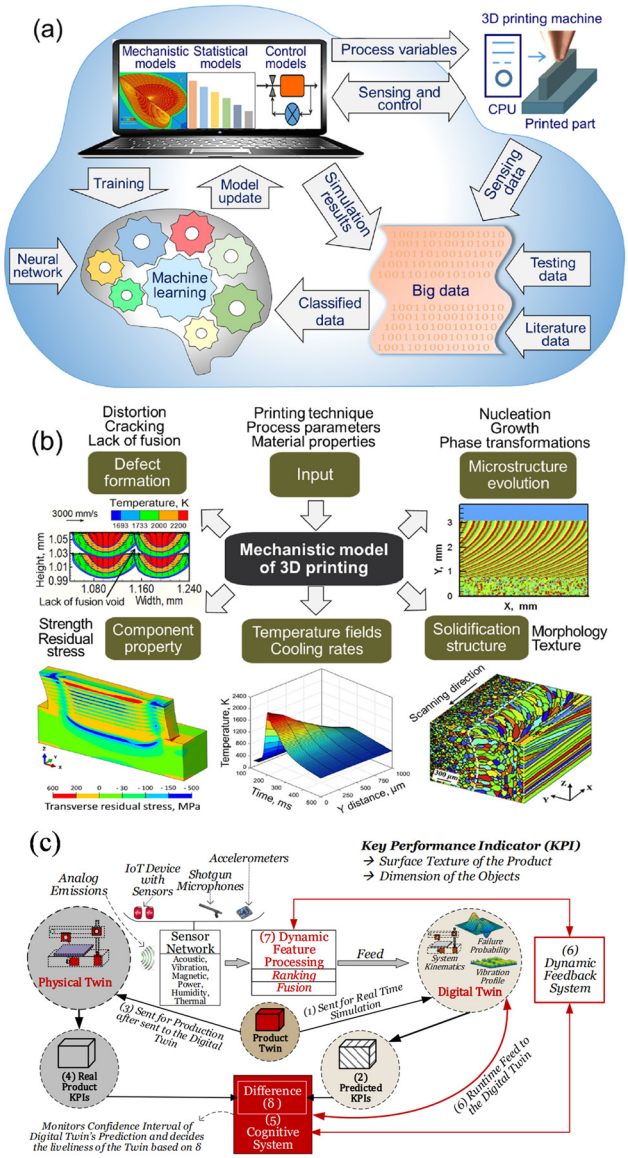

Fig. 32 Digital-twin concepts for AM: (a) digital-twin workflow for AM and (b) mechanistic model of 3D printing, adapted from ref. 280 (reused with permission, license number 6260630476580); and (c) dynamic data-driven application system-enabled digital twin of an AM cyber-physical system ref. 281 (open access).

© 2026 The Author(s). Published by the Royal Society of Chemistry

Open Access Article. Published on 19 June 2026. Downloaded on 6/19/2026 11:23:52 PM. This article is licensed under a Creative Commons Attribution 3.0 Unported Licence.

CAM twin synchronizes design files, machine states, sensor streams, inspection results, and predicted quality states, but its outputs remain limited to visualization, anomaly alerts, offline parameter recommendations, or post-build acceptance decisions. An active CAM twin adds state estimation, uncertainty-aware decision logic, and validated actuation, allowing deposition parameters such as laser power, scan speed, feed rate, extrusion temperature, bead pressure, cooling rate, toolpath scheduling, or local repair actions to be adjusted when sensor evidence indicates drift from the qualified process window. This distinction is critical: passive monitoring primarily strengthens traceability, whereas active control changes the manufacturing history of the part and therefore requires controller-stability analysis, latency reporting, fail-safe rules, and evidence that corrective actions improve microstructure or properties rather than only the sensor signal.[25,275,276,279]

8. Roadmap for ML-enabled CAM: from sensing to benchmarking, closed-loop control, and digital twins (2025–2035)

To transition ML-CAM from promising demonstrations to a reproducible, certifiable, and industrially scalable practice, a staged roadmap is required that connects sensor-based data collection, standardized benchmarking, real-time process control, and digital twin/cloud integration. The roadmap below is aligned with the literature showing that (i) multi-modal *in situ* sensing is the prerequisite for robust inference and defect observability, (ii) community benchmarking is essential for trustworthy model comparisons, and (iii) closed-loop control and digital twins demand low-latency data pipelines and validated physics-data hybrid models.[25,274,276]

8.2 Phase 1 (0–2 years): sensor-based data collection and analysis-ready datasets

Objectives: establish reliable, well-annotated datasets that enable supervised ML, cross-platform comparison, and downstream model development.

1. Multi-modal sensing stacks (process, part, and environment): deploy synchronized thermal and visible imaging, acoustic and vibration sensing, and power, force, and position measurements, supplemented where applicable by subsurface sensing. Emphasize calibration, accurate time-stamping, and multimodal sensor fusion to capture both defect signatures and process signatures.[274,282]

2. Ground-truth linking for supervised ML: Build paired datasets that connect *in situ* sensor streams with *ex situ* metrology and inspection (*e.g.*, X-ray microCT/CT, microscopy, and mechanical testing), enabling traceable labels, uncertainty quantification, and model validation.[274,282]

3. Data governance and interoperability: Define minimal yet sufficient metadata (*e.g.*, machine, material, lot, toolpath, and environment), along with sampling specifications and standardized storage formats, to ensure dataset reuse and interoperability across laboratories and platforms.[274]

Deliverable (end of phase 1): public or consortium datasets featuring consistent metadata, documented sensor calibration, and standardized baseline splits (training, validation, and test sets), suitable for benchmarking and reproducible ML development.

8.3 Phase 2 (2–5 years): standardized ML-CAM benchmarking protocols

Objectives: enable fair, reproducible, and transferable evaluation of ML-enabled CAM models and control strategies across machines, materials, and laboratories.

1. Benchmark test cases and measurement challenges: adapt the AM-Bench concept, combining controlled builds, rich multimodal measurements, and shared prediction challenges, to CAM-relevant materials and processes. Such benchmarks enable direct, like-for-like comparison of models, inference pipelines, and control strategies.[277]

2. Benchmark metrics beyond accuracy: require reporting of performance metrics that reflect operational relevance, including receiver operating characteristic (ROC)- or probability-of-detection (POD)-style curves (false-alarm *versus* miss-rate trade-offs), robustness across builds and machines, and uncertainty calibration. These metrics are particularly critical for defect detection and anomaly monitoring tasks.[283]

3. Reproducibility checklist: standardize reporting of data preprocessing steps, feature construction, domain-shift mitigation strategies, and inference latency (to assess real-time readiness), together with explicit dataset and version identifiers.

Deliverable (end of phase 2): a community-defined ML-CAM benchmarking protocol encompassing shared datasets, standardized metrics, and reporting guidelines, validated through multi-laboratory round-robin studies.

Regulatory acceptance of ML-driven QA should build on the phase 2 benchmarking protocol, but it will require more than benchmark accuracy. For CAM, the evidence package should document data provenance, feedstock lot and conditioning history, machine configuration, sensor calibration, software and model version, training and validation splits, uncertainty bounds, out-of-distribution tests, and all process interventions performed during closed-loop operation. Certification bodies will also need clear separation between model-assisted evidence and final acceptance criteria: ML can prioritize inspection, detect process drift, recommend parameter changes, or support a digital-thread audit, but part release should remain tied to validated quality characteristics, mechanical allowables, inspection capability, and documented process control. Existing AM qualification and critical-application standards provide a starting point for production-site qualification, process control, and documentation, but CAM-specific adoption requires additional consensus on anisotropic test specimens, fiber-orientation and interface descriptors, benchmark builds, model change-control procedures, cybersecurity of the digital thread, and procedures for revalidation after feedstock, machine, sensor, or software changes.[27,283,284]

Open Access Article. Published on 19 June 2026. Downloaded on 6/19/2026 11:23:52 PM. This article is licensed under a Creative Commons Attribution 3.0 Unported Licence.

8.3 Phase 3 (3–7 years): real-time process control systems (closed-loop ML)

Objectives: transition ML-enabled CAM from passive monitoring and offline optimization to reliable, adaptive, and certifiable *in situ* process control.

1. From monitoring to diagnosis and action: progress from offline optimization and online detection toward adaptive *in situ* control strategies capable of defect avoidance, mitigation, or repair. This requires fast ML inference on streaming data, coupled with control-theoretic guardrails to ensure stability and safety.[274,276]

2. Measurement science for closed-loop feasibility: prioritize measurands and sensing modalities that are demonstrably linked to quality outcomes, recognizing that inadequate or weakly correlated measurements remain a primary barrier to effective real-time control.[190,275]

3. Edge deployment and fail-safe logic: implement low-latency edge inference for time-critical control loops and incorporate uncertainty-aware decision logic to prevent unsafe interventions when models operate outside their training distribution.

Deliverable (end of phase 3): demonstrated closed-loop ML control on benchmark CAM problems, with quantified improvements in process stability, latency, and part quality.

8.4 Phase 4 (5–10 years): integration with digital twins and cloud platforms (digital thread)

Objectives: integrate ML-enabled CAM into scalable, traceable, and qualification-ready digital ecosystems that support prediction, control, and lifecycle management across distributed manufacturing environments.

1. Hybrid physics-data digital twins: combine validated multiphysics models with ML-based surrogate models to achieve near-real-time prediction of process and part states (*e.g.*, thermal fields and distortion). Such hybrid digital twins enable ''what-if'' control decisions and predictive quality assessment during manufacturing.[25,36]

2. Digital thread data packaging: implement end-to-end traceability across the manufacturing lifecycle, spanning design, process planning, *in situ* sensing, inspection, and certification, through standardized digital data packages. This digital thread is essential for qualification, auditability, and regulated deployment of CAM systems.[283]

3. Cloud and remote twin ecosystems: use cloud and cloud-edge infrastructures for scalable data storage, model lifecycle management, federated benchmarking, and remote monitoring and control. Emerging validated digital-twin ecosystems demonstrate the feasibility of real-time synchronization and large-scale analytics across distributed manufacturing assets.[285,286]

4. Twin-enabled advanced control: progress toward digital-twin-enabled model predictive control and optimization frameworks that tightly integrate prediction, decision-making, and constraint handling. Such approaches support robust operation across varying jobs, materials, and process conditions.[37]

Deliverable (end of phase 4): a deployable ML-CAM digital-twin framework spanning edge and cloud resources, capable of supporting qualification evidence, audit trails, and continuous process improvement across the digital thread.

9. Conclusions

CAM is entering a decisive transition from geometry-driven prototyping to performance-directed production of architected, multifunctional, and application-specific composite systems. However, its broader industrial translation remains limited by composite-specific uncertainty arising from nonuniform reinforcement dispersion, orientation drift, incomplete interfacial bonding, defect-sensitive property scatter, and insufficient standardization across materials, machines, and process routes. The synthesis presented in this review shows that these limitations cannot be resolved by optimizing materials, process parameters, or data-driven models in isolation. Instead, the composite interface must be treated as the central organizing variable linking feedstock architecture, process physics, microstructural evolution, defect formation, and final performance. Dispersion, orientation, interphase formation, void morphology, lack of fusion, residual stress, and anisotropic property scatter are therefore best understood as coupled outcomes of a process–structure–property–control system, with distinct manifestations across vat photopolymerization, binder jetting, material extrusion, selective laser sintering, directed energy deposition, and emerging hybrid or multi-material CAM platforms.

A major conclusion of this review is that the role of ML in CAM is rapidly shifting from retrospective data analysis toward active participation in materials selection, toolpath and topology design, *in situ* monitoring, process optimization, and qualification-oriented decision-making. ML is increasingly valuable not because it replaces mechanistic understanding, but because it can connect heterogeneous data streams, reveal process-sensitive correlations, accelerate parameter-space exploration, and support closed-loop control when embedded within physically constrained workflows. This transition is especially important for emerging CAM inflection points, including high-productivity volumetric stereolithography, scalable binder-jet strategies, advanced polymer-composite extrusion, support-free selective laser sintering, variability reduction in directed energy deposition, and spatially controlled hybrid and multi-material manufacturing. For fusion-based metal and composite systems, process maps should extend beyond nominal heat input and bead geometry to include solidification descriptors such as thermal gradient, solidification rate, their ratio, and cooling-rate products, thereby linking processing conditions to segregation, reinforcement redistribution, residual stress, cracking susceptibility, and interfacial stability.

Despite these advances, the field still lacks a qualification-oriented evidentiary framework capable of converting promising laboratory demonstrations into transferable, certifiable manufacturing practices. Mechanical strength alone is no

© 2026 The Author(s). Published by the Royal Society of Chemistry

Open Access Article. Published on 19 June 2026. Downloaded on 6/19/2026 11:23:52 PM. This article is licensed under a Creative Commons Attribution 3.0 Unported Licence.

longer an adequate basis for process comparison or deployment claims. Future CAM benchmarking must integrate anisotropy ratios, fatigue performance, interlaminar strength, fracture metrics, porosity and defect-size distributions, dimensional accuracy, surface topography, build rate, energy input, throughput, and process repeatability. Similarly, multiscale simulations should progress from idealized homogenization toward experimentally calibrated, defect-informed, cohesive/interphase-aware models that are validated against full-field strain measurements, microscopy, X-ray microCT, and failure observations. Such benchmarking and modeling discipline is essential for separating genuine process capability from geometry-specific, machine-specific, or dataset-specific performance.

The next stage of CAM development should therefore follow a staged pathway that links sensing, benchmarking, modeling, control, and certification evidence within a qualification-ready digital thread. Priority actions include establishing synchronized multimodal sensing with robust calibration, spatial registration, and time-stamping; building paired datasets that connect *in situ* process signatures to *ex situ* ground truth; defining community-level benchmarking protocols and operational metrics beyond prediction accuracy; demonstrating closed-loop control using low-latency inference, uncertainty-aware decision rules, and safety guardrails; and integrating hybrid physics-data digital twins with lifecycle traceability. These digital threads should also include design-of-experiments planning, build-wise, batch-wise, geometry-wise, and machine-wise validation splits, external validation, out-of-distribution detection, model-version tracking, and auditable regulatory evidence dossiers.

Future ML-CAM studies should explicitly state the intended function of each model: passive monitoring, offline optimization, design-space exploration, process-window mapping, or active closed-loop control. Model selection should be justified by the data modality and manufacturing decision being addressed. Tabular surrogates, Gaussian-process models, Bayesian methods, and ensemble learners are well suited for process–structure–property mapping; CNNs, vision transformers, and segmentation models are appropriate for spatial defects, melt-pool signatures, and reinforcement clustering; recurrent, transformer, and state-space architectures are suitable for toolpath-linked temporal signals; and reinforcement learning or model-predictive control is appropriate for sequential process decisions. In data-scarce regimes, transfer learning, domain adaptation, self-supervised learning, simulation pretraining, and physics-informed learning offer promising routes, but only when accompanied by physical consistency checks, uncertainty calibration, explainability, and independent validation. Accuracy alone should not be treated as qualification evidence unless predictions are traceable to composite descriptors, bounded by calibrated uncertainty, and interpretable in terms of process physics and microstructural mechanisms.

Overall, the most compelling outlook is that scalable and certifiable CAM will emerge from the convergence of interface-aware feedstock design, process-resolved multiscale modeling, standardized benchmarking, and ML-enabled closed-loop control. The field's central challenge is no longer simply to print complex composite geometries, but to manufacture composite performance with reproducible evidence. Achieving this goal will require passive-to-active digital-twin ecosystems in which calibrated sensors, physics-guided models, uncertainty-aware ML, guarded actuation, and auditable qualification records mature together. Such integration would transform CAM from a largely empirical and demonstration-driven technology into a predictive, traceable, and certification-ready manufacturing platform for aerospace, biomedical, energy, mobility, and other safety-critical applications.

Author contributions

Md Zillur Rahman: conceptualization, validation, supervision, project administration, writing - original draft, writing - review and editing; H K Mahedi Azad: data curation, investigation, methodology, writing - original draft; Morad Hossain Diganto: investigation, methodology, writing - original draft.

Conflicts of interest

The authors declare that they have no conflict of interest.

Data availability

Data will be made available upon request.

References

1 A. Islam and M. Z. Rahman, Recent advances in additive manufacturing techniques: An in-depth review, *Comprehensive Materials Processing*, Elsevier, 2nd edn, 2024.
2 S. Ford and M. Despeisse, Additive manufacturing and sustainability: an exploratory study of the advantages and challenges, *J. Cleaner Prod.*, 2016, **137**, 1573–1587.
3 M. A. Shahriar, M. H. Kobir, S. Rahman, M. Z. Rahman and B. Saha, Overview of additive manufacturing and applications of 3D printed composites, *Comprehensive Materials Processing*, Elsevier, 2nd edn, 2024.
4 H. A. Hegab, Design for additive manufacturing of composite materials and potential alloys: a review, *Manuf. Rev.*, 2016, **3**, 11.
5 A. Islam and M. Z. Rahman, Composite additive manufacturing: An overview of current state, limitations, and progress, *Comprehensive Materials Processing*, Elsevier, 2nd edn, 2024.
6 A. M. Arka, *et al.*, A review on additively manufactured materials in biomedical applications, *Comprehensive Materials Processing*, Elsevier, 2nd edn, 2024.
7 E. D. Herderick, Progress in additive manufacturing, *Jom*, 2015, **67**(3), 580–581.
8 A. Islam and M. Z. Rahman, Recent advances in additive manufacturing of ceramic and graphene and their

Open Access Article. Published on 19 June 2026. Downloaded on 6/19/2026 11:23:52 PM. This article is licensed under a Creative Commons Attribution 3.0 Unported Licence.

applications, *Comprehensive Materials Processing*, 2nd edn, Elsevier, 2024.
9 P. Parandoush and D. Lin, A review on additive manufacturing of polymer-fiber composites, *Compos. Struct.*, 2017, **182**, 36–53.
10 K. Chen, *et al.*, A review of machine learning in additive manufacturing: design and process, *Int. J. Adv. Manuf. Technol.*, 2024, **135**(3), 1051–1087.
11 S. S. Babu, A.-H. I. Mourad, K. H. Harib and S. Vijayavenkataraman, Recent developments in the application of machine-learning towards accelerated predictive multiscale design and additive manufacturing, *Virtual Phys. Prototyping*, 2023, **18**(1), e2141653.
12 S. Park, W. Shou, L. Makatura, W. Matusik and K. K. Fu, 3D printing of polymer composites: Materials, processes, and applications, *Matter*, 2022, **5**(1), 43–76.
13 R. Velu, F. Raspall and S. Singamneni, 3D printing technologies and composite materials for structural applications, *Green Composites for Automotive Applications*, Elsevier, 2019, pp. 171–196.
14 M. M. Rahman, S. B. Rayhan, J. Sultana and M. Z. Rahman, Additive manufacturing techniques, their challenges, and additively manufactured composites for advanced engineering applications, *Comprehensive Materials Processing*, Elsevier, 2nd edn, 2023.
15 H. R. Jani and M. Z. Rahman, Modeling and simulation of additively manufactured composites, *Comprehensive Materials Processing*, Elsevier, 2nd edn, 2024.
16 M. Pagac, *et al.*, A review of vat photopolymerization technology: materials, applications, challenges, and future trends of 3D printing, *Polymers*, 2021, **13**(4), 598.
17 S. M. A. Nipu, *et al.*, 13.12 – Additive manufacturing-based composites for sensors and other applications, *Comprehensive Materials Processing*, ed. S. Hashmi, Elsevier, Oxford, 2nd edn, 2024, pp. 214–240.
18 S. Salifu, O. Ogunbiyi and P. A. Olubambi, Potentials and challenges of additive manufacturing techniques in the fabrication of polymer composites, *Int. J. Adv. Manuf. Technol.*, 2022, **122**(2), 577–600.
19 E. H. Sabuz and M. Z. Rahman, 13.04 – Modeling and simulation on additive manufacturing of composite materials, *Comprehensive Materials Processing*, ed. S. Hashmi, Elsevier, Oxford, 2nd edn, 2024, pp. 77–90.
20 A. P. Deshmankar, J. S. Challa, A. R. Singh and S. P. Regalla, A Review of the Applications of Machine Learning for Prediction and Analysis of Mechanical Properties and Microstructures in Additive Manufacturing, *J. Comput. Inf. Sci. Eng.*, 2024, **24**(12), 120801.
21 G. Vashishtha, S. Chauhan, R. Zimroz, N. Yadav, R. Kumar and M. K. Gupta, Current applications of machine learning in additive manufacturing: a review on challenges and future trends, *Arch. Comput. Methods Eng.*, 2024, 1–34.
22 J. Jiang, A survey of machine learning in additive manufacturing technologies, *Int. J. Comput. Integr. Manuf.*, 2023, **36**(9), 1258–1280.
23 L. Tudorache, Ö. Babur, S. S. Lucas and M. van den Brand, Current approaches to digital twins in additive manufacturing: a systematic literature review, *Prog. Addit. Manuf.*, 2025, **10**(12), 10819–10853.
24 L. Zhang, *et al.*, Digital twins for additive manufacturing: a state-of-the-art review, *Appl. Sci.*, 2020, **10**(23), 8350.
25 T. Shen and B. Li, Digital twins in additive manufacturing: a state-of-the-art review, *Int. J. Adv. Manuf. Technol.*, 2024, **131**(1), 63–92.
26 K. Yanamandra, G. L. Chen, X. Xu, G. Mac and N. Gupta, Reverse engineering of additive manufactured composite part by toolpath reconstruction using imaging and machine learning, *Compos. Sci. Technol.*, 2020, **198**, 108318.
27 ISO/ASTM 52920:2023:Additive manufacturing—Qualification principles—Requirements for industrial additive manufacturing processes and production sites, I. O. F. Standardization, 2023.
28 Z. Chen, C. Han, M. Gao, S. Y. Kandukuri and K. Zhou, A review on qualification and certification for metal additive manufacturing, *Virtual Phys. Prototyping*, 2022, **17**(2), 382–405.
29 X. Qi, G. Chen, Y. Li, X. Cheng and C. Li, Applying neural-network-based machine learning to additive manufacturing: current applications, challenges, and future perspectives, *Engineering*, 2019, **5**(4), 721–729.
30 Z. Jin, Z. Zhang, K. Demir and G. X. Gu, Machine learning for advanced additive manufacturing, *Matter*, 2020, **3**(5), 1541–1556.
31 C. Wang, X. P. Tan, S. B. Tor and C. Lim, Machine learning in additive manufacturing: State-of-the-art and perspectives, *Addit. Manuf.*, 2020, **36**, 101538.
32 M. Shusteff, *et al.*, One-step volumetric additive manufacturing of complex polymer structures, *Sci. Adv.*, 2017, **3**(12), eaao5496.
33 M. Ziaee and N. B. Crane, Binder jetting: A review of process, materials, and methods, *Addit. Manuf.*, 2019, **28**, 781–801.
34 G. X. Gu, C.-T. Chen, D. J. Richmond and M. J. Buehler, Bioinspired hierarchical composite design using machine learning: simulation, additive manufacturing, and experiment, *Mater. Horiz.*, 2018, **5**(5), 939–945.
35 K. V. Wong and A. Hernandez, A review of additive manufacturing, *Int. Scholarly Res. Not.*, 2012, **2012**(1), 208760.
36 H. Mu, F. He, L. Yuan, H. Hatamian, P. Commins and Z. Pan, Online distortion simulation using generative machine learning models: A step toward digital twin of metallic additive manufacturing, *J. Ind. Inf. Integr.*, 2024, **38**, 100563.
37 V. D. Kolate, M. K. Chaudhary, S. Mane and M. Devadhe, Digital twin–enabled model predictive control in additive manufacturing: critical review, research challenges, and future directions, *Mater. Manuf. Processes*, 2025, 1–17.
38 Y. Regassa, H. G. Lemu and B. Sirabizuh, Trends of using polymer composite materials in additive manufacturing, *IOP Conf. Ser.:Mater. Sci. Eng.*, 2019, 659, 1, p. 012021.

© 2026 The Author(s). Published by the Royal Society of Chemistry

Open Access Article. Published on 19 June 2026. Downloaded on 6/19/2026 11:23:52 PM. This article is licensed under a Creative Commons Attribution 3.0 Unported Licence.

39 X. Wang, M. Jiang, Z. Zhou, J. Gou and D. Hui, 3D printing of polymer matrix composites: A review and prospective, *Composites, Part B*, 2017, **110**, 442–458.
40 N. P. Padture, Advanced structural ceramics in aerospace propulsion, *Nat. Mater.*, 2016, **15**(8), 804–809.
41 N. Travitzky, *et al.*, Additive manufacturing of ceramic-based materials, *Adv. Eng. Mater.*, 2014, **16**(6), 729–754.
42 Z. Lu, J. Cao, Z. Song, D. Li and B. Lu, Research progress of ceramic matrix composite parts based on additive manufacturing technology, *Virtual Phys. Prototyp.*, 2019, **14**(4), 333–348.
43 H. K. M. Azad and M. Z. Rahman, Ceramic matrix composites with particulate reinforcements—Progress over the past 15 years, *Comprehensive Materials Processing*, Elsevier, 2nd edn, 2024, pp. 395–408.
44 H. K. M. Azad and M. Z. Rahman, A critical review of developments in the characterization of metal matrix composites with particulate reinforcements, *Comprehensive Materials Processing*, Elsevier, 2nd edn, 2024, pp. 442–458.
45 M. P. Behera, T. Dougherty and S. Singamneni, Conventional and additive manufacturing with metal matrix composites: a perspective, *Proc. Manuf.*, 2019, **30**, 159–166.
46 A. Mussatto, I. U. Ahad, R. T. Mousavian, Y. Delaure and D. Brabazon, Advanced production routes for metal matrix composites, *Eng. Rep.*, 2021, **3**(5), e12330.
47 A. Alfaify, M. Saleh, F. M. Abdullah and A. M. Al-Ahmari, Design for additive manufacturing: A systematic review, *Sustainability*, 2020, **12**(19), 7936.
48 S. Ford, L. Mortara and T. Minshall, The emergence of additive manufacturing: introduction to the special issue, 2016.
49 A. others Standard, Standard terminology for additive manufacturing technologies, ASTM Int, ed: F2792–12a, 2012.
50 I. Gibson, *et al.*, *Additive manufacturing technologies*, Springer, 2021.
51 R. Singh, *et al.*, Powder bed fusion process in additive manufacturing: An overview, *Mater. Today: Proc.*, 2020, **26**, 3058–3070.
52 F. M. Mwema and E. T. Akinlabi, *Fused deposition modeling: strategies for quality enhancement*, Springer nature, 2020.
53 X. Li, *et al.*, Qualify assessment for extrusion-based additive manufacturing with 3D scan and machine learning, *J. Manuf. Process.*, 2023, **90**, 274–285.
54 S. C. Daminabo, S. Goel, S. A. Grammatikos, H. Y. Nezhad and V. K. Thakur, Fused deposition modeling-based additive manufacturing (3D printing): techniques for polymer material systems, *Mater. Today Chem.*, 2020, **16**, 100248.
55 M. A. Mahmood, A. I. Visan, C. Ristoscu and I. N. Mihailescu, Artificial neural network algorithms for 3D printing, *Materials*, 2020, **14**(1), 163.
56 I. Gibson, *et al.*, *Additive manufacturing technologies*, Springer, 2021.
57 A. Mostafaei, *et al.*, Binder jet 3D printing—Process parameters, materials, properties, modeling, and challenges, *Prog. Mater. Sci.*, 2021, **119**, 100707.
58 A. Levy, *et al.*, Ultrasonic additive manufacturing of steel: method, post-processing treatments and properties, *J. Mater. Process. Technol*, 2018, **256**, 183–189.
59 S. L. Sing and W. Y. Yeong, Emerging Materials for Additive Manufacturing, *Material*, 2022, **16**, 127.
60 A. Dass and A. Moridi, State of the art in directed energy deposition: From additive manufacturing to materials design, *Coatings*, 2019, **9**(7), 418.
61 M. Ahmadifar, K. Benfriha, M. Shirinbayan and A. Tcharkhtchi, Additive manufacturing of polymer-based composites using fused filament fabrication (FFF): a review, *Appl. Compos. Mater.*, 2021, **28**(5), 1335–1380.
62 P. Consul, K.-U. Beuerlein, G. Luzha and K. Drechsler, Effect of extrusion parameters on short fiber alignment in fused filament fabrication, *Polymers*, 2021, **13**(15), 2443.
63 Y. Zhang, Y. Yu, L. Wang, Y. Li, F. Lin and W. Yan, Dispersion of reinforcing micro-particles in the powder bed fusion additive manufacturing of metal matrix composites, *Acta Mater.*, 2022, **235**, 118086.
64 W. Du, X. Ren, Z. Pei and C. Ma, Ceramic binder jetting additive manufacturing: a literature review on density, *J. Manuf. Sci. Eng.*, 2020, **142**(4), 040801.
65 A. Lores, N. Azurmendi, I. Agote and E. Zuza, A review on recent developments in binder jetting metal additive manufacturing: materials and process characteristics, *Powder Metallurgy*, 2019, **62**(5), 267–296.
66 S. Hasanov, *et al.*, Review on additive manufacturing of multi-material parts: Progress and challenges, *J. Manuf. Mater. Process.*, 2021, **6**(1), 4.
67 A. Elkaseer, K. J. Chen, J. C. Janhsen, O. Refle, V. Hagenmeyer and S. G. Scholz, Material jetting for advanced applications: A state-of-the-art review, gaps and future directions, *Addit. Manuf.*, 2022, **60**, 103270, DOI: 10.1016/j.addma.2022.103270.
68 D. S. Thomas and S. W. Gilbert, Costs and cost effectiveness of additive manufacturing, *NIST Spec. Publ.*, 2014, **1176**, 12.
69 D.-G. Ahn, Directed energy deposition (DED) process: state of the art, *Int. J. Precis. Eng. Manuf. – Green Technol.*, 2021, **8**(2), 703–742.
70 D. Li, A review of microstructure evolution during ultrasonic additive manufacturing, *Int. J. Adv. Manuf. Technol.*, 2021, **113**(1), 1–19.
71 J. Huang, Q. Qin and J. Wang, A review of stereolithography: Processes and systems, *Processes*, 2020, **8**(9), 1138.
72 B. E. Kelly, I. Bhattacharya, H. Heidari, M. Shusteff, C. M. Spadaccini and H. K. Taylor, Volumetric additive manufacturing *via* tomographic reconstruction, *Science*, 2019, **363**(6431), 1075–1079.
73 D. Loterie, P. Delrot and C. Moser, High-resolution tomographic volumetric additive manufacturing, *Nat. Commun.*, 2020, **11**(1), 852.
74 J. W. Halloran, Ceramic stereolithography: additive manufacturing for ceramics by photopolymerization, *Annu. Rev. Mater. Res.*, 2016, **46**(1), 19–40.

Open Access Article. Published on 19 June 2026. Downloaded on 6/19/2026 11:23:52 PM. This article is licensed under a Creative Commons Attribution 3.0 Unported Licence.

75 J. R. Tumbleston, *et al.*, Continuous liquid interface production of 3D objects, *Science*, 2015, **347**(6228), 1349–1352.
76 T. D. Ngo, A. Kashani, G. Imbalzano, K. T. Nguyen and D. Hui, Additive manufacturing (3D printing): A review of materials, methods, applications and challenges, *Composites, Part B*, 2018, **143**, 172–196.
77 A. N. Dickson, K.-A. Ross and D. P. Dowling, Additive manufacturing of woven carbon fibre polymer composites, *Compos. Struct.*, 2018, **206**, 637–643.
78 Q. Wei, R. Yang, X. Zhao, J. Zhou, Y. An and S. Yang, Fused deposition modeling of carbon-reinforced polymer matrix composites: a comprehensive review, *Polym. Compos.*, 2023, **44**(9), 5313–5345.
79 R. Matsuzaki, *et al.*, Three-dimensional printing of continuous-fiber composites by in-nozzle impregnation, *Sci. Rep.*, 2016, **6**(1), 23058.
80 H. L. Tekinalp, *et al.*, Highly oriented carbon fiber–polymer composites *via* additive manufacturing, *Compos. Sci. Technol.*, 2014, **105**, 144–150.
81 M. Yakout and M. Elbestawi, Additive manufacturing of composite materials: an overview, in Proceedings of the 6th International Conference on Virtual Machining Process Technology (VMPT), Montréal, QC, Canada, 2017, vol. 29.
82 H. Dou, *et al.*, Effect of process parameters on tensile mechanical properties of 3D printing continuous carbon fiber-reinforced PLA composites, *Materials*, 2020, **13**(17), 3850.
83 W. E. Frazier, Metal additive manufacturing: a review, *J. Mater. Eng. Perform.*, 2014, **23**(6), 1917–1928.
84 S. Bose, D. Ke, H. Sahasrabudhe and A. Bandyopadhyay, Additive manufacturing of biomaterials, *Prog. Mater. Sci.*, 2018, **93**, 45–111.
85 E. O. Olakanmi, R. F. Cochrane and K. W. Dalgarno, A review on selective laser sintering/melting (SLS/SLM) of aluminium alloy powders: Processing, microstructure, and properties, *Prog. Mater. Sci.*, 2015, **74**, 401–477.
86 M. Attaran, The rise of 3-D printing: The advantages of additive manufacturing over traditional manufacturing, *Bus. Horiz.*, 2017, **60**(5), 677–688.
87 D. Herzog, V. Seyda, E. Wycisk and C. Emmelmann, Additive manufacturing of metals, *Acta Mater.*, 2016, **117**, 371–392.
88 T. DebRoy, *et al.*, Additive manufacturing of metallic components–process, structure and properties, *Prog. Mater. Sci.*, 2018, **92**, 112–224.
89 J. Zuback and T. Debroy, The hardness of additively manufactured alloys, *Materials*, 2018, **11**(11), 2070.
90 A. Hehr and M. Norfolk, A comprehensive review of ultrasonic additive manufacturing, *Rapid Prototyp. J.*, 2019, **26**(3), 445–458.
91 K. Ishfaq, Z. Abas, M. Saravana Kumar and M. A. Mahmood, Review of recent trends in ultrasonic additive manufacturing: current challenges and future prospects, *Rapid Prototyp. J.*, 2023, **29**(6), 1195–1211.
92 A. Kumar, A. Dixit and S. Sreenivasa, Mechanical properties of additively manufactured polymeric composites using sheet lamination technique and fused deposition modeling: A review, *Polym. Adv. Technol.*, 2024, **35**(4), e6396.
93 F. Honarvar and A. Varvani-Farahani, A review of ultrasonic testing applications in additive manufacturing: Defect evaluation, material characterization, and process control, *Ultrasonics*, 2020, **108**, 106227.
94 K. V. Wong and A. Hernandez, A review of additive manufacturing, *Int. Scholarly Res. Not.*, 2012, **2012**, 208760.
95 C. K. Chua and K. F. Leong, *3D Printing and additive manufacturing: Principles and applications (with companion media pack)-of rapid prototyping*, World Scientific Publishing Company, 2014.
96 M. Shusteff, R. M. Panas, J. Henriksson, B. E. Kelly and A. E. Browar, Additive fabrication of 3d structures by holographic lithography, in 2016 International Solid Freeform Fabrication Symposium, 2016, University of Texas at Austin.
97 H. L. Van Der Laan, M. A. Burns and T. F. Scott, Volumetric photopolymerization confinement through dual-wavelength photoinitiation and photoinhibition, *ACS Macro Lett.*, 2019, **8**(8), 899–904.
98 X. Zheng, *et al.*, Multiscale metallic metamaterials, *Nat. Mater.*, 2016, **15**(10), 1100–1106.
99 X. Lv, F. Ye, L. Cheng, S. Fan and Y. Liu, Fabrication of SiC whisker-reinforced SiC ceramic matrix composites based on 3D printing and chemical vapor infiltration technology, *J. Eur. Ceram. Soc.*, 2019, **39**(11), 3380–3386.
100 D. A. Snelling, C. B. Williams, C. T. Suchicital and A. P. Druschitz, Binder jetting advanced ceramics for metal-ceramic composite structures, *Int. J. Adv. Manuf. Technol.*, 2017, **92**, 531–545.
101 J. Sun, *et al.*, A review on additive manufacturing of ceramic matrix composites, *J. Mater. Sci. Technol.*, 2023, **138**, 1–16.
102 I. Gibson, *et al.*, Binder jetting, *Addit. Manufact. Technol.*, 2021, 237–252.
103 A. Qattawi, B. Alrawi and A. Guzman, Experimental optimization of fused deposition modelling processing parameters: a design-for-manufacturing approach, *Procedia Manuf.*, 2017, **10**, 791–803.
104 K. Rajan, M. Samykano, K. Kadirgama, W. S. W. Harun and M. M. Rahman, Fused deposition modeling: process, materials, parameters, properties, and applications, *Int. J. Adv. Manuf. Technol.*, 2022, **120**(3–4), 1531–1570.
105 N. N. Kumbhar and A. Mulay, Post processing methods used to improve surface finish of products which are manufactured by additive manufacturing technologies: a review, *J. Inst. Eng. (India): Ser. D*, 2018, **99**, 481–487.
106 K. Bryll, E. Piesowicz, P. Szymański, W. Ślączka and M. Pijanowski, Polymer composite manufacturing by FDM 3D printing technology, *MATEC Web of Conferences*, EDP Sciences, 2018, vol. 237, p. 02006.
107 M. Nikzad, S. H. Masood and I. Sbarski, Thermomechanical properties of a highly filled polymeric composites for fused deposition modeling, *Mater. Design*, 2011, **32**(6), 3448–3456.

© 2026 The Author(s). Published by the Royal Society of Chemistry

Open Access Article. Published on 19 June 2026. Downloaded on 6/19/2026 11:23:52 PM. This article is licensed under a Creative Commons Attribution 3.0 Unported Licence.

108 K. Rajan, M. Samykano, K. Kadirgama, W. S. W. Harun and M. M. Rahman, Fused deposition modeling: process, materials, parameters, properties, and applications, *Int. J. Adv. Manuf. Technol.*, 2022, **120**(3), 1531–1570.
109 N. N. Kumbhar and A. Mulay, Post processing methods used to improve surface finish of products which are manufactured by additive manufacturing technologies: a review, *J. Inst. Eng. (India): Ser. D*, 2018, **99**(4), 481–487.
110 A. Mazzoli, Selective laser sintering in biomedical engineering, *Med. Biol. Eng. Comput.*, 2013, **51**, 245–256.
111 S. Yuan, Y. Zheng, C. K. Chua, Q. Yan and K. Zhou, Electrical and thermal conductivities of MWCNT/polymer composites fabricated by selective laser sintering, *Composites, Part A*, 2018, **105**, 203–213.
112 W. Han, L. Kong and M. Xu, Advances in selective laser sintering of polymers, *Int. J. Extreme Manuf.*, 2022, 042002.
113 Y. A. Gueche, N. M. Sanchez-Ballester, S. Cailleaux, B. Bataille and I. Soulairol, Selective laser sintering (SLS), a new chapter in the production of solid oral forms (SOFs) by 3D printing, *Pharmaceutics*, 2021, **13**(8), 1212.
114 D.-G. Ahn, Directed energy deposition (DED) process: State of the art, *Int. J. Precis. Eng. Manuf. – Green Technol.*, 2021, **8**, 703–742.
115 I. Z. Era and Z. Liu, Effect of process parameters on tensile properties of SS 316 prepared by directional energy deposition, *Procedia CIRP*, 2021, **103**, 115–121.
116 D. Svetlizky, *et al.*, Directed energy deposition (DED) additive manufacturing: Physical characteristics, defects, challenges and applications, *Mater. Today*, 2021, **49**, 271–295.
117 J. C. Lippold, *Welding metallurgy and weldability*, John Wiley & Sons, 2014.
118 T. DebRoy, *et al.*, Additive manufacturing of metallic components–process, structure and properties, *Prog. Mater. Sci.*, 2018, **92**, 112–224.
119 G. Langelandsvik, O. M. Akselsen, T. Furu and H. J. Roven, Review of aluminum alloy development for wire arc additive manufacturing, *Materials*, 2021, **14**(18), 5370.
120 D. Han and H. Lee, Recent advances in multi-material additive manufacturing: methods and applications, *Curr. Opin. Chem. Eng.*, 2020, **28**, 158–166, DOI: 10.1016/j.coche.2020.03.004.
121 A. García-Collado, J. Blanco, M. K. Gupta and R. Dorado-Vicente, Advances in polymers based Multi-Material Additive-Manufacturing Techniques: State-of-art review on properties and applications, *Addit. Manuf.*, 2022, **50**, 102577.
122 A. Verma, A. Kapil, D. Klobčar and A. Sharma, A review on multiplicity in multi-material additive manufacturing: process, capability, scale, and structure, *Materials*, 2023, **16**(15), 5246.
123 S. M. A. Nipu, *et al.*, Advances and perspectives in multi-material additive manufacturing of heterogenous metal-polymer components, *npj Adv. Manuf.*, 2025, **2**(1), 31.
124 M. Rajeshirke, I. Fidan, V. Naikwadi, S. Alkunte, A. Gupta and M. Mohammadizadeh, Material extrusion–based multi-material 3D printing: a holistic review of recent advances, *Int. J. Adv. Manuf. Technol.*, 2025, 1–26.
125 A. Nazir, *et al.*, Multi-material additive manufacturing: A systematic review of design, properties, applications, challenges, and 3D printing of materials and cellular metamaterials, *Mater. Des.*, 2023, **226**, 111661.
126 S. Vikneswaran, P. Nagarajan, S. Dinesh, K. S. Kumar and A. Megalingam, Investigation of the tensile behaviour of polylactic acid, acrylonitrile butadiene styrene, and polyethylene terephthalate glycol materials, *Mater. Today: Proc.*, 2022, **66**, 1093–1098.
127 D. Baca and R. Ahmad, The impact on the mechanical properties of multi-material polymers fabricated with a single mixing nozzle and multi-nozzle systems *via* fused deposition modeling, *Int. J. Adv. Manuf. Technol.*, 2020, **106**(9), 4509–4520.
128 N. A. Lee, *et al.*, Sequential multimaterial additive manufacturing of functionally graded biopolymer composites, *3D Print. Addit. Manuf.*, 2020, **7**(5), 205–215.
129 H. Sun, *et al.*, Multi-material ceramic hybrid additive manufacturing based on vat photopolymerization and material extrusion compound process, *Addit. Manuf.*, 2025, **97**, 104627.
130 K. E. Neely, K. C. Galloway and A. M. Strauss, Multi-material additively manufactured composite reactive materials *via* continuous filament direct ink writing, *Addit. Manuf.*, 2020, **35**, 101332.
131 N. Putra, M. Mirzaali, I. Apachitei, J. Zhou and A. Zadpoor, Multi-material additive manufacturing technologies for Ti-, Mg-, and Fe-based biomaterials for bone substitution, *Acta Biomater.*, 2020, **109**, 1–20.
132 J. Pragana, R. F. Sampaio, I. Bragança, C. Silva and P. Martins, Hybrid metal additive manufacturing: A state–of–the-art review, *Adv. Ind. Manuf. Eng.*, 2021, **2**, 100032.
133 B. Freitas, V. Richhariya, M. Silva, A. Vaz, S. F. Lopes and Ó. Carvalho, A review of hybrid manufacturing: integrating subtractive and additive manufacturing, *Materials*, 2025, **18**(18), 4249.
134 M. Á. Rabalo, A. García and E. M. Rubio, Emerging Trends in Hybrid Additive and Subtractive Manufacturing, *Appl. Sci.*, 2025, **15**(11), 6102.
135 M. Rabalo, E. Rubio, B. Agustina and A. Camacho, Hybrid additive and subtractive manufacturing: evolution of the concept and last trends in research and industry, *Procedia CIRP*, 2023, **118**, 741–746.
136 Y. Wang, *et al.*, The process planning for additive and subtractive hybrid manufacturing of powder bed fusion (PBF) process, *Mater. Des.*, 2023, **227**, 111732.
137 K. Palanikumar, M. Mudhukrishnan and P. Soorya Prabha, Technologies in additive manufacturing for fiber reinforced composite materials: a review, *Curr. Opin. Chem. Eng.*, 2020, **28**, 51–59.
138 S. Ramírez-Revilla, D. Camacho-Valencia, E. G. Gonzales-Condori and G. Márquez, Evaluation and comparison of the degradability and compressive and tensile properties

Open Access Article. Published on 19 June 2026. Downloaded on 6/19/2026 11:23:52 PM. This article is licensed under a Creative Commons Attribution 3.0 Unported Licence.

of 3D printing polymeric materials: PLA, PETG, PC, and ASA, *MRS Commun.*, 2023, **13**(1), 55–62.

139 S. Ekşi and C. Karakaya, Effects of Process Parameters on Tensile Properties of 3D-Printed PLA Parts Fabricated with the FDM Method, *Polymers*, 2025, **17**(14), 1934.

140 M. Algarni and S. Ghazali, Comparative study of the sensitivity of pla, abs, peek, and petg's mechanical properties to fdm printing process parameters, *Crystals*, 2021, **11**(8), 995.

141 E. Kargar and A. Ghasemi-Ghalebahman, Experimental investigation on fatigue life and tensile strength of carbon fiber-reinforced PLA composites based on fused deposition modeling, *Sci. Rep.*, 2023, **13**(1), 18194.

142 A. Zakręcki, J. Cieślik, A. Bazan and P. Turek, Innovative Approaches to 3D printing of PA12 Forearm orthoses: A Comprehensive analysis of mechanical properties and production efficiency, *Materials*, 2024, **17**(3), 663.

143 M. R. Omar, *et al.*, Effect of polyamide-12 material compositions on mechanical properties and surface morphology of SLS 3D printed part, *J. Mech. Eng.*, 2022, **19**(1), 57–70.

144 A. Mansoura, S. Dehghan, N. Barka and S. S. Kangranroudi, Investigation into the effect of process parameters on density, surface roughness, and mechanical properties of 316L stainless steel fabricated by selective laser melting, *Int. J. Adv. Manuf. Technol.*, 2024, **130**(5), 2547–2562.

145 M. Bakhtiarian, H. Omidvar, A. Mashhuriazar, Z. Sajuri and C. H. Gur, The effects of SLM process parameters on the relative density and hardness of austenitic stainless steel 316L, *J. Mater. Res. Technol.*, 2024, **29**, 1616–1629.

146 I. La Fé-Perdomo, J. Ramos-Grez, R. Mujica and M. Rivas, Surface roughness Ra prediction in Selective Laser Melting of 316L stainless steel by means of artificial intelligence inference, *J. King Saud Univ., Eng. Sci.*, 2023, **35**(2), 148–156.

147 Y. Deng, Z. Mao, N. Yang, X. Niu and X. Lu, Collaborative optimization of density and surface roughness of 316L stainless steel in selective laser melting, *Materials*, 2020, **13**(7), 1601.

148 N. Sanaei and A. Fatemi, Defects in additive manufactured metals and their effect on fatigue performance: A state-of-the-art review, *Prog. Mater. Sci.*, 2021, **117**, 100724.

149 H. Zhang, *et al.*, 3D printing of continuous carbon fibre reinforced polymer composites with optimised structural topology and fibre orientation, *Compos. Struct.*, 2023, **313**, 116914.

150 R. Shougat, E. H. Sabuz, G. Najmul Quader and M. Mahboo, Effect of Building Orientation & Post Processing Material on Mechanical Properties of 3D Printed Parts, *Proceedings of the International Conference on Mechanical, Industrial and Energy Engineering*, Khulna, Bangladesh, 2016, pp. 26–27.

151 J. Fu, S. Qu, J. Ding, X. Song and M. Fu, Comparison of the microstructure, mechanical properties and distortion of stainless steel 316 L fabricated by micro and conventional laser powder bed fusion, *Addit. Manuf.*, 2021, **44**, 102067.

152 E. H. Sabuz and M. Z. Rahman, *Modeling and simulation on additive manufacturing of composite materials*, 2023.

153 A. El Moumen, T. Kanit and A. Imad, Numerical evaluation of the representative volume element for random composites, *Eur. J. Mech.-A/Solids*, 2021, **86**, 104181.

154 B. Brenken, E. Barocio, A. Favaloro, V. Kunc and R. B. Pipes, Fused filament fabrication of fiber-reinforced polymers: A review, *Addit. Manuf.*, 2018, **21**, 1–16.

155 F. Ning, W. Cong, J. Qiu, J. Wei and S. Wang, Additive manufacturing of carbon fiber reinforced thermoplastic composites using fused deposition modeling, *Composites, Part B*, 2015, **80**, 369–378.

156 M. Caminero, J. Chacón, I. García-Moreno and J. Reverte, Interlaminar bonding performance of 3D printed continuous fibre reinforced thermoplastic composites using fused deposition modelling, *Polym. Test.*, 2018, **68**, 415–423.

157 Q. He, H. Wang, K. Fu and L. Ye, 3D printed continuous CF/PA6 composites: Effect of microscopic voids on mechanical performance, *Compos. Sci. Technol.*, 2020, **191**, 108077.

158 I. Ezzaraa, *et al.*, Numerical modeling based on finite element analysis of 3D-printed wood-polylactic acid composites: a comparison with experimental data, *Forests*, 2023, **14**(1), 95.

159 A. Özen and D. Auhl, Modeling of the mechanical properties of fused deposition modeling (FDM) printed fiber reinforced thermoplastic composites by asymptotic homogenization, *Compos. Adv. Mater.*, 2022, **31**, 26349833221132296.

160 T. A. Dutra, R. T. L. Ferreira, H. B. Resende, L. M. Oliveira, B. J. Blinzler and L. E. Asp, Identification of representative equivalent volumes on the microstructure of 3d-printed fiber-reinforced thermoplastics based on statistical characterization, *Polymers*, 2022, **14**(5), 972.

161 M. Gljušćić, M. Franulović, D. Lanc and A. Žerovnik, Representative volume element for microscale analysis of additively manufactured composites, *Addit. Manuf.*, 2022, **56**, 102902.

162 T. A. Dutra, R. T. L. Ferreira, H. B. Resende, B. J. Blinzler and L. E. Asp, Mechanism based failure of 3D-printed continuous carbon fiber reinforced thermoplastic composites, *Compos. Sci. Technol.*, 2021, **213**, 108962.

163 W.-G. Jiang, R.-Z. Zhong, Q. H. Qin and Y.-G. Tong, Homogenized finite element analysis on effective elastoplastic mechanical behaviors of composite with imperfect interfaces, *Int. J. Mol. Sci.*, 2014, **15**(12), 23389–23407.

164 D. K. Singh, A. Vaidya, V. Thomas, M. Theodore, S. Kore and U. Vaidya, Finite element modeling of the fiber-matrix interface in polymer composites, *J. Compos. Sci.*, 2020, **4**(2), 58.

165 J. Gan, H. Gao, S. Wen, Y. Zhou, S. Tan and L. Duan, Simulation, forming process and mechanical property of Cu-Sn-Ti/diamond composites fabricated by selective laser melting, *Int. J. Refract. Met. Hard Mater.*, 2020, **87**, 105144.

166 D. Gu, Y. Yang, L. Xi, J. Yang and M. Xia, Laser absorption behavior of randomly packed powder-bed during selective laser melting of SiC and TiB2 reinforced Al matrix composites, *Opt. Laser Technol.*, 2019, **119**, 105600.

© 2026 The Author(s). Published by the Royal Society of Chemistry

Open Access Article. Published on 19 June 2026. Downloaded on 6/19/2026 11:23:52 PM. This article is licensed under a Creative Commons Attribution 3.0 Unported Licence.

167 Y. Woo, T. Hwang, I. Oh, D. Seo and Y. Moon, Analysis on selective laser melting of WC-reinforced H13 steel composite powder by finite element method, *Adv. Mech. Eng.*, 2019, **11**(1), 1687814018822200.
168 B. AlMangour, D. Grzesiak, J. Cheng and Y. Ertas, Thermal behavior of the molten pool, microstructural evolution, and tribological performance during selective laser melting of TiC/316L stainless steel nanocomposites: Experimental and simulation methods, *J. Mater. Process. Technol*, 2018, **257**, 288–301.
169 S. Westbeek, J. Van Dommelen, J. Remmers and M. Geers, Multiphysical modeling of the photopolymerization process for additive manufacturing of ceramics, *Eur. J. Mech.-A Solids*, 2018, **71**, 210–223.
170 S. Westbeek, J. J. Remmers, J. Van Dommelen and M. G. Geers, Multi-scale process simulation for additive manufacturing through particle filled vat photopolymerization, *Comput. Mater. Sci.*, 2020, **180**, 109647.
171 I. M. Alarifi, Mechanical properties and numerical simulation of FDM 3D printed PETG/carbon composite unit structures, *J. Mater. Res. Technol.*, 2023, **23**, 656–669.
172 A. D. Pertuz, S. Díaz-Cardona and O. A. González-Estrada, Static and fatigue behaviour of continuous fibre reinforced thermoplastic composites manufactured by fused deposition modelling technique, *Int. J. Fatigue*, 2020, **130**, 105275.
173 O. A. González-Estrada, A. D. P. Comas and J. G. D. Rodríguez, Monotonic load datasets for additively manufactured thermoplastic reinforced composites, *Data Brief*, 2020, **29**, 105295.
174 A. D. Pertuz-Comas, J. G. Díaz, O. J. Meneses-Duran, N. Y. Niño-Álvarez and J. León-Becerra, Flexural fatigue in a polymer matrix composite material reinforced with continuous Kevlar fibers fabricated by additive manufacturing, *Polymers*, 2022, **14**(17), 3586.
175 P. Yuan and D. Gu, Molten pool behaviour and its physical mechanism during selective laser melting of TiC/AlSi10Mg nanocomposites: simulation and experiments, *J. Phys. D:Appl. Phys.*, 2015, **48**(3), 035303.
176 C. Wang, X. Tan, S. B. Tor and C. Lim, Machine learning in additive manufacturing: State-of-the-art and perspectives, *Addit. Manuf.*, 2020, **36**, 101538.
177 T. Xue, T. J. Wallin, Y. Menguc, S. Adriaenssens and M. Chiaramonte, Machine learning generative models for automatic design of multi-material 3D printed composite solids, *Extreme Mech. Lett.*, 2020, **41**, 100992.
178 Y. Zhou, H. Lu, G. Wang, J. Wang and W. Li, Voxelization modelling based finite element simulation and process parameter optimization for Fused Filament Fabrication, *Mater. Design*, 2020, **187**, 108409.
179 G. Tapia, A. H. Elwany and H. Sang, Prediction of porosity in metal-based additive manufacturing using spatial Gaussian process models, *Addit. Manuf.*, 2016, **12**, 282–290.
180 R. Cai, W. Wen, K. Wang, Y. Peng, S. Ahzi and F. Chinesta, Tailoring interfacial properties of 3D-printed continuous natural fiber reinforced polypropylene composites through parameter optimization using machine learning methods, *Mater. Today Commun.*, 2022, **32**, 103985.
181 K. Xu, J. Lyu and S. Manoochehri, In situ process monitoring using acoustic emission and laser scanning techniques based on machine learning models, *J. Manuf. Process.*, 2022, **84**, 357–374.
182 F. Kaji, H. Nguyen-Huu, A. Budhwani, J. A. Narayanan, M. Zimny and E. Toyserkani, A deep-learning-based *in situ* surface anomaly detection methodology for laser directed energy deposition *via* powder feeding, *J. Manuf. Process.*, 2022, **81**, 624–637.
183 R. Cai, K. Wang, W. Wen, Y. Peng, M. Baniassadi and S. Ahzi, Application of machine learning methods on dynamic strength analysis for additive manufactured polypropylene-based composites, *Polym. Test.*, 2022, **110**, 107580.
184 A. Marko, S. Bähring, J. Raute, M. Biegler and M. Rethmeier, Quality Prediction in Directed Energy Deposition Using Artificial Neural Networks Based on Process Signals, *Appl. Sci.*, 2022, **12**(8), 3955.
185 V. Karkaria, *et al.*, Towards a digital twin framework in additive manufacturing: Machine learning and bayesian optimization for time series process optimization, *J. Manuf. Syst.*, 2024, **75**, 322–332.
186 G. Vashishtha, S. Chauhan, R. Zimroz, N. Yadav, R. Kumar and M. K. Gupta, Current Applications of Machine Learning in Additive Manufacturing: A Review on Challenges and Future Trends, *Arch. Comput. Methods Eng.*, 2025, **32**(4), 2635–2668, DOI: 10.1007/s11831-024-10215-2.
187 S. Manivannan, Automatic quality inspection in additive manufacturing using semi-supervised deep learning, *J. Intell. Manuf.*, 2023, **34**(7), 3091–3108.
188 A. Oleff, B. Küster, M. Stonis and L. Overmeyer, Process monitoring for material extrusion additive manufacturing: a state-of-the-art review, *Prog. Addit. Manuf.*, 2021, **6**(4), 705–730.
189 L. Chen, *et al.*, *In situ* process monitoring and adaptive quality enhancement in laser additive manufacturing: a critical review, *J. Manuf. Syst.*, 2024, **74**, 527–574.
190 M. Mani, S. Feng, L. Brandon, A. Donmez, S. Moylan and R. Fesperman, Measurement science needs for real-time control of additive manufacturing powder-bed fusion processes, *Additive manufacturing handbook*, CRC Press, 2017, 629–652.
191 B. Kavas, *et al.*, *In situ* controller autotuning by Bayesian optimization for closed-loop feedback control of laser powder bed fusion process, *Addit. Manuf.*, 2025, **99**, 104641.
192 A. Dean and D. Voss, *Design and analysis of experiments*, Springer, 1999.
193 G. E. Box and K. B. Wilson, On the experimental attainment of optimum conditions, *Breakthroughs in statistics: methodology and distribution*, Springer, 1992, pp. 270–310.
194 G. E. Box and D. W. Behnken, Some new three level designs for the study of quantitative variables, *Technometrics*, 1960, **2**(4), 455–475.

Open Access Article. Published on 19 June 2026. Downloaded on 6/19/2026 11:23:52 PM. This article is licensed under a Creative Commons Attribution 3.0 Unported Licence.

195 F. Kartal, Mechanical performance optimization in FFF 3D printing using Taguchi design and machine learning approach with PLA/walnut Shell composites filaments, *J. Vinyl Addit. Technol.*, 2025, **31**(3), 622–638.
196 R. D. Maalihan, Modelling the toughness of nanostructured polyhedral oligomeric silsesquioxane composites fabricated by stereolithography 3D printing: a response surface methodology and artificial neural network approach, *Materials Science Forum*, 2022, Trans Tech Publications, vol. 1053, pp. 41–46.
197 A. Deka and J. F. Hall, A framework for optimizing process parameters in fused deposition modeling using predictive modeling coupled response surface methodology, *Int. J. Adv. Manuf. Technol.*, 2024, **131**(1), 447–466.
198 C.-T. Chen and G. X. Gu, Machine learning for composite materials, *MRs Communications*, 2019, **9**(2), 556–566.
199 Z. Yang, *et al.*, Deep learning approaches for mining structure-property linkages in high contrast composites from simulation datasets, *Comput. Mater. Sci.*, 2018, **151**, 278–287.
200 M. Mathieu, M. Henaff and Y. LeCun, Fast training of convolutional networks through ffts, *arXiv*, 2013, preprint, arXiv:1312.5851, DOI: 10.48550/arXiv.1312.5851.
201 J. Bruna, W. Zaremba, A. Szlam and Y. LeCun, Spectral networks and locally connected networks on graphs, *arXiv*, 2013, preprint, arXiv:1312.6203, DOI: 10.48550/arXiv.1312.6203.
202 D. Palaz, M. M. Doss and R. Collobert, Convolutional neural networks-based continuous speech recognition using raw speech signal, in 2015 IEEE International Conference on Acoustics, Speech and Signal Processing (ICASSP), 2015, IEEE, pp. 4295–4299.
203 S. A. Shevchik, C. Kenel, C. Leinenbach and K. Wasmer, Acoustic emission for in situ quality monitoring in additive manufacturing using spectral convolutional neural networks, *Addit. Manuf.*, 2018, **21**, 598–604.
204 Y. Zhang, G. S. Hong, D. Ye, K. Zhu and J. Y. Fuh, Extraction and evaluation of melt pool, plume and spatter information for powder-bed fusion AM process monitoring, *Mater. Design*, 2018, **156**, 458–469.
205 J. Klein, M. Jaretzki, M. Schwarzenberger, S. Ihlenfeldt and W.-G. Drossel, Automated porosity assessment of parts produced by laser powder bed fusion using convolutional neural networks, *Procedia CIRP*, 2021, **104**, 1434–1439.
206 M. A. Ansari, A. Crampton, R. Garrard, B. Cai and M. Attallah, A Convolutional Neural Network (CNN) classification to identify the presence of pores in powder bed fusion images, *Int. J. Adv. Manuf. Technol.*, 2022, **120**(7), 5133–5150.
207 M. Qin, J. Ding, S. Qu, X. Song, C. C. Wang and W.-H. Liao, Deep reinforcement learning based toolpath generation for thermal uniformity in laser powder bed fusion process, *Addit. Manuf.*, 2024, **79**, 103937.
208 X. Lu, Q. Chen, Z. Yang, S. Liu, P. Chen and F. Dong, Prediction of porosity in parts using coaxial melt pool imaging and deep learning methods, *Mater. Today Commun.*, 2025, **45**, 112280.
209 M. Mozaffar, A. Ebrahimi and J. Cao, Toolpath design for additive manufacturing using deep reinforcement learning, *arXiv*, 2020, preprint, arXiv:2009.14365, DOI: 10.48550/arXiv.2009.14365.
210 X. Sun, *et al.*, Machine learning-evolutionary algorithm enabled design for 4D-printed active composite structures, *Adv. Funct. Mater.*, 2022, **32**(10), 2109805.
211 J. García-Ávila, D. d J. Torres Serrato, C. A. Rodriguez, A. V. Martínez, E. R. Cedillo and J. I. Martínez-López, Predictive Modeling of Soft Stretchable Nanocomposites Using Recurrent Neural Networks, *Polymers*, 2022, **14**(23), 5290.
212 S. Jaypuria, S. K. Gupta and D. K. Pratihar, Comparative study of feed-forward and recurrent neural networks in modeling of electron beam welding, *Advances in Additive Manufacturing and Joining: Proceedings of AIMTDR 2018*, Springer, 2019, pp. 521–531.
213 G. L. Chen, K. Yanamandra and N. Gupta, Artificial neural networks framework for detection of defects in 3D-printed fiber reinforcement composites, *JOM*, 2021, **73**(7), 2075–2084.
214 Y.-C. Hsu, C.-H. Yu and M. J. Buehler, Using deep learning to predict fracture patterns in crystalline solids, *Matter*, 2020, **3**(1), 197–211.
215 M. Mozaffar, R. Bostanabad, W. Chen, K. Ehmann, J. Cao and M. Bessa, Deep learning predicts path-dependent plasticity, *Proc. Natl. Acad. Sci.*, 2019, **116**(52), 26414–26420.
216 J. Schmidhuber, Deep learning in neural networks: An overview, *Neural Networks*, 2015, **61**, 85–117.
217 X. Zha, H. Ren, Z. Chen, H. Tang, D. Zhao and Y. Xiong, Strengthening mechanical performance with machine learning-assisted toolpath planning for additive manufacturing of continuous fiber reinforced polymer composites, *J. Manuf. Process.*, 2025, **141**, 1416–1432.
218 A. Kiadarbandsari, M. V. Ehteshamfar and H. Adibi, Ensemble machine learning for predicting surface roughness improvement in chemo-mechanical post-processing of additive manufacturing dental parts, *Prog. Addit. Manuf.*, 2025, 1–15.
219 I. Mahapatra, N. Chikkanna, K. Shanmugam, J. Rengaswamy and V. Ramachandran, Evaluation of tensile properties of 3D-printed lattice composites: Experimental and machine learning-based predictive modelling, *Composite Part A*, 2025, **193**, 108823.
220 W. Tian, Q. Li, Q. Wang, D. Chen and W. Gao, Additive manufacturing error quantification on stability of composite sandwich plates with lattice-cores through machine learning technique, *Compos. Struct.*, 2024, **327**, 117645.
221 T.-W. Chang, K.-W. Liao, C.-C. Lin, M.-C. Tsai and C.-W. Cheng, Predicting magnetic characteristics of additive manufactured soft magnetic composites by machine learning, *Int. J. Adv. Manuf. Technol.*, 2021, **114**, 3177–3184.
222 S. Mahadevan, P. Nath and Z. Hu, Uncertainty quantification for additive manufacturing process improvement: Recent advances, *ASCE-ASME J. Risk Uncertain. Eng. Syst. B: Mech. Eng.*, 2022, **8**(1), 010801.

 © 2026 The Author(s). Published by the Royal Society of Chemistry

Open Access Article. Published on 19 June 2026. Downloaded on 6/19/2026 11:23:52 PM. This article is licensed under a Creative Commons Attribution 3.0 Unported Licence.

223 M. Faegh, S. Ghungrad, J. P. Oliveira, P. Rao and A. Haghighi, A review on physics-informed machine learning for process-structure-property modeling in additive manufacturing, *J. Manuf. Process.*, 2025, **133**, 524–555.
224 Y. Tang, M. R. Dehaghani and G. G. Wang, Review of transfer learning in modeling additive manufacturing processes, *Addit. Manuf.*, 2023, **61**, 103357.
225 M. Raissi, P. Perdikaris and G. E. Karniadakis, Physics-informed neural networks: A deep learning framework for solving forward and inverse problems involving nonlinear partial differential equations, *J. Comput. Phys.*, 2019, **378**, 686–707.
226 A. Kiadarbandsari, M. V. Ehteshamfar and H. Adibi, Ensemble machine learning for predicting surface roughness improvement in chemo-mechanical post-processing of additive manufacturing dental parts, *Prog. Addit. Manuf.*, 2025, **10**(10), 7409–7423.
227 T.-W. Chang, K.-W. Liao, C.-C. Lin, M.-C. Tsai and C.-W. Cheng, Predicting magnetic characteristics of additive manufactured soft magnetic composites by machine learning, *Int. J. Adv. Manuf. Technol.*, 2021, **114**(9), 3177–3184.
228 C. Blundell, J. Cornebise, K. Kavukcuoglu and D. Wierstra, Weight uncertainty in neural network, *International conference on machine learning*, PMLR, 2015, pp. 1613–1622.
229 Y. Gal and Z. Ghahramani, Dropout as a bayesian approximation: Representing model uncertainty in deep learning, in international conference on machine learning, 2016, PMLR, pp. 1050–1059.
230 B. Lakshminarayanan, A. Pritzel and C. Blundell, Simple and scalable predictive uncertainty estimation using deep ensembles, *Adv. Neural Inf. Process. Syst.*, 2017, **30**, 1–12.
231 S. H. Bang, R. Ak, A. Narayanan, Y. T. Lee and H. Cho, A survey on knowledge transfer for manufacturing data analytics, *Comput. Ind.*, 2019, **104**, 116–130.
232 C. F. Lui, A. Maged and M. Xie, A novel image feature based self-supervised learning model for effective quality inspection in additive manufacturing, *J. Intell. Manuf.*, 2024, **35**(7), 3543–3558.
233 M. V. Bimrose, *et al.*, Detecting and classifying hidden defects in additively manufactured parts using deep learning and X-ray computed tomography, *J. Intell. Manuf.*, 2025, **36**(5), 3465–3479.
234 M. Seeger, Gaussian processes for machine learning, *Int. J. Neural Syst.*, 2004, **14**(02), 69–106.
235 D. Hendrycks and K. Gimpel, A baseline for detecting misclassified and out-of-distribution examples in neural networks, *arXiv*, 2016, preprint, arXiv:1610.02136, DOI: 10.48550/arXiv.1610.02136.
236 S. M. Lundberg and S.-I. Lee, A unified approach to interpreting model predictions, *Adv. Neural Inf. Process. Syst.*, 2017, **30**, 1–10.
237 A. N. Angelopoulos and S. Bates, Conformal prediction: A gentle introduction, *Found. Trends Mach. Learn.*, 2023, **16**(4), 494–591.
238 G. Vashishtha, S. Chauhan, R. Zimroz, N. Yadav, R. Kumar and M. K. Gupta, Current Applications of Machine Learning in Additive Manufacturing: A Review on Challenges and Future Trends: G. Vashishtha *et al.*, *Arch. Comput. Methods Eng.*, 2025, **32**(4), 2635–2668.
239 C. Rudin, Stop explaining black box machine learning models for high stakes decisions and use interpretable models instead, *Nat. Mach. Intell.*, 2019, **1**(5), 206–215.
240 A. B. Arrieta, *et al.*, Explainable Artificial Intelligence (XAI): Concepts, taxonomies, opportunities and challenges toward responsible AI, *Inform. Fusion*, 2020, **58**, 82–115.
241 Y. Huang, *et al.*, 3D printing of topologically optimized wing spar with continuous carbon fiber reinforced composites, *Composites, Part B*, 2024, **272**, 111166.
242 P. Cheng, *et al.*, 3D printed continuous fiber reinforced composite lightweight structures: A review and outlook, *Composites, Part B*, 2023, **250**, 110450.
243 C. Sun, *et al.*, A shape-performance synergistic strategy for design and additive manufacturing of continuous fiber reinforced transfemoral prosthetic socket, *Composites, Part B*, 2024, **281**, 111518.
244 P. K. Mishra and T. Jagadesh, Applications and Challenges of 3D Printed Polymer Composites in the Emerging Domain of Automotive and Aerospace: A Converged Review, *J. Inst. Eng. (India): Ser. D*, 2022, 1–18.
245 C. J. Choudhari, P. S. Thakare and S. K. Sahu, 3D printing of composite sandwich structures for aerospace applications, *High-performance composite structures: additive manufacturing and processing*, Springer, 2021, pp. 45–73.
246 S. C. Joshi and A. A. Sheikh, 3D printing in aerospace and its long-term sustainability, *Virtual Phys. Prototyping*, 2015, **10**(4), 175–185.
247 U. Fasel, D. Keidel, L. Baumann, G. Cavolina, M. Eichenhofer and P. Ermanni, Composite additive manufacturing of morphing aerospace structures, *Manuf. Lett.*, 2020, **23**, 85–88.
248 J. Frketic, T. Dickens and S. Ramakrishnan, Automated manufacturing and processing of fiber-reinforced polymer (FRP) composites: An additive review of contemporary and modern techniques for advanced materials manufacturing, *Addit. Manuf.*, 2017, **14**, 69–86.
249 B. Castanie, C. Bouvet and M. Ginot, Review of composite sandwich structure in aeronautic applications, *Compos., Part C: Open Access*, 2020, **1**, 100004.
250 L. J. Kumar and C. Krishnadas Nair, Current trends of additive manufacturing in the aerospace industry, *Advances in 3D printing & additive manufacturing technologies*, 2017, pp. 39–54.
251 A. Azarov, V. Kolesnikov and A. Khaziev, Development of equipment for composite 3D printing of structural elements for aerospace applications, *IOP Conf. Ser.:Mater. Sci. Eng.*, 2020, **934**(1), 012049.
252 R. Liu, Z. Wang, T. Sparks, F. Liou and J. Newkirk, Aerospace applications of laser additive manufacturing, *Laser additive manufacturing*, Elsevier, 2017, pp. 351–371.
253 M. Attaran, Additive manufacturing: the most promising technology to alter the supply chain and logistics, *J. Serv. Sci. Manag.*, 2017, **10**(03), 189.

Open Access Article. Published on 19 June 2026. Downloaded on 6/19/2026 11:23:52 PM. This article is licensed under a Creative Commons Attribution 3.0 Unported Licence.

254 J. C. Vasco, Additive manufacturing for the automotive industry, *Additive Manufacturing*, Elsevier, 2021, pp. 505–530.
255 A. A. Hassen, *et al.*, Scaling Up metal additive manufacturing process to fabricate molds for composite manufacturing, *Addit. Manuf.*, 2020, **32**, 101093.
256 V. K. Balla, K. H. Kate, J. Satyavolu, P. Singh and J. G. D. Tadimeti, Additive manufacturing of natural fiber reinforced polymer composites: Processing and prospects, *Composites, Part B*, 2019, **174**, 106956.
257 M. Sargini, S. Masood, S. Palanisamy, E. Jayamani and A. Kapoor, Additive manufacturing of an automotive brake pedal by metal fused deposition modelling, *Mater. Today: Proc.*, 2021, **45**, 4601–4605.
258 E. Dalpadulo, A. Petruccioli, F. Gherardini and F. Leali, A review of automotive spare-part reconstruction based on additive manufacturing, *J. Manuf. Mater. Process.*, 2022, **6**(6), 133.
259 S. Curran, *et al.*, Big area additive manufacturing and hardware-in-the-loop for rapid vehicle powertrain prototyping: A case study on the development of a 3-D-printed Shelby Cobra, *SAE Technical Paper*, pp. 0148–7191, 2016.
260 E. B. Joyee and Y. Pan, Additive manufacturing of multi-material soft robot for on-demand drug delivery applications, *J. Manuf. Process.*, 2020, **56**, 1178–1184.
261 N. W. Bartlett, *et al.*, A 3D-printed, functionally graded soft robot powered by combustion, *Science*, 2015, **349**(6244), 161–165.
262 H. K. Yap, H. Y. Ng and C.-H. Yeow, High-force soft printable pneumatics for soft robotic applications, *Soft Rob.*, 2016, **3**(3), 144–158.
263 B. Khatri, K. Lappe, D. Noetzel, K. Pursche and T. Hanemann, A 3D-printable polymer-metal soft-magnetic functional composite—Development and characterization, *Materials*, 2018, **11**(2), 189.
264 N. C. Benack, T. Wang, K. Matthews and M. L. Taheri, Additive manufacturing methods for soft magnetic composites (SMCs), *Microsc. Microanal.*, 2018, **24**(S1), 1066–1067.
265 M. R. E. U. Shougat, *Physical Reservoir Computing Using Nonlinear System*, North Carolina State University, 2023.
266 J. D. Carrico, T. Hermans, K. J. Kim and K. K. Leang, 3D-printing and machine learning control of soft ionic polymer-metal composite actuators, *Sci. Rep.*, 2019, **9**(1), 17482.
267 M. R. E. U. Shougat, S. Kennedy and E. Perkins, A self-sensing shape memory alloy actuator physical reservoir computer, *IEEE Sensors Lett.*, 2023, **7**(5), 1–4.
268 S. Kennedy, M. R. E. U. Shougat and E. Perkins, Robust self-sensing shape memory alloy actuator using a machine learning approach, *Sens. Actuators, A*, 2023, **354**, 114255.
269 Z. Quan, *et al.*, Additive manufacturing of multi-directional preforms for composites: opportunities and challenges, *Mater. Today*, 2015, **18**(9), 503–512.
270 R. Whenish, R. Velu, S. Anand Kumar and L. Ramprasath, Additive manufacturing technologies for biomedical implants using functional biocomposites, *High-performance composite structures: additive manufacturing and processing*, Springer, 2021, pp. 25–44.
271 X. Han, *et al.*, Carbon fiber reinforced PEEK composites based on 3D-printing technology for orthopedic and dental applications, *J. Clin. Med.*, 2019, **8**(2), 240.
272 Y. Xia, *et al.*, Selective laser sintering fabrication of nano-hydroxyapatite/poly-ε-caprolactone scaffolds for bone tissue engineering applications, *Int. J. Nanomed.*, 2013, 4197–4213.
273 J. Singh and P. M. Pandey, Machine learning for materials developments in metals additive manufacturing, *Machine Learning for Powder-Based Metal Additive Manufacturing*, Elsevier, 2025, pp. 43–75.
274 Y. Fu, A. Downey, L. Yuan, A. Pratt and Y. Balogun, In situ monitoring for fused filament fabrication process: A review, *Addit. Manuf.*, 2021, **38**, 101749.
275 M. Mani, B. M. Lane, M. A. Donmez, S. C. Feng and S. P. Moylan, A review on measurement science needs for real-time control of additive manufacturing metal powder bed fusion processes, *Int. J. Prod. Res.*, 2017, **55**(5), 1400–1418.
276 D. R. Gunasegaram, *et al.*, Machine learning-assisted *in situ* adaptive strategies for the control of defects and anomalies in metal additive manufacturing, *Addit. Manuf.*, 2024, **81**, 104013.
277 B. M. Lane, B. J. Simonds, J. E. Seppala and L. E. Levine, Don't Miss the 2022 Additive Manufacturing Benchmark Test Series and Conference, *JOM*, 2022, **74**(4), 1274–1276.
278 ISO/ASTM 52904:2024: Additive manufacturing of metals—Process characteristics and performance—Metal powder bed fusion process to meet critical applications, 2024.
279 T. Debroy, W. Zhang, J. Turner and S. S. Babu, Building digital twins of 3D printing machines, *Scr. Mater.*, 2017, **135**, 119–124.
280 T. Mukherjee and T. DebRoy, A digital twin for rapid qualification of 3D printed metallic components, *Appl. Mater. Today*, 2019, **14**, 59–65.
281 S. Chhetri, S. Faezi and M. Al Faruque, Digital twin of manufacturing systems: technical report on digital twin project, *Center for Embedded and Cyber-physical Systems (CECS)*, University of California, Irvine, CA, USA, 2017.
282 Y. AbouelNour and N. Gupta, *In situ* monitoring of subsurface and internal defects in additive manufacturing: A review, *Mater. Des.*, 2022, **222**, 111063.
283 H. C. de Winton, F. Cegla and P. A. Hooper, A method for objectively evaluating the defect detection performance of *in situ* monitoring systems, *Addit. Manuf.*, 2021, **48**, 102431.
284 ISO/ASTM 52904:2024 Additive manufacturing of metals—Process characteristics and performance—Metal powder bed fusion process to meet critical applications, I. O. f. Standardization, 2024.
285 M. Pantelidakis, K. Mykoniatis, J. Liu and G. Harris, A digital twin ecosystem for additive manufacturing using a real-time development platform, *Int. J. Adv. Manuf. Technol.*, 2022, **120**(9), 6547–6563.
286 C. Liu, L. Le Roux, C. Körner, O. Tabaste, F. Lacan and S. Bigot, Digital twin-enabled collaborative data management for metal additive manufacturing systems, *J. Manuf. Syst.*, 2022, **62**, 857–874.

© 2026 The Author(s). Published by the Royal Society of Chemistry